Neurochemical methods for the sub-second measurement of neurotransmitter release

By

Thomas Field

Submitted to the graduate degree program in Chemistry and the Graduate Faculty of the University of Kansas in partial fulfillment of the requirements for the degree of Doctor of Philosophy.

_____

Chair: Michael Johnson Ph.D.

_____

Cindy Berrie Ph.D.

_____

Rich Givens Ph.D.

_____

Susan Lunte Ph.D.

_____

Black Peterson Ph.D.

Date Defended: 16th August 2017

The dissertation committee for Thomas Field certifies that this is the approved version of the following dissertation:

Neurochemical methods for the sub-second measurement of neurotransmitter release

_____

Chair: Michael Johnson Ph.D.

Date Approved: 8-31-17

Abstract

This dissertation is a compilation of work on the development of new methods and models to study neurochemical changes. Using fast-scan cyclic voltammetry to measure electroactive species is the common theme that ties these projects together. This electrochemical technique is the method that we have chosen to either apply to a new animal model for sub-second neurotransmitter release, zebrafish, or in conjunction with photochemistry.

In the 1st chapter we discuss work that we have done to develop caged compounds for use in neurochemical experiments. We discuss work on the synthesis of caged thiols and phenols and how we have probed their photochemical mechanisms. We also discuss work we have done on developing a novel probe to measure electrochemical changes while simultaneously carrying out photochemical reactions.

In the next two chapters we discuss work we have done in zebrafish studying sub-second dopamine release. We have shown that it is possible to measure dopamine release from both whole brain preparations *ex vivo* as well as sagittal and coronal slices. We discuss the pharmacology of this release as well as unique characteristics of the uptake plots. We also examine how different uptake inhibitors effect the kinetics of the dopamine uptake.

Finally we discuss work we have done on the chemotherapy induced changes in zebrafish dopamine release. We look at 2 drugs, 5-FU and carboplatin, and two treatment pathways, habitat water and food. We show that there is a pathway dependent attenuation for both of the drugs studied that is not correlated with apparent changes in uptake. The food delivery pathway was found to have an effect on dopamine release on a much shorter time scale then the habitat water treatment pathway.

Acknowledgments

I want to acknowledge many people who made this all possible. First off my lab mates and Mike for supporting me day by day and helping push me when I needed it to get stuff done when it needed to get done. My friends in grad school also were a great help, they made sure I stayed sane and didn't get too high or too low and I thank them for that. Finally I want to thank my family, my parents and brother and my grandparents and aunts and uncles. Without all of their support I never would have finished all of this.

Table of Contents

Chapter 1: Introduction

1.1 Dopamine: Synthesis, release, and uptake

Dopamine is a monoamine neurotransmitter found in a wide range of vertebrate species including fish, rodents and humans. This neurotransmitter is involved in many neurological processes which include memory and learning [1], reward and addiction[2, 3], and movement[4, 5]. Deficiencies in dopamine neurotransmission have also been observed in many neurological conditions, such as Huntington's Diesease[6-9], Parkinson's Disease[10, 11] , Alzheimer's Disease[12, 13] , multiple sclerosis[14], and Chemotherapy induced cognitive impairment[15].

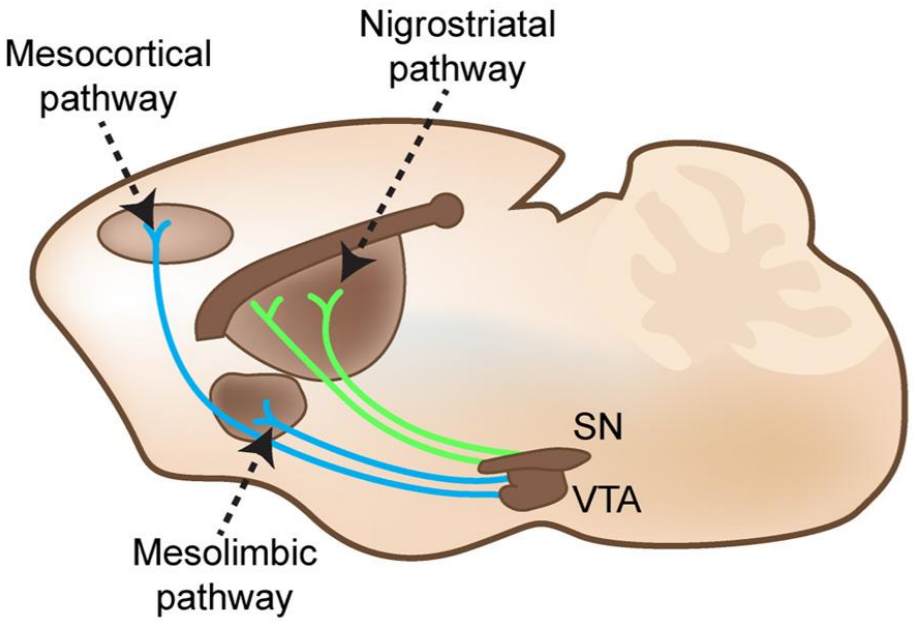

Figure 1: Major dopamine pathways in the adult mouse brain. The Nigrostriatal pathway is green and the mesolimbic and mesocortical pathways are blue. Reproduced with permission from Frontiers in neuroscience [16]

In mammals, the dopaminergic system has major projections that extend from the ventral tegmental and the substantia nigra to the neostriatum, limbic cortex and other limbic structures.[17, 18] The first projection listed is termed the nigrostriatal system and controls movement[19] (Figure

1). These last two projections are termed the mesocortical and mesolimbic systems respectively, and have been implicated in learning, reward and addiction[20, 21](Figure 1).

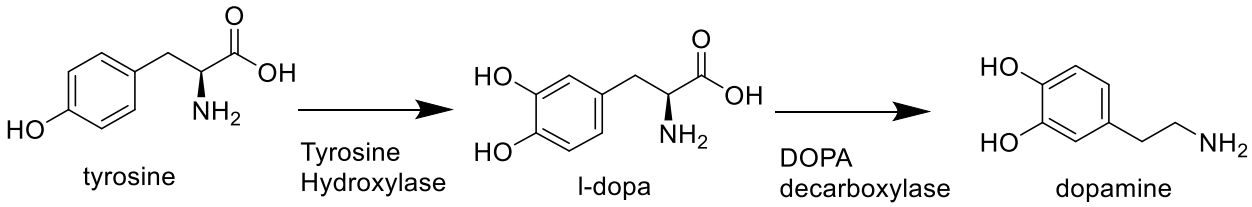

Figure 1: Dopamine synthesis in neurons.

Dopamine is synthesized intracellularly from tyrosine in the pathway shown in Figure 2. The rate-determining step of the entire process is the conversion of tyrosine to L-DOPA by tyrosine hydroxylase. L-DOPA can then be converted to dopamine by DOPA decarboxylase. Once dopamine is synthesized, it is packaged in vesicles within the neuron by the vesicular monoamine transporter 2 (VMAT2) [17], a membrane-bound protein that utilizes a proton gradient to transport monoamines into the vesicles.[22] When an action potential occurs, these vesicles merge with the cell membrane and dopamine is released into the synapse by a process called exocytosis. Dopamine released into the synapse can: 1) be taken up by presynaptic dopamine transporters (DAT), 2) bind to post- or pre-synaptic receptors, or 3) diffuse out of the synapse.

Depending on its location in the brain, dopamine can be metabolized by monoamine oxidase to DOPAC or by catechol-*O*-methyl-transferase (COMT) to 2-methoxytyramine[23] (Figure 3). Both of these products are then converted into homovanillic acid by COMT and MAO, respectively. In rodents and primates, DOPAC and HVA are the two most common metabolites. 3-MT is found in much smaller amounts.[17]

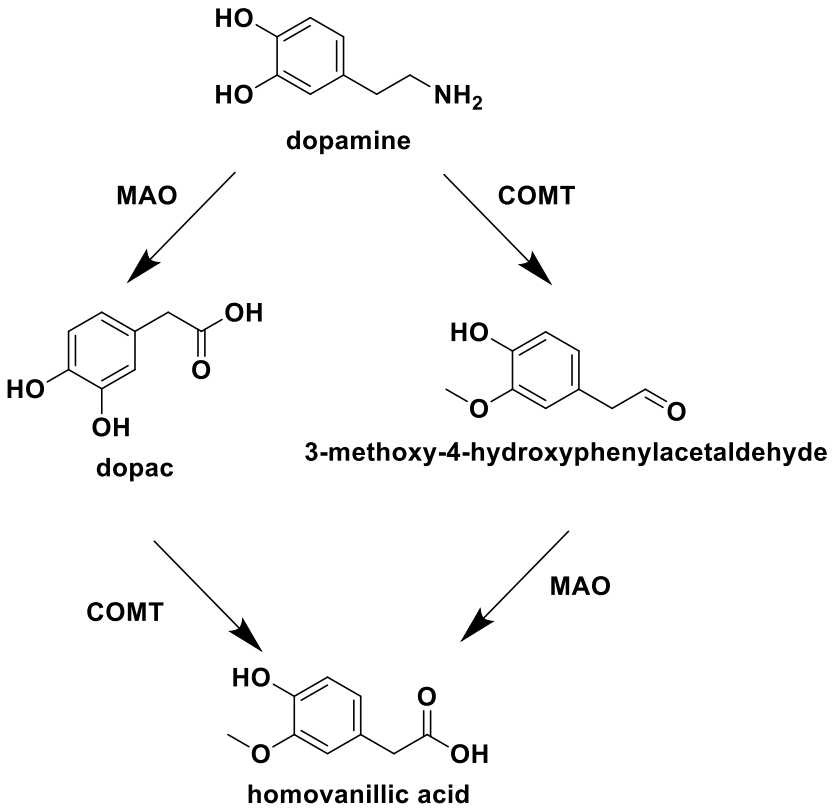

Figure 3: Scheme showing the metabolism of dopamine. Dopamine can be consumed through 2 pathways to be converted into either DOPAC or 3-MT. Both of these compounds would then be converted into HVA.

1.2 Dopamine receptors

Dopamine receptors, which are found both postsynaptically and presynaptcally, are G-protein coupled receptors that activate or inhibit neuronal function by either upregulating or downregulating adenylyl cyclase, respectively[24]. They are organized into two main classes, D_1-like and D_2-like. The D_1-like class includes D_1 and D_5 receptors and activate adenylyl cyclase, while D_2-like receptors include D_2, D_3 and D_4 receptors and inhibit adenylyl cyclase. All types of dopamine receptors are transmembrane receptors that have 7 hydrophobic transmembrane domains[24].

We are primarily interested in presynaptic D2 receptors because they are the dopamine autoreceptors[17]. As mentioned above, an action potential can cause a neuron to release dopamine

and that dopamine can either be reuptaken or interact with post or presynaptic receptors. The D2 autoreceptors are a special class of presynaptic receptors in that when dopamine interacts with them dopamine released is stopped directly by the activation of potassium channels to depolarize the neuron or stopped indirectely by modulating tyrosine hydroxylase and DAT[17, 25]. Drugs that manipulate D2 autoreceptor activation are useful because they modulate the amount of dopamine released: antagonists such as sulpiride[26], raclopride[27], and eticlopride[28] enhance the dopamine signal while agonists such as quinpirole[29] suppress the signal.

1.3 Voltammetry history and theory

The field of voltammetry was started in 1922 with the development of polarography by Jarsolav Heyrovsky. These early methods took hours and only had the ability to take measurements from a linear sweep of voltage. In 1942 Archie Hickling developed the first 3 electrode potentiostat[30], which facilitated measurements obtained by CV and linear sweep voltammetry by allowing a counter electrode to be added to the system. The modern electrochemical cell used in voltammetry experiments has 3 electrodes: the working electrode, the reference electrode, and the counter electrode (Figure 4). For a given measurement cycle, a potential is applied to the working electrode, moving from a holding potential to a switching potential and back to a holding potential over a time scale that is dependent on the scan rate of the experiment. As that potential changes, electroactive species can be oxidized or reduced. This electrochemical process leads to a faradaic current that can be measured. By plotting the current observed vs the potential applied chemical information can be ascertained. These plots are called voltammagrams[31] and are unique to the compound that is oxidized and reduced allowing for chemical identification.

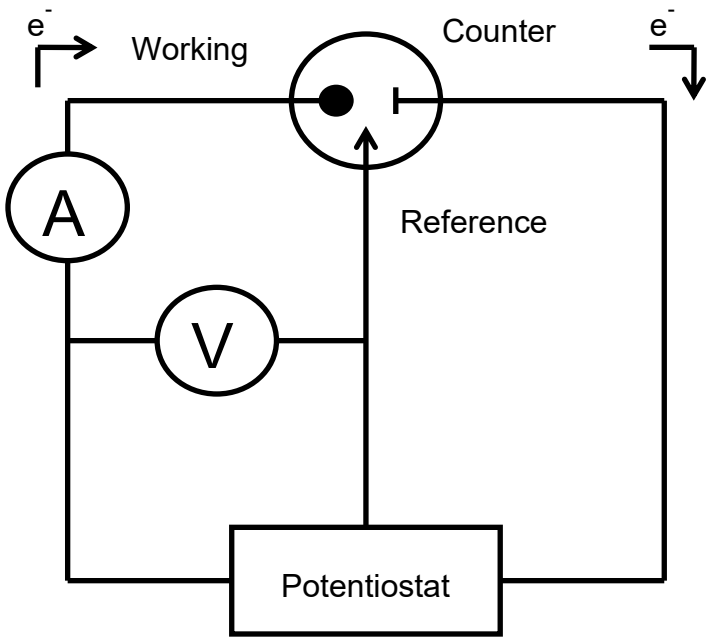

Figure 4: A diagram of a 3-electrode system, The potentiostat is able to isolate the current from from the reference electrode by passing it through the counter electrode.

The potential at a working electrode is obtained by comparison with a reference electrode [31] In reality, a system only needs two electrodes to make measurements, a working electrode and a reference electrode. However, in a 2-electrode setup, the reference electrode is coupled directly with the working electrode to carry out the faradaic reaction. This system makes accurate control of applied potential impractical due to IR drop, a phenomenon in which the potential decreases as current increases, according to Ohm's law ($E = IR$)[32]. In order to mitigate this problem, a mostly inert electrode, known as the counter electrode, is introduced into the system. In the three electrode system, this electrode completes the circuit so current can pass, thereby keeping the reference electrode potential constant.

The reactions our group studies can be described by the Nernst equation (Equation 1) because they are reversible (a reaction where the reduction and oxidation potential are separated by less than 0.058 Volts/n)[31]. This equation describes how the concentration of oxidized and reduced species changes over time as a function of applied potential (E). In Equation 1, E^0 is the

formal reduction potential of the analyte, *R* is the universal gas constant, *n* is the number of electrons per reaction, and *F* is the faraday constant.[31]

$$Equation\ 1: E = E^o + \frac{RT}{nF} * \ln(\frac{[ox]}{[red]})$$

The peak current for a reversible reaction can be described by the Randles-Sevcik equation (Equation 2)[31].

$$Equation\ 2: i_p = (2.69\ x\ 10^5) n^{\frac{3}{2}} A D^{\frac{1}{2}} C \upsilon^{\frac{1}{2}}$$

In this equation, i_p is the peak oxidation current, n is the number of electrons transferred in the reaction, A is the electrode area (cm^2), D is the diffusion coefficient for the molecule of interest (cm^2/s), C is the concentration of the species oxidized (mol/cm^3) and ν is the scan rate (V/s). This equation describes a relationship in which the concentration of the species oxidized is directly related to the scan rate, area of the electrode, and the current measured at the electrode. This means that, as long as the electrode area and scan rate are held constant, the concentration and faradaic current are directly related and can be interconverted. This interconversion allows the measurement of concentrations of electroactive species.

1.4 Electrochemical measurement of neurotransmitters with fast-scan cyclic voltammetry (FSCV)

The electrochemical measurement of neurotransmitters in brain tissue was first published in 1973 by Ralph N Adams and coworkers, who used carbon paste electrodes to measure ascorbic acid by CV [33]. In the early 1980s, independent work by Wightman[34] and Millar[35] resulted in the development of fast-scan cyclic voltammetry (FSCV) at carbon-fiber microelectrodes[36, 37]. In brief, FSCV is a technique in which a triangular potential waveform (-0.4 V to +1.3 V to -0.4 V as used in our laboratory for the detection of dopamine) is applied at a

high scan rate (>100 V/s) [38, 39]. The carbon-fiber microelectrodes used in our laboratory have a diameter of 7 μm and are trimmed to ~50 μm in length (Figure 5).

FSCV has several advantages that make it suitable for neurobiological applications: 1) the small electrode size provides high spatial resolution, thereby allowing specific brain structures to be selected; 2) carbon is biologically inert; 3) the diffusional properties and microelectrodes allow steady state (or quasi steady state) currents to be quickly attained, thereby allowing high temporal resolution measurements; and 4) the small currents measured allow CV measurements to be obtained using a 2-electrode system in highly resistive environments, such as brain tissue[40, 41]. Because the high scan rate generates a large, non-faradaic current, which results from charging of the electric double layer, a background subtraction process is required to reliably identify the faradaic currents produced by the chemical species of interest, such as dopamine. This background subtraction method is illustrated in Figure 6. For a given measurement, a series of CVs is collected at a predetermined application frequency (typically 10 CVs/s) for a pre-determined period of time (typically on the order of 20 s). The average current of 10 CVs obtained when dopamine is not present (we are neglecting basal dopamine levels in this case) is subtracted from the CVs obtained throughout the entire data set. Because the background current at a given scan rate is quite stable, subtraction of this current removes this current and, ideally, leaves all other signals of interest[42]. Because the remaining faradaic signal is directly dependent upon concentration, each electrode can be calibrated in a flow cell against standard solutions to determine concentration.

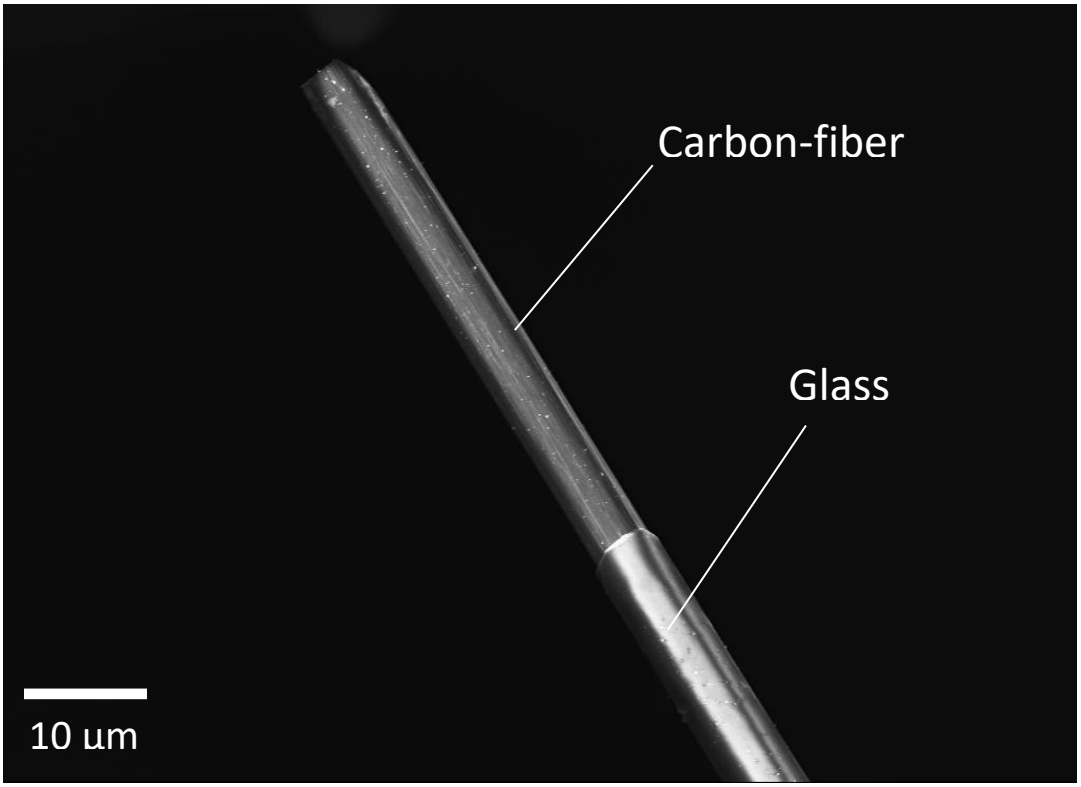

Figure 5: An SEM image of a carbon fiber microelectrode. This image was obtained at KU microscopy and analytical imaging lab.

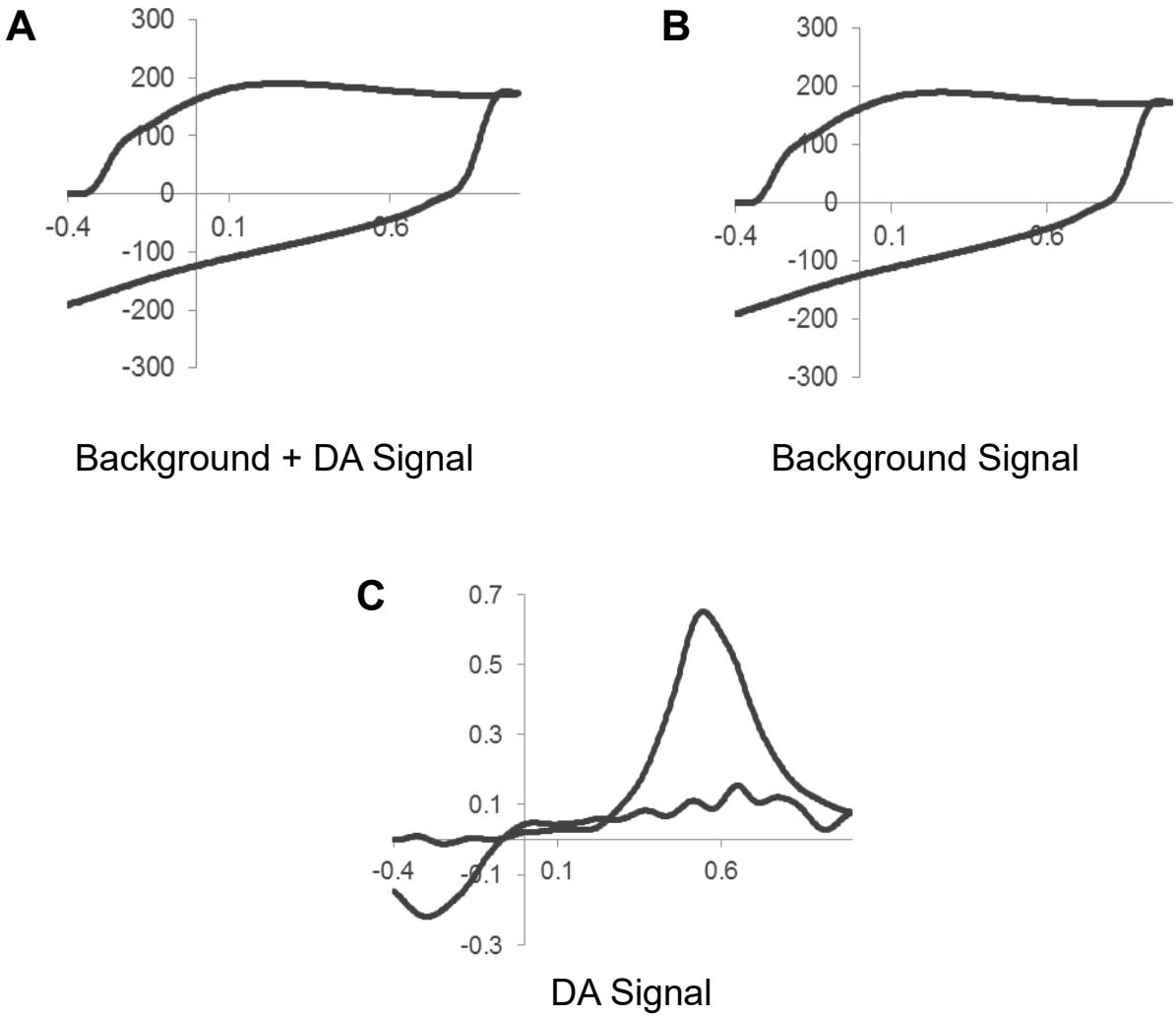

Figure 6: An illustration of the background subtraction process. (A) is the signal from dopamine plus the charging current, (B) is the background current alone taken from scans before the dopamine signal was introduced. (C) Is the signal after B is subtracted from A leaving just the dopamine signal with the indicative dopamine CV.

1.5 Electrochemical measurement of dopamine with FSCV

The compound of interest throughout this work, as mentioned above, is dopamine and here its electrochemistry will be briefly discussed. Dopamine is a monamine that can be oxidized at 0.6 V at a carbon-fiber microelectrode (versus a Ag/AgCl electrode) to dopamine orthoquinone, which can then be reduced back to dopamine at -0.2 V (Figure 7) in a reversible process. This process gives a distinct CV shown in Figure 6 that can be used to identify the

signal. This faradaic oxidation current can then be used to determine the concentration of dopamine, because of the Randles-Sevcik discussed above, by calibration against standard dopamine solutions. In our work, a waveform of -0.4 V to 1.3 V to -0.4 V at 400 V/s, applied every 100 ms, is used to measure dopamine. We selected a switching potential of 1.3 V instead of the standard switching potential of 1.0 V to enhance adsorption of dopamine to the electrode, making it more sensitive.[43] This increase in absorption is caused by an increase in ester and carboxylic acid groups on the carbon surface which can interact with the amine group on dopamine.[44, 45]

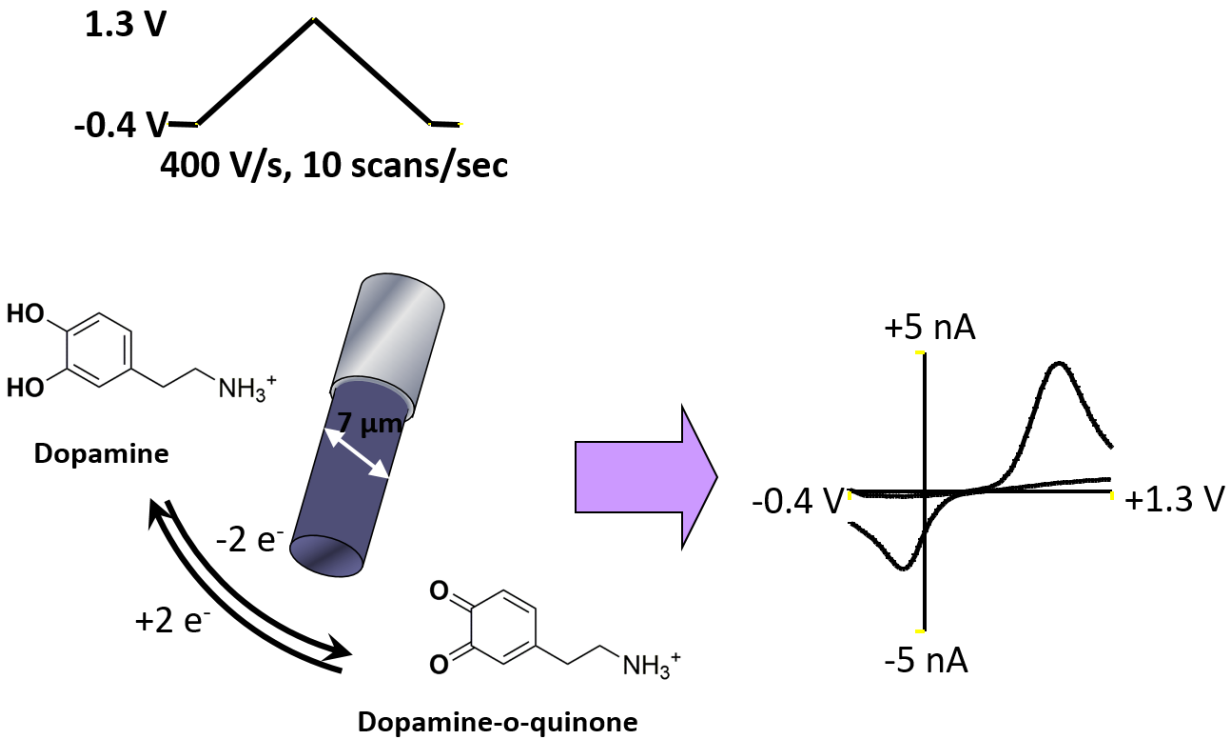

Figure 7: Fast-scan cyclic voltammetry of dopamine. A waveform of -0.4 to 1.3 V and back to -0.4 V at 400 V/s is applied once every ten seconds. As the voltage is scanned toward the positive potential, dopamine is oxidized to dopamine-*o*-quinone. As the potential is scanned back to the negative potential, dopamine-*o*-quinone is reduced to form dopamine. After background subtraction, the measured currents providing the observed CV.

1.6 Zebrafish as model organisms for neurochemical analysis

The use of model organisms is essential to simulate the complex environment of the human brain. Model organisms used range from simple invertebrates such as fruit flies[46, 47] to complex mammalian systems such as mice, rats, and primates[48, 49]. FSCV at carbon fiber microelectrodes in rodents has been used extensively to study dopamine both *in vitro*[6, 15, 50, 51] and *in vivo*[52-55]. Rodents have been used to increase our basic understanding of how neurotransmitter release relates to behavior[50, 51, 54] as well as disorders and diseases including addiction[52, 53], neurodegeneration[6, 55] , Huntington's Disease[6], Parkinson's Disease[55] and Chemotherapy induced cognitive impariment[15].

While rodents are useful model organsims, there are disadvantages to using them 1) the creation of genetically altered mammals is costly and time-consuming; 2) treating rats or mice using injection methods are both difficult and stressful on both the animal and the experimenter.

One of the main goals of our group recently has been the development of zebrafish as a new model for neurochemical studies. Zebrafish, first developed by George Streisinger in the 1970s [56] as a model for development[57], also are a useful model organism for the study of neuronal function because they:

1. are a vertebrate, unlike fruit flies or *C. elegans*, and, therefore, have greater anatomical similarity to humans.
2. have a completely sequenced genome that has ~ 70% similarity to the human genome.[58]
3. can be easily housed in large numbers cheaply and have a short life cycle with a large amount of offspring.
4. can be genetically modified easily unlike rodents[59]

5. possess complex brains of ideal size that can be kept alive in a perfusion chamber away from the body[60], unlike rodents.
6. are easy to treat with pharmacological agents, which often can be given to them by simply adding it to their water habitat[61, 62] as well as food[63].
7. they react to pharmacological agents similarly to how rodents react.[64]

1.6.1 Zebrafish vs rodent neuroanatomy

Extensive staining studies have been used to elucidate the zebrafish's neuroanatomy. These studies have shown that dopamine, norepinephrine, histamine, and serotonin are all present in the zebrafish central nervous system[65]. The catecholamine system, and more specifically the dopamine system, retains many of the same proteins. Zebrafish and rodents both have tyrosine hydroxylase (although zebrafish have 2 distinct versions of the protein[66]), MAO (although zebrafish only have one version of MAO)[65, 67, 68], COMT, and all of the families of dopamine receptors (though zebrafish have 8 whereas rodents have 5)[65]. The dopaminergic system in zebrafish has been studied using histology. It has been shown that one of the main projections is an ascending system from the diecephelon to the ventral telecephelon [69, 70]. Based on staining studies, it is thought that this system is similar to the mesolimbic system in rodents.

Rink and Wulliman[71] used histochemical staining against tyrosine hydroxylase to show that there were dopaminergic neurons present in the fore brain. These neurons were mainly found in the diencephalon and the telencephalon with projections running from the former to the later. They also noted that because of the evolutionary history of dopaminergic pathways there is a possibility that these neurons are similar to the mesolimbic system in mammals, even though these neurons are not found in the midbrain.

The neuroanatomy of zebrafish has also been studied after application of known neurotoxins with well documented effects in rodents. After larval zebrafish were treated with 1-methyl-4-phenyl-1,2,3,6-tetrahydropyridine (MPTP) and 1-methyl-4-phenylpyridinium (MPP+), Panula et al[72] observed a decreases in tyrosine hydroxylase labeled neurons in the diencephalon. This loss of neurons was associated with decrease in swimming speed. There was also a decreased in total dopamine content as measured by HPLC. Similar loss of diencephalic dopamine neurons and decrease in movement after MPTP treatment have also been reported by Lam et al.[73] and Bretaud et al. [74] Since there was a decrease in movement coupled with the neuronal death in these studies it has been proposed that part of the diencephalon is similar to the rodent substantia nigra.

1.7 Previous studies in Zebrafish

Neurotransmitter levels in zebrafish have been previously measured directly by both real time electrochemical measurements as well as by HPLC methods. Zebrafish neurotransmission has also been studied using electrophysiological methods. This section will briefly review these studies, with an emphasis on studies drawing comparisons between zebrafish and mammals in order to try to make the argument that zebrafish are a viable model to study disorders that effect humans.

1.7.1 HPLC measurements in zebrafish

Robert Gerlai's group has used HPLC coupled to electrochemical detection to measure the amount of dopamine and serotonin as well their metabolites DOPAC and 5-HIAA. These measurements were conducted both post and pretreatment with alcohol[75, 76]. Gerlai and coworkers showed that as the adult fish were treated with increasing amounts of ethanol the amount of all the compounds studied increased.[75] They also showed that when the embryos were

treated with ethanol the amount of the compounds studied decreased. [76] His group has also showed that the strain of fish effects how the attenuation of neurotransmitter content after treatment of the embryo with alcohol presents itself, with some strains mitigating the effects[77].

Panula and coworkers showed dopamine content was attenuated after adult fish were injected with the catecholaminergic toxins 6-hydroxydopamine (6-OHDA) and 1-methyl-4-phenyl-1,2,3,6-tetrahydropyrdine (MPTP).[78] [72]The amount of dopamine was reduced to about 40 % of the saline value after 1 week of MPTP treatment and to 59% of control values after 6-OHDA treatment.[78] They also showed that the zebrafish locomotion was decreased for both treatments, something that would also be expected for rodents treated with these same drugs.

I have selected these two specific examples to illustrate how zebrafish have been used to study important process such as fetal alcohol syndrome and neurodegeneration. Zebrafish have also been studied with HPLC methods to study cocaine withdrawal [79] , stress [80], and the maturation of zebrafish behavior[81].

1.7.2 Electrophysiological measurements in zebrafish

Electrophysiology has been applied to zebrafish in order to study the neuronal firing associated and correlate it with observed behavioral effects. Work has been done by Baier and coworkers showing that zebrafish react to pentylenetetrazole similarly to what is observed in rodents with a large increase in movement that is correlated with an increase in seizure like neuronal firing in the optic tectum[82]. They also showed that anticonvulsant agents (valproic acid and diazepam) reduced the amount of seizure like neuron firing, just as would be expected in mammals.

Douglass *et al* studied induced escape behavior in zebrafish and correlated the behavior with electrophysiology studies to try to elucidate what neuronal families were firing[83]. In order to

do these studies they expressed channelrhodopsin-2 in neurons that are known to be involved in these escape movements. They then showed, in larvae zebrafish, that there was no basal firing of these modified cells, that there was firing of the cells when light was introduced and that this firing was related to the observed escape behavior. Electrophisology has also been used to study photochemically induced neuron silencing[84], Dravet syndrome[85, 86] and Mauthner cells[87]. While electrophysiology can be used to determine when cells are firing it can't provide specific information about neurotransmitter release like FSCV is able to.

1.7.3 Real time release measurement in zebrafish

To the best of our knowledge, two other groups have made real time measurements of neurotransmitter release in zebrafish. Jones *et al.* made evoked neurotransmitter release measurements in sagittal zebrafish slices[88] with FSCV after the application of both chemical and electrical stimulation from the brain slice. They demonstrated that dopamine was one of the components of a mixture that included pH change and histamine. This was determined by using GBR 12909 and cocaine to pharmacologically manipulate the dopamine portion of the signal as well as by using principal component analysis to isolate the dopamine signal from the other components. They determined that the $[DA]_{max}$ was about 100 nM after stimulation.

Shang *et al* were able to measure real time dopamine release using amperometry in larval zebrafish after scent stimulatoin[89]. They showed that the signal observed was dopamine using pharmacological manipulations and staining studies. They applied nomifensine and observed both an increase in the signal as well as a decline in uptake. They also used calcium imaging in conjunction with staining to show dopamine neurons were firing after the application of their stimulation.

As can be seen by the brief review of current work done in the zebrafish brain, it is already a model that has been shown to be able to model disease states such as alcoholism and epilepsy as well as neurodegeneration. It is also clear that real time measurements are possible using electrochemistry, as has been demonstrated in both adult brain slices and larvae. In this dissertation we discuss work that expands on this previous work by moving into real time measurements in whole intact adult zebrafish brains *ex vivo*[60] as well as work we have done to expand zebrafish as a model of chemotherapy induced cognitive impairment.

1.8 Outline of chapters

Chapter 2 discusses work I have done towards the development and application of photochemical probes to study biological systems. It includes work we have done with both phenol and thiol moieties and our attempts to develop new and biologically relevant molecules that contain those previously mentioned moieites. I also discuss work that has been done towards the development of a device to simultaneously apply, uncage and measure these compounds in tissue samples.

Chapter 3 discusses the initial development of methods to measure dopamine from zebrafish whole brains *ex vivo* done by Mimi Shin. It also discusses how the identity of the released neurotransmitter was determined and examines the pharmacology of that signal. Finally, unique characteristics of the release and uptake curves in zebrafish are examined and explained.

Chapter 4 discusses work that has been done examining the effects of chemotherapy treatment, specifically 5-FU and carboplatin, on the neurochemistry of the zebrafish brain. Comparisons are also drawn between this work and the work done by Sam Kaplan and Rachel Ginther in order to demonstrate that the phenomena observed in the zebrafish is similar to what is observed in rodents.

Concluding remarks are provided in Chapter 5.

1.8 References

[1] Aarts, E., van Holstein, M., and Cools, R. (2011) Striatal dopamine and the interface between motivation and cognition, *Frontiers in psychology 2*.

[2] Kelley, A. E., and Berridge, K. C. (2002) The neuroscience of natural rewards: relevance to addictive drugs, *Journal of Neuroscience 22*, 3306-3311.

[3] Oei, N. Y., Rombouts, S. A., Soeter, R. P., van Gerven, J. M., and Both, S. (2012) Dopamine modulates reward system activity during subconscious processing of sexual stimuli, *Neuropsychopharmacology 37*, 1729-1737.

[4] Barnéoud, P., Descombris, E., Aubin, N., and Abrous, D. N. (2000) Evaluation of simple and complex sensorimotor behaviours in rats with a partial lesion of the dopaminergic nigrostriatal system, *European Journal of Neuroscience 12*, 322-336.

[5] Cousins, M., and Salamone, J. (1996) Involvement of ventrolateral striatal dopamine in movement initiation and execution: a microdialysis and behavioral investigation, *Neuroscience 70*, 849-859.

[6] Johnson, M. A., Rajan, V., Miller, C. E., and Wightman, R. M. (2006) Dopamine release is severely compromised in the R6/2 mouse model of Huntington's disease, *Journal of neurochemistry 97*, 737-746.

[7] Ortiz, A. N., Kurth, B. J., Osterhaus, G. L., and Johnson, M. A. (2010) Dysregulation of intracellular dopamine stores revealed in the R6/2 mouse striatum, *Journal of neurochemistry 112*, 755-761.

[8] Ortiz, A. N., Kurth, B. J., Osterhaus, G. L., and Johnson, M. A. (2011) Impaired dopamine release and uptake in R6/1 Huntington's disease model mice, *Neuroscience letters 492*, 11-14.

[9] Ortiz, A. N., Osterhaus, G. L., Lauderdale, K., Mahoney, L., Fowler, S. C., von Hoersten, S., Riess, O., and Johnson, M. A. (2012) Motor function and dopamine release measurements in transgenic Huntington's disease model rats, *Brain Res. 1450*, 148-156.

[10] Sitte, H. H., Pifl, C., Rajput, A. H., Hörtnagl, H., Tong, J., Lloyd, G. K., Kish, S. J., and Hornykiewicz, O. (2017) Dopamine and noradrenaline, but not serotonin, in the human claustrum are greatly reduced in patients with Parkinson's disease: possible functional implications, *European Journal of Neuroscience 45*, 192-197.

[11] Isaias, I. U., Trujillo, P., Summers, P., Marotta, G., Mainardi, L., Pezzoli, G., Zecca, L., and Costa, A. (2016) Neuromelanin Imaging and Dopaminergic Loss in Parkinson's Disease, *Frontiers in aging neuroscience 8*.

[12] Moreno-Castilla, P., Rodriguez-Duran, L. F., Guzman-Ramos, K., Barcenas-Femat, A., Escobar, M. L., and Bermudez-Rattoni, F. (2016) Dopaminergic neurotransmission dysfunction induced by amyloid-beta transforms cortical long-term potentiation into long-term depression and produces memory impairment, *Neurobiology of aging 41*, 187-199.

[13] Kemppainen, S., Lindholm, P., Galli, E., Lahtinen, H. M., Koivisto, H., Hamalainen, E., Saarma, M., and Tanila, H. (2015) Cerebral dopamine neurotrophic factor improves long-term memory in APP/PS1 transgenic mice modeling Alzheimer's disease as well as in wild-type mice, *Behav Brain Res 291*, 1-11.

[14] Melnikov, M., Belousova, O., Murugin, V., Pashenkov capital Em, C., and Boysmall ka, C. o. C. A. (2016) The role of dopamine in modulation of Th-17 immune response in multiple sclerosis, *Journal of neuroimmunology 292*, 97-101.

[15] Kaplan, S. V., Limbocker, R. A., Gehringer, R. C., Divis, J. L., Osterhaus, G. L., Newby, M. D., Sofis, M. J., Jarmolowicz, D. P., Newman, B. D., Mathews, T. A., and Johnson, M. A. (2016) Impaired Brain Dopamine and Serotonin Release and Uptake in Wistar Rats Following Treatment with Carboplatin, *ACS Chem. Neurosci. 7*, 689-699.

[16] Money, K., and Stanwood, G. (2013) Developmental origins of brain disorders: roles for dopamine, *Frontiers in cellular neuroscience 7*.

[17] Cooper, J. R., Bloom, F. E., and Roth, R. H. (2003) *The biochemical basis of neuropharmacology*, Oxford University Press.

[18] Björklund, A., and Dunnett, S. B. (2007) Dopamine neuron systems in the brain: an update, *Trends in neurosciences 30*, 194-202.

[19] Deumens, R., Blokland, A., and Prickaerts, J. (2002) Modeling Parkinson's disease in rats: an evaluation of 6-OHDA lesions of the nigrostriatal pathway, *Experimental neurology 175*, 303-317.

[20] Nestler, E. J., and Carlezon, W. A. (2006) The mesolimbic dopamine reward circuit in depression, *Biological psychiatry 59*, 1151-1159.

[21] Tzschentke, T. (2001) Pharmacology and behavioral pharmacology of the mesocortical dopamine system, *Progress in neurobiology 63*, 241-320.

[22] Wimalasena, K. (2011) Vesicular Monoamine Transporters: Structure-Function, Pharmacology, and Medicinal Chemistry, *Medicinal research reviews 31*, 483-519.

[23] Smythies, J., and Galzigna, L. (1998) The oxidative metabolism of catecholamines in the brain: a review, *Biochimica et Biophysica Acta (BBA) - General Subjects 1380*, 159-162.

[24] Brady, S., Siegel, G., Albers, R. W., and Price, D. (2005) *Basic Neurochemistry: Molecular, Cellular and Medical Aspects*, Elsevier Science.

[25] Ford, C. P. (2014) The role of D2-autoreceptors in regulating dopamine neuron activity and transmission, *Neuroscience 282*, 13-22.

[26] O'connor, S., and Brown, R. (1982) The pharmacology of sulpiride—a dopamine receptor antagonist, *General Pharmacology: The Vascular System 13*, 185-193.

[27] Köhler, C., Hall, H., Ögren, S.-O., and Gawell, L. (1985) Specific in vitro and in vivo binding of 3H-raclopride a potent substituted benzamide drug with high affinity for dopamine D-2 receptors in the rat brain, *Biochemical pharmacology 34*, 2251-2259.

[28] Martelle, J. L., and Nader, M. A. (2008) A Review of the Discovery, Pharmacological Characterization, and Behavioral Effects of the Dopamine D2-Like Receptor Antagonist Eticlopride, *CNS neuroscience & therapeutics 14*, 248-262.

[29] Eilam, D., and Szechtman, H. (1989) Biphasic effect of D-2 agonist quinpirole on locomotion and movements, *European journal of pharmacology 161*, 151-157.

[30] Hickling, A. (1942) Studies in electrode polarisation. Part IV.—The automatic control of the potential of a working electrode, *Transactions of the Faraday Society 38*, 27-33.

[31] Kissinger, P. T., and Heineman, W. R. (1983) Cyclic voltammetry, *Journal of Chemical Education 60*, 702.

[32] Hayes, M., Kuhn, A., and Patefield, W. (1977) Techniques for the determination of ohmic drop in half-cells and full cells: A review, *Journal of Power Sources 2*, 121-136.

[33] Kissinger, P. T., Hart, J. B., and Adams, R. N. (1973) Voltammetry in brain tissue — a new neurophysiological measurement, *Brain Research 55*, 209-213.

[34] Stamford, J. A., Kruk, Z. L., Millar, J., and Wightman, R. M. (1984) Striatal dopamine uptake in the rat: in vivo analysis by fast cyclic voltammetry, *Neuroscience letters 51*, 133-138.

[35] Armstrong-James, M., and Millar, J. (1984) High-speed cyclic voltammetry and unit recording with carbon fibre microelectrodes, *Measurement of Neurotransmitter Release in vivo*, 209-226.

[36] Ponchon, J. L., Cespuglio, R., Gonon, F., Jouvet, M., and Pujol, J. F. (1979) Normal pulse polarography with carbon fiber electrodes for in vitro and in vivo determination of catecholamines, *Analytical Chemistry 51*, 1483-1486.

[37] Dayton, M., Brown, J., Stutts, K., and Wightman, R. (1980) Faradaic electrochemistry at microvoltammetric electrodes, *Analytical Chemistry 52*, 946-950.

[38] Stamford, J. A., Kruk, Z. L., and Millar, J. (1986) Sub-second striatal dopamine release measured by in vivo voltammetry, *Brain research 381*, 351-355.

[39] Millar, J., Stamford, J. A., Kruk, Z. L., and Wightman, R. M. (1985) Electrochemical, pharmacological and electrophysiological evidence of rapid dopamine release and removal in the rat caudate nucleus following electrical stimulation of the median forebrain bundle, *European journal of pharmacology 109*, 341-348.

[40] Fleischmann, M., and Pons, S. (1987) The behavior of microelectrodes, *Analytical Chemistry 59*, 1391A-1399A.

[41] Kissinger, P., and Heineman, W. R. (1996) *Laboratory Techniques in Electroanalytical Chemistry, revised and expanded*, CRC press.

[42] Venton, B. J., and Wightman, R. M. (2003) Psychoanalytical electrochemistry: dopamine and behavior, ACS Publications.

[43] Heien, M. L., Phillips, P. E., Stuber, G. D., Seipel, A. T., and Wightman, R. M. (2003) Overoxidation of carbon-fiber microelectrodes enhances dopamine adsorption and increases sensitivity, *Analyst 128*, 1413-1419.

[44] Yue, Z., Jiang, W., Wang, L., Gardner, S., and Pittman, C. U. (1999) Surface characterization of electrochemically oxidized carbon fibers, *Carbon 37*, 1785-1796.

[45] Bath, B. D., Michael, D. J., Trafton, B. J., Joseph, J. D., Runnels, P. L., and Wightman, R. M. (2000) Subsecond adsorption and desorption of dopamine at carbon-fiber microelectrodes, *Analytical chemistry 72*, 5994-6002.

[46] Vickrey, T. L., Condron, B., and Venton, B. J. (2009) Detection of endogenous dopamine changes in Drosophila melanogaster using fast-scan cyclic voltammetry, *Analytical chemistry 81*, 9306-9313.

[47] Makos, M. A., Han, K.-A., Heien, M. L., and Ewing, A. G. (2009) Using in vivo electrochemistry to study the physiological effects of cocaine and other stimulants on the Drosophila melanogaster dopamine transporter, *ACS chemical neuroscience 1*, 74-83.

[48] Weerts, E. M., Fantegrossi, W. E., and Goodwin, A. K. (2007) The value of nonhuman primates in drug abuse research, *Experimental and clinical psychopharmacology 15*, 309.

[49] Chaumette, T., Lebouvier, T., Aubert, P., Lardeux, B., Qin, C., Li, Q., Accary, D., Bezard, E., Bruley des Varannes, S., and Derkinderen, P. (2009) Neurochemical plasticity in the enteric nervous system of a primate animal model of experimental Parkinsonism, *Neurogastroenterology & Motility 21*, 215-222.

[50] John, C. E., and Jones, S. R. (2007) Voltammetric characterization of the effect of monoamine uptake inhibitors and releasers on dopamine and serotonin uptake in mouse caudate-putamen and substantia nigra slices, *Neuropharmacology 52*, 1596-1605.

[51] Ferris, M. J., Calipari, E. S., Yorgason, J. T., and Jones, S. R. (2013) Examining the complex regulation and drug-induced plasticity of dopamine release and uptake using voltammetry in brain slices, *ACS chemical neuroscience 4*, 693-703.

[52] Robinson, D. L., and Wightman, R. M. (2007) Rapid dopamine release in freely moving rats.

[53] Covey, D. P., Roitman, M. F., and Garris, P. A. (2014) Illicit dopamine transients: reconciling actions of abused drugs, *Trends in neurosciences 37*, 200-210.

[54] Flagel, S. B., Clark, J. J., Robinson, T. E., Mayo, L., Czuj, A., Willuhn, I., Akers, C. A., Clinton, S. M., Phillips, P. E., and Akil, H. (2011) A selective role for dopamine in stimulus-reward learning, *Nature 469*, 53-57.

[55] Lohr, K. M., Bernstein, A. I., Stout, K. A., Dunn, A. R., Lazo, C. R., Alter, S. P., Wang, M., Li, Y., Fan, X., and Hess, E. J. (2014) Increased vesicular monoamine transporter enhances dopamine release and opposes Parkinson disease-related neurodegeneration in vivo, *Proceedings of the National Academy of Sciences 111*, 9977-9982.

[56] Grunwald, D. J., and Eisen, J. S. (2002) Headwaters of the zebrafish—emergence of a new model vertebrate, *Nature reviews genetics 3*, 717-724.

[57] Streisinger, G., Walker, C., Dower, N., Knauber, D., and Singer, F. (1981) Production of clones of homozygous diploid zebra fish (Brachydanio rerio), *Nature 291*, 293-296.

[58] Howe, K., and Clark, M. D., and Torroja, C. F., and Torrance, J., and Berthelot, C., and Muffato, M., and Collins, J. E., and Humphray, S., and McLaren, K., and Matthews, L.,

and McLaren, S., and Sealy, I., and Caccamo, M., and Churcher, C., and Scott, C., and Barrett, J. C., and Koch, R., and Rauch, G.-J., and White, S., and Chow, W., and Kilian, B., and Quintais, L. T., and Guerra-Assuncao, J. A., and Zhou, Y., and Gu, Y., and Yen, J., and Vogel, J.-H., and Eyre, T., and Redmond, S., and Banerjee, R., and Chi, J., and Fu, B., and Langley, E., and Maguire, S. F., and Laird, G. K., and Lloyd, D., and Kenyon, E., and Donaldson, S., and Sehra, H., and Almeida-King, J., and Loveland, J., and Trevanion, S., and Jones, M., and Quail, M., and Willey, D., and Hunt, A., and Burton, J., and Sims, S., and McLay, K., and Plumb, B., and Davis, J., and Clee, C., and Oliver, K., and Clark, R., and Riddle, C., and Eliott, D., and Threadgold, G., and Harden, G., and Ware, D., and Mortimer, B., and Kerry, G., and Heath, P., and Phillimore, B., and Tracey, A., and Corby, N., and Dunn, M., and Johnson, C., and Wood, J., and Clark, S., and Pelan, S., and Griffiths, G., and Smith, M., and Glithero, R., and Howden, P., and Barker, N., and Stevens, C., and Harley, J., and Holt, K., and Panagiotidis, G., and Lovell, J., and Beasley, H., and Henderson, C., and Gordon, D., and Auger, K., and Wright, D., and Collins, J., and Raisen, C., and Dyer, L., and Leung, K., and Robertson, L., and Ambridge, K., and Leongamornlert, D., and McGuire, S., and Gilderthorp, R., and Griffiths, C., and Manthravadi, D., and Nichol, S., and Barker, G., and Whitehead, S., and Kay, M., and Brown, J., and Murnane, C., and Gray, E., and Humphries, M., and Sycamore, N., and Barker, D., and Saunders, D., and Wallis, J., and Babbage, A., and Hammond, S., and Mashreghi-Mohammadi, M., and Barr, L., and Martin, S., and Wray, P., and Ellington, A., and Matthews, N., and Ellwood, M., and Woodmansey, R., and Clark, G., and Cooper, J., and Tromans, A., and Grafham, D., and Skuce, C., and Pandian, R., and Andrews, R., and Harrison, E., and Kimberley, A., and Garnett, J., and

Fosker, N., and Hall, R., and Garner, P., and Kelly, D., and Bird, C., and Palmer, S., and Gehring, I., and Berger, A., and Dooley, C. M., and Ersan-Urun, Z., and Eser, C., and Geiger, H., and Geisler, M., and Karotki, L., and Kirn, A., and Konantz, J., and Konantz, M., and Oberlander, M., and Rudolph-Geiger, S., and Teucke, M., and Osoegawa, K., and Zhu, B., and Rapp, A., and Widaa, S., and Langford, C., and Yang, F., and Carter, N. P., and Harrow, J., and Ning, Z., and Herrero, J., and Searle, S. M. J., and Enright, A., and Geisler, R., and Plasterk, R. H. A., and Lee, C., and Westerfield, M., and de Jong, P. J., and Zon, L. I., and Postlethwait, J. H., and Nusslein-Volhard, C., and Hubbard, T. J. P., and Crollius, H. R., and Rogers, J., and Stemple, D. L. (2013) The zebrafish reference genome sequence and its relationship to the human genome, *Nature 496*, 498-503.

[59] Lieschke, G. J., and Currie, P. D. (2007) Animal models of human disease: zebrafish swim into view, *Nature Reviews Genetics 8*, 353-367.

[60] Shin, M., Field, T. M., Stucky, C. S., Furgurson, M. N., and Johnson, M. A. (2017) Ex Vivo Measurement of Electrically Evoked Dopamine Release in Zebrafish Whole Brain, *ACS Chemical Neuroscience*.

[61] Zon, L. I., and Peterson, R. T. (2005) In vivo drug discovery in the zebrafish, *Nature reviews Drug discovery 4*, 35-44.

[62] Gerlai, R., Lahav, M., Guo, S., and Rosenthal, A. (2000) Drinks like a fish: zebra fish (Danio rerio) as a behavior genetic model to study alcohol effects, *Pharmacology biochemistry and behavior 67*, 773-782.

[63] Sterling, M., Karatayev, O., Chang, G.-Q., Algava, D., and Leibowitz, S. (2015) Model of voluntary ethanol intake in zebrafish: effect on behavior and hypothalamic orexigenic peptides, *Behavioural brain research 278*, 29-39.

[64] Kalueff, A. V., Stewart, A. M., and Gerlai, R. (2014) Zebrafish as an emerging model for studying complex brain disorders, *Trends in pharmacological sciences 35*, 63-75.

[65] Panula, P., Chen, Y.-C., Priyadarshini, M., Kudo, H., Semenova, S., Sundvik, M., and Sallinen, V. (2010) The comparative neuroanatomy and neurochemistry of zebrafish CNS systems of relevance to human neuropsychiatric diseases, *Neurobiology of disease 40*, 46-57.

[66] Yamamoto, K., Ruuskanen, J. O., Wullimann, M. F., and Vernier, P. (2010) Two tyrosine hydroxylase genes in vertebrates: new dopaminergic territories revealed in the zebrafish brain, *Molecular and Cellular Neuroscience 43*, 394-402.

[67] Anichtchik, O., Sallinen, V., Peitsaro, N., and Panula, P. (2006) Distinct structure and activity of monoamine oxidase in the brain of zebrafish (Danio rerio), *Journal of Comparative Neurology 498*, 593-610.

[68] Aldeco, M., Arslan, B. K., and Edmondson, D. E. (2011) Catalytic and inhibitor binding properties of zebrafish monoamine oxidase (zMAO): comparisons with human MAO A and MAO B, *Comparative Biochemistry and Physiology Part B: Biochemistry and Molecular Biology 159*, 78-83.

[69] Rink, E., and Wullimann, M. F. (2001) The teleostean (zebrafish) dopaminergic system ascending to the subpallium (striatum) is located in the basal diencephalon (posterior tuberculum), *Brain research 889*, 316-330.

[70] Rink, E., and Wullimann, M. F. (2004) Connections of the ventral telencephalon (subpallium) in the zebrafish (Danio rerio), *Brain Res 1011*, 206-220.

[71] Rink, E., and Wullimann, M. F. (2001) The teleostean (zebrafish) dopaminergic system ascending to the subpallium (striatum) is located in the basal diencephalon (posterior tuberculum), *Brain Res. 889*, 316-330.

[72] Sallinen, V., Torkko, V., Sundvik, M., Reenilä, I., Khrustalyov, D., Kaslin, J., and Panula, P. (2009) MPTP and MPP+ target specific aminergic cell populations in larval zebrafish, *Journal of Neurochemistry 108*, 719-731.

[73] Lam, C. S., Korzh, V., and Strahle, U. (2005) Zebrafish embryos are susceptible to the dopaminergic neurotoxin MPTP, *European Journal of Neuroscience 21*, 1758-1762.

[74] Bretaud, S., Lee, S., and Guo, S. (2004) Sensitivity of zebrafish to environmental toxins implicated in Parkinson's disease, *Neurotoxicology and teratology 26*, 857-864.

[75] Chatterjee, D., and Gerlai, R. (2009) High precision liquid chromatography analysis of dopaminergic and serotoninergic responses to acute alcohol exposure in zebrafish, *Behavioural brain research 200*, 208-213.

[76] Buske, C., and Gerlai, R. (2011) Early embryonic ethanol exposure impairs shoaling and the dopaminergic and serotoninergic systems in adult zebrafish, *Neurotoxicology and teratology 33*, 698-707.

[77] Mahabir, S., Chatterjee, D., and Gerlai, R. (2014) Strain dependent neurochemical changes induced by embryonic alcohol exposure in zebrafish, *Neurotoxicology and teratology 41*, 1-7.

[78] Anichtchik, O. V., Kaslin, J., Peitsaro, N., Scheinin, M., and Panula, P. (2004) Neurochemical and behavioural changes in zebrafish Danio rerio after systemic administration of 6-hydroxydopamine and 1-methyl-4-phenyl-1, 2, 3, 6-tetrahydropyridine, *Journal of neurochemistry 88*, 443-453.

[79] Patiño, M. A. L., Yu, L., Yamamoto, B. K., and Zhdanova, I. V. (2008) Gender differences in zebrafish responses to cocaine withdrawal, *Physiology & behavior 95*, 36-47.

[80] Tran, S., Chatterjee, D., and Gerlai, R. (2014) Acute net stressor increases whole-body cortisol levels without altering whole-brain monoamines in zebrafish, *Behavioral neuroscience 128*, 621.

[81] Mahabir, S., Chatterjee, D., Buske, C., and Gerlai, R. (2013) Maturation of shoaling in two zebrafish strains: a behavioral and neurochemical analysis, *Behavioural brain research 247*, 1-8.

[82] Baraban, S., Taylor, M., Castro, P., and Baier, H. (2005) Pentylenetetrazole induced changes in zebrafish behavior, neural activity and c-fos expression, *Neuroscience 131*, 759-768.

[83] Douglass, A. D., Kraves, S., Deisseroth, K., Schier, A. F., and Engert, F. (2008) Escape behavior elicited by single, channelrhodopsin-2-evoked spikes in zebrafish somatosensory neurons, *Current Biology 18*, 1133-1137.

[84] Arrenberg, A. B., Del Bene, F., and Baier, H. (2009) Optical control of zebrafish behavior with halorhodopsin, *Proceedings of the National Academy of Sciences 106*, 17968-17973.

[85] Baraban, S. C., Dinday, M. T., and Hortopan, G. A. (2013) Drug screening in Scn1a zebrafish mutant identifies clemizole as a potential Dravet syndrome treatment, *Nature communications 4*.

[86] Baraban, S. C. (2013) Forebrain electrophysiological recording in larval zebrafish, *Journal of visualized experiments: JoVE*.

[87] Hatta, K., and Korn, H. (1998) Physiological properties of the Mauthner system in the adult zebrafish, *Journal of Comparative Neurology 395*, 493-509.

[88] Jones, L. J., McCutcheon, J. E., Young, A. M., and Norton, W. H. (2015) Neurochemical measurements in the zebrafish brain, *Frontiers in behavioral neuroscience 9*.

[89] Shang, C.-f., Li, X.-q., Yin, C., Liu, B., Wang, Y.-f., Zhou, Z., and Du, J.-l. (2015) Amperometric monitoring of sensory-evoked dopamine release in Awake Larval Zebrafish, *Journal of Neuroscience 35*, 15291-15294.

Chapter 2: Development of photochemical methods for the study of neurochemical processes

Abstract

In this chapter we discuss the synthesis of model compounds to examine the photochemistry of p-hydroxyphenacyl (pHP) protected thiols and phenols. We were able to successfully synthesize a model phenol, pHP-*p*-cyanophenol, that was shown to cleanly undergo deprotection chemistry via the photo-favorskii rearrangement. A pHP protected thiol was also synthesized and was shown to likely undergo an uncaging mechanism involving homolytic cleavage via a radical mechanism. Finally, an optrode that can detect dopamine in both a flow cell and brain slice, as well as direct light to tissue in the vicinity of the electrode, will be discussed.

2.1 Introduction

Caged compounds are molecules that have been chemically protected by a group that can be photochemically removed (an uncaging reaction scheme for the pHP group is shown in Figure 1) [1, 2]. When the uncaging occurs, the protected compound is released (red) and a byproduct of the cage is produced (blue). This photochemical reactivity has led to a great deal of interest in using these compounds for biological applications because of the ability to deprotect the compound of interest in a spatial and temporally resolved way without the introduction of harsh external chemicals to the sample. These properties are highly relevant in biological studies because of the high level of spatial heterogeneity that can be observed in these living systems.

The ideal caged compound for biological studies should satisfy four important criteria: 1) The compound must be rendered biologically inert by the introduction of the photoprotecting group. 2) The compound of interest must be released in high yield while limiting other undesired

products. 3) The group must undergo photolysis with light that does not have sufficient energy to damage the tissue of interest. 4) The byproduct of the photorelease must be biologically inert and not interfere with the photochemical reaction of uncaging [1-3].

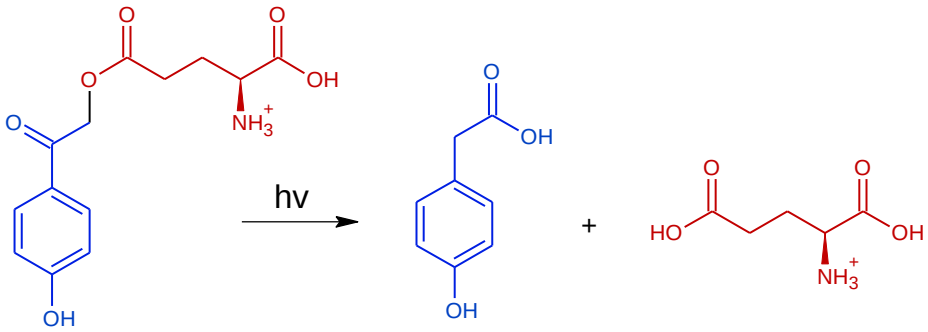

Figure 1: An example uncaging reaction using the p-hydroxyphenacyl (pHP) protecting group. The photoprotecting group in blue on the reactants side is chemically bonded to the leaving group of interest in red. When light (hv) is applied, a photochemical reaction takes place that releases the leaving group in red and produces a byproduct of the caging group in blue on the products side.

2.1.1 Photoprotecting groups

Many photoremovable groups have been used in the field of biological research[4], including *o*-nitorbenzyl[5, 6], benzoins[7, 8],and coumaryl groups[9]. The *o*-nitrobenyl group is one of the most extensively used groups[3] because of its ease of synthesis and high levels of compatibility with functional groups of biological interest. While it is the most common, it does not satisfy all 4 of the requirements outlined above, since the byproduct of the photochemical reaction, 2-nitrosobenzaldehyde, is toxic to biological systems[10]. Therefore it has been necessary for researchers to look for alternative protecting groups that can be used in biological systems. One such protecting group, and the one that will be studied in this chapter, is pHP (Figure 1).

The pHP protecting group was developed by Richard Givens at the University of Kansas in 1996 [11, 12] and has many attributes that make it an attractive alternative to *o*-nitrobenzyl. The photochemical byproduct of pHP is 4-hydroxyphenylacetic acid (4HPAA) , a nontoxic

compound that has a absorption blue shifted away from the parent caged compounds [11] . The pHP protecting group has also been shown to have high quantum yields, rapid rates of photorelease, and high aqueous solubility [13]. This protecting group undergoes a photo-favorskii type rearrangement mechanism, shown in Scheme 1, when the reaction is carried out in solvents containing an aqueous component [14, 15]. All of these factors taken together make pHP a promising group for our chemistry.

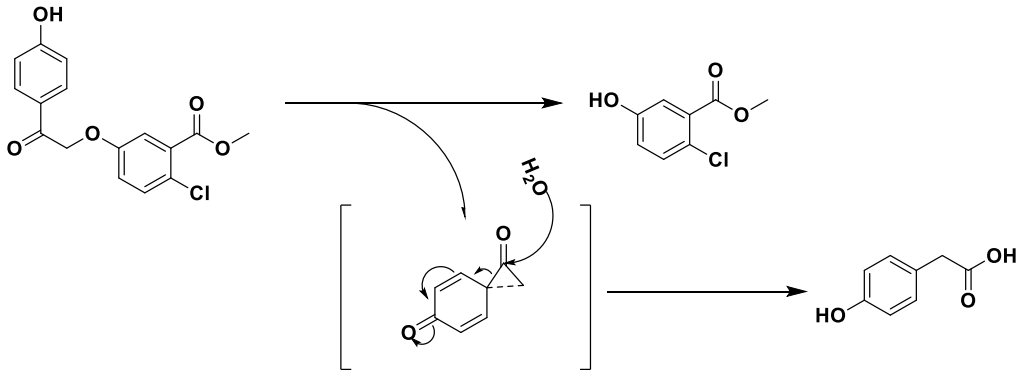

Scheme 1: Photo-favorskii rearrangement of a pHP caged compound

The pHP protecting group has been used successfully with leaving groups that are conjugates of strong acids (amino acids[11], phosphates[16], carboxylates[17]), however, there has been limited success with phenolate based leaving groups[18]. Phenols are an important moiety found in D2 receptor antagonists, such as eticlopride and raclopride. In this work we hoped to expand the application of pHP to phenolate containing compounds in order to modulate these antagonists' chemistry. Another group that we have become interested in are thiols, which are important in glutathione peroxidase chemistry. One of the main goals of this chapter is to show our work in the development of phenol and thiol based pHP compounds with the eventual goal of protecting compounds that are relevant to neurochemical studies. Additionally, we show progress made on developing a probe that can be used *in vivo* to photorelease caged compounds while measuring sub-second neurotransmitter release.

2.1.2 Electrochemical tracking of photochemical reactions

As was mentioned above the byproduct of the photo-favorskii rearrangment of pHP, 4-HPAA, is electrochemically active[19]. This property allows for the electrochemical quantification and tracking of the photochemical release of non-electrochemically active compounds. Our lab has shown this using a pHP protected glutamate. We have also shown that it is possible to measure the uncaging of pHP protected glutamate and the electrically stimulated release of in brain slices (Figure 2).

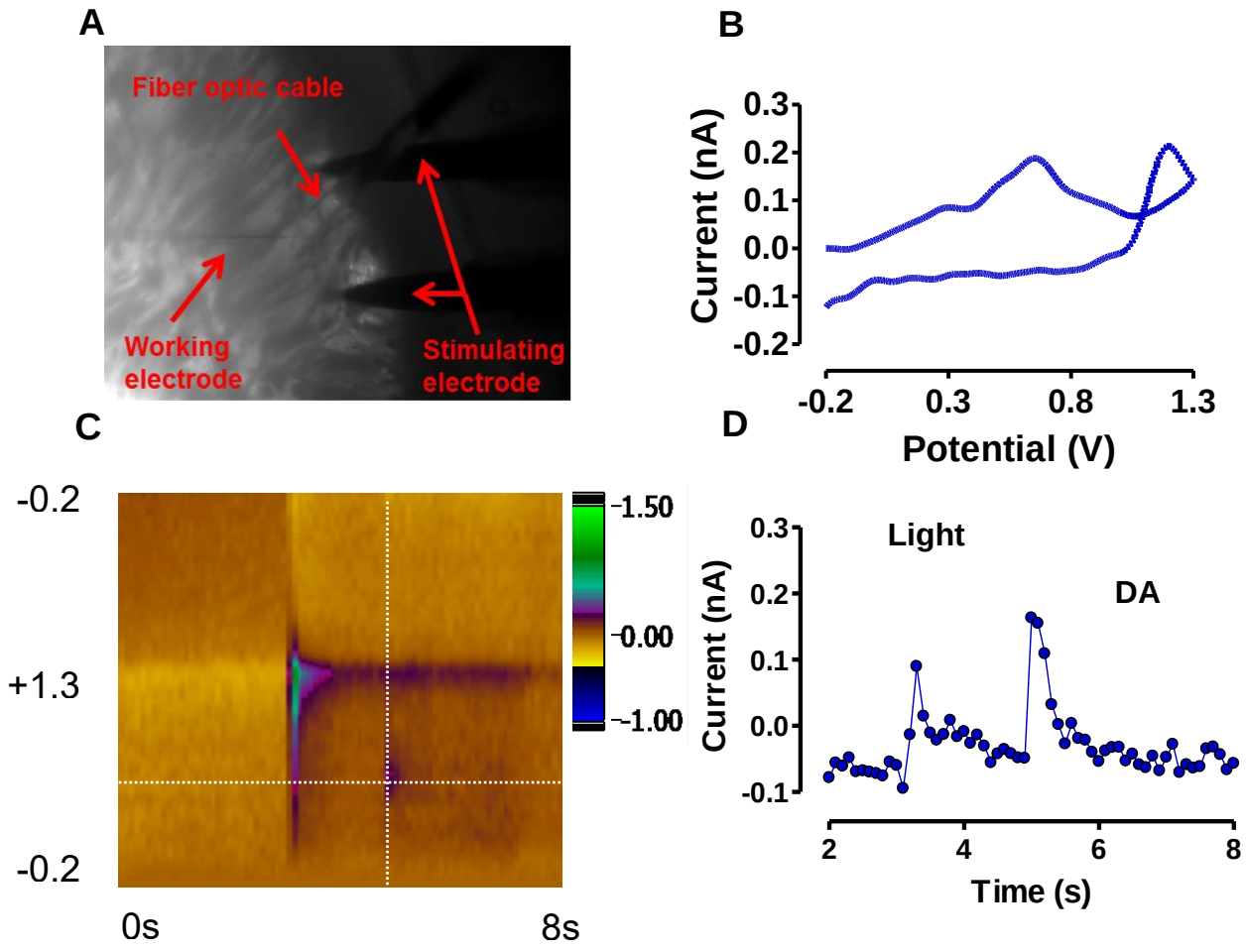

Figure 2: (A) In a brain slice the working electrode is placed in between the biphasic stimulating electrode. A 200 µm fiber optic is placed over the working electrode. (B) The cyclic voltammogram taken at the dotted line is in panel C. It shows characteristics of dopamine with an oxidation peak at 0.6 V and of 4-HPAA with an oxidation peak at 1.3 V. (C) The color plot for a recording. The signal at 3 seconds represents the light artifact and 4-hpaa oxidation at 3 seconds when light is introduced. The signal at 5 seconds where the dotted white lines cross is the electrically stimulated dopamine release. (D) The current vs time plot showing the light artifact at 3 seconds and the dopamine signal at 5 seconds.

One of the main difficulties our lab has discovered when attempting to do these experiments is the difficulty in aligning the fiber optic light guide with the working electrode and the difficulty in minimizing the amount of valuable caged compound that needs to be used in these experiments. In order to try to overcome these difficulties our group has also worked on developing an "optrode" that would contain a working electrode, a fiber optic cable, and a silica

capillary for the injection of the compounds of interest. The reminder of this chapter will be a discussion of our work in trying to develop novel caged compounds and optrode technology.

2.2 Methods

2.2.1 2-bromo-1-(4-hydroxyphenyl)ethan-1-one

A 100mL round bottom flask was charged with 1g *p*-hydroxyacetophenone (7.35mmol) and 3.6g $CuBr_2$ (16.2mmol) and 1:1 $CHCl_3$: ethyl acetate (v:v). This mixture was stirred under reflux for 6 hours or until the solution turned from green to red. This solution was run through a silica plug yielding an amber liquid. Solvent was removed under vacuum. The product was purified by recrystallization in toluene giving a purple crystal. H^1 NMR 400mHz ($CDCl_3$) δ 4.41(2H, s), δ 6.92(2H, d), δ 7.95(2H, d).

2.2.2 4-(2-(4-hydroxyphenyl)-2-oxoethoxy)benzonitrile

A 100 mL round bottom flask was charged with 0.352 K_2CO_3 and 0.303g 4-cyanophenol in THF and was stirred at 4 C. To this mixture a solution of 0.5 g 2-bromo-1-(4-hydroxyphenyl)ethan-1-one in THF was added dropwise over 1 hour. After this addition, the reacting mixture was allowed to return to rt and stirred for an additional 24 hours. The solvent was removed under vacuum to yield a crude solid. The product was purified via flash chromatography with 3:1 hexanes: ethyl acetate. Product was a fine white powder. Yield-23%. H^1 NMR 400mHz (CD_3CN) δ 5.48(2H, s) δ 6.95(2H, d) δ 7.05(2H, d) δ 7.67(2H, d) δ 7.92(2H, d). HRMS, M-H, 252.0661, found, 252.0655.

2.2.3 1-(4-(Benzyloxy)phenyl)ethan-1-one**:**

A 250 ml round bottom was charged with 1.01 g (7.42 mmol) of *p*-hydroxyacetophenone, 3.00 g (21.7 mmol) of K_2CO_3, and acetonitrile. This solution was stirred at rt while 0.880 ml (7.35 mmol) of benzyl bromide was added dropwise and the final solution was stirred for 20

hours. The solvent was removed under vacuum and the resulting white residue was dissolved in 1:1 H_2O:ethyl acetate (v:v) and extracted with 30 ml 1 M NaOH 4 times. The combined organics was dried with $MgSO_4$ and the solvent was removed with reduced pressure giving a white solid. White solid (1.36 g, 82%), H^1NMR (400 MHz, $CDCl_3$) δ 2.56 (s, 3H), 5.14 (s, 2H), 7.01 (d, J = 8 Hz, 2H), 7.42 (m, 5H), 7.94 (d, J = 8 Hz, 2H).

2.2.4 2-Bromo-1-(4-phenoxyphenyl)ethan-1-one**:**

A 250 ml round bottom was charged with 513.7 mg (2.27 mmol) of 1-(4-(4-methoxyphenoxy)phenyl)ethan-1-one and 1085 mg (4.86 mmol) of copper(II) bromide in 30 ml of 1:1 $CHCl_3$: ethyl acetate (v:v). The solution was brought to reflux, turning brown then green, and run until completion was determined by TLC (4-6 hours). The green solution was filtered through a silica plug and the solvent was removed under vacuum resulting in brown oil. This oil was recrystallized in absolute ethanol and 2-bromo-1-(4-phenoxyphenyl)ethan-1-one, a brown/tan solid, was collected via vacuum filtration. Tan solid (330.2 mg 47.7%), H^1 NMR (400 MHz, $CDCl_3$) δ 4.41 (s, 2H), 5.16 (s, 2H), 7.05 (d, J = 12 Hz, 2H), 7.43 (m, 5H), 7.98 (d, J= 8Hz,2H)

2.2.5 Methyl 5-chloro-2-(2-oxo-2-(4-phenoxyphenyl)ethoxy)benzoate**:**

A 50 ml round bottom was charged with 37.3 mg (0.12 mmol) of 2-bromo-1-(4-phenoxyphenyl)ethan-1-one , 49.06 mg (0.355 mmol) of K_2CO_3 and 48.8 mg (0.262 mmol) of methyl-5-chlorosalicylate dissolved in 30 ml acetonitrile. The resulting solution was stirred at rt and run until completion was determined by TLC. The solvent was removed under vacuum and the resulting red-brown residue was dissolved in 1:1 H_2O: ethyl acetate (v:v) and extracted 3x with 20 ml 1 M NaOH. The solution was filtered and solvent removed under vacuum to a crude yellow-red solid. The solid was purified with flash chromatography (ethyl acetate: n-hexane 1:4,

v:v). Yield: 14.8 mg, 29.5%. H^1 NMR (400 MHz, $CDCl_3$) δ 3.88 (s, 3H), 5.15 (s, 2H), 5.30 (s, 2H), 6.84 (d, J = 8 Hz, 1H), 7.04 (d, J=8 Hz, 2H), 7.41 (m, 5H), 7.80 (d, J= 4Hz, 1H), 8.02 (d, J= 8 Hz, 2H)

2.2.6 1-(4-((4-Nitrobenzyl)oxy)phenyl)ethan-1-one**:**

An oven dried 100 ml round bottom was charged with 1.54 g (11.1 mmol) of K_2CO_3 , 640 mg of 4-nitrobenzyl chloride and 495 mg of *p*-hydroxyacetophenone in acetonitrile. This solution was stirred for 4 hours at reflux turning a cloudy white then a tan brown. The solvent was removed under vacuum and the brown solid was dissolved in 1:1 water:ethyl acetate (v:v). The organic layer was extracted three times with 30 ml 1 M NaOH and dried over $MgSO_4$. The solvent was removed under vacuum resulting in a red crude. This solid was recrystallized in hot ethanol and a tan solid was collected via vacuum filtration. Tan solid (697 mg 69.3%). H^1NMR (400 MHz, $CDCl_3$) δ 2.59 (s, 3H), 5.27 (s, 2H), 7.03 (d, J = 8 Hz, 2H), 7.64 (d, J = 8 Hz, 2H), 7.98 (d, J = 8 Hz, 2H), 8.29 (d, J = 8 Hz, 2H).

2.2.7 1-(4-(4-Methoxyphenoxy)phenyl)ethan-1-one:

A oven dried 100 ml round bottom was charged with 212.3 mg (1.56 mmol) of *p*-hydroxyacetophenone , 612.4 mg (4.43 mmol) of K_2CO_3 and acetonitrile. The resulting solution was stirred at rt while 0.203 ml (1.47 mmol) of 4-methoxybenzyl chloride was added dropwise, this solution was then stirred for 18 hours. The solvent was removed under reduced pressure and the residue was dissolved in 1:1 H_2O: ethyl acetate (v:v). This solution was extracted 3x with 30ml of 1 M NaOH and the combined organic layers were dried over $MgSO_4$. The solvent was removed under reduced pressure to give 1-(4-(4-methoxyphenoxy)phenyl)ethan-1-one as a white, crude solid. The solid was purified recrystallized in hot ethanol giving a white crystalline solid. White solid (330 mg 17%), H^1 NMR (400 MHz, $CDCl_3$) δ 2.57(s, 3H), 3.83 (s, 3H), 5.06

(s, 2H), 6.94 (d, J = 8Hz, 2H), 7.01 (d, J= 8Hz, 2H), 7.37 (d, J = 8 Hz, 2H), 7.94 (d, J= 12 Hz, 2H).

2.2.8 4-(2-bromoacetyl)phenyl acetate**:**

An oven dried round bottom was charged with 1.01 g of 2-bromo-1-(4-hydroxyphenyl)ethan-1-one and 900 ml of triethyl amine in anhydrous diethyl ether. This solution was stirred under N_2 ice while 0.428 ml of acetyl chloride (6 mmol) was added over a 15 minute period. The resulting solution was stirred at room temperature for 4 hours turning white and cloudy. After 4 hours he solution was washed twice with 10 ml of water, 5% soda ash and saturated sodium chloride then dried of magnesium sulfate. The organic layer was rotovapped down to a tan solid. Tan solid (1.0 g 83 %) H^1 NMR (400 MHz, $CDCl_3$) δ 2.36 (s, 3H), 4.45 (s, 2 H), 7.26 (m, 2H), 8.06 (d, 2 H, J = 8).

2.2.9 Dimethyl-2-mercaptosuccinate:

An oven dried round bottom was charged with 3.01 grams of (14 mmol) of mercaptosuccinic acid 0.14 of H_2SO_4 (1.39 mmol) in methanol. This mixture as stirred for 4 hours after which water was added to quench the reaction. This water methanol mixture was extracted with ether. The ether layer was then washed with 5% soda ash and dried with $MgSO_4$, the solvent was then removed via vacuum leaving a clear oil (1.84 g, 47%) H^1 NMR (400 MHz, $CDCl_3$) δ 2.23(d, J = 4, 1H), 2.77 (dd, J = 8, 24, 1H), 3.02 (dd, J = 8, 24, 1H), 3.70 (s, 3H), 3.77 (s, 3H)

2.2.10 Dimethyl 2-((2-(4-hydroxyphenyl)-2-oxoethyl)thio)succinate: (Compound 4)

An oven dried round bottom was charged with 1.00 g (3.5 mmol) of dimethyl 2-((2-(4-hydroxyphenyl)-2-oxoethyl)thio)succinate, 585 mg of K_2CO_3 (4.24 mmol) and 759 mg of pHP Br (3.53 mmol) in acetonitrile. This was stirred for 5 hours at room temperature, the solvent was

removed via vacuum leaving a crude solid. The solid was dissolved in ethyl acetate and extracted with water. The organic was then washed with 5% soda ash and the solvent was removed via vacumn to a ten solid. (yield 751 mg, 41 %) H^1 NMR (400 MHz, $CDCl_3$) δ 2.23(d, J = 4, 1H), 2.79 (dd, J = 4, 20, 1H), 3.03 (dd, J = 8, 24, 1H), 3.70 (s, 3H), 3.75 (s, 3H), 5.77 (s, 2H), 6.91 (d, J = 8, 2H), 7.92 (d, J = 8, 2H)

2.2.11 General Photolysis Procedure-UV analysis:

5mg 2,4-cyanophenoxy-4-hydroxyacetophenone was dissolved in 5mL 20% aqueous acetonitrile, buffered at pH 7.4 with a phosphate buffer. Solution was transferred to pyrex test tube. Samples were irradiated with Rayonet reactor under 8 300nm white lamps. Samples for UV analysis were prepared by removing 50μL aliquots of irradiated sample with calibrated micropipette and diluted to 2mL in a volumetric flask. UV spectrum were taken after every 3 minutes of irradiation.

2.2.12 General Photolysis Procedure- NMR analysis

1mL of 3.5 x 10^{-3} M solution in 20% D_2O D_3-Acetonitrile was prepared and placed in a pyrex test tube for photolysis. A 0.6mL aliquot was removed in order to take an NMR spectrum after which it was returned to the test tube for further irradiation.

2.2.13 General Photolysis Procedure-Mass spectrometry analysis

A 2mM solution of Compound 4 were prepared 5 mL 10% aqueous acetonitrile. Samples were irradiated with a Rayonet reactor under 8 300 nm white lamps for 10 minutes. Samples were analyzed using a eluent mixture of acetonitrile and water and a gradient of a 15 minute ramp from 95% organic, 5 % aqueous to 65 % organic, 35 % aqueous, 5 minutes to 1:1 organic aqueous, 1 minute to 5 % organic, 95 % aqueous, 1 minute to 95 % organic, 5 % aqueous followed by a hold at the same ratio for 4 additional minutes. The flow rate was held at 1.5 mL

throughout and the separation was conducted on a 15 cm C18 Ascentis column. Mass spectrometry analysis was conducted using a electrospray ionization source in negative mode coupled to a triple quadrupole detector.

2.2.14 Actinometer

0.006M ferrioxalate in 0.05M H_2SO_4 was irradiated with the same lamps, test tube, and volume as photolysis procedures. The preparation of an actinometer has been described previously[20]. To a 10mL volumetric flask was added 0.5mL buffer pH 7.4 phosphate buffer, 2mL 0.1% phenanthroline, 0.9mL 0.05M Sulfuric acid, and 0.1mL of irradiated solution. The absorbance of a prepared solution was measured and checked against a blank. The difference in optical density was converted to concentration using a calibration curve. The change in concentration was converted to mol/min and light output was determined by dividing this number by 1.24[20]. The calibration curve was constructed by dissolving $FeSO_4$ in distilled water and diluting to a range of concentrations from $1.03x10^{-3}$ to $1.24x10^{-4}$M. Solutions were prepared for analysis by adding, volumes of aqueous Fe^{3+} to make the desired concentration, a volume of 0.05M sulfuric acid to make the total volume 5mL, 1mL 0.1% phenanthroline, 2mL pH 7.4 phosphate buffer, and distilled water to a total volume of 10 mL. The optical density was measured at 510nm.

2.2.15 Quantum Yield Determination

Change in concentration over time was determined by converting absorbance of product to concentration using a calibration curve constructed by measuring absorbance of concentrations over area of interest. The slope of the curve of concentration vs time represents the rate of change of M/min which can be changed to mol/min by multiplying by the volume irradiated. This value was divided by the light output determined by the ferrioxalate actinometer.

2.2.6 Animals:

Mice (Charles River Laboratories, Inc., Wilmington, MA, USA), were housed 5 per cage in plastic cages with food and water available *ad libitum* in a temperature/humidity-controlled environment. Animals were placed on a 12 hour light/dark cycle. All experiments were carried out in accordance with the National Institutes of Health *Guide for the Care and Use of Laboratory Animals.* All procedures were approved by the University of Kansas Institutional Animal Care and Use Committee.

2.2.17 Brain Slices:

Brain slices were harvested as previously described[21]. In summary, mice were deeply anesthetized by isofurane inhalation and decapitated. The brain was then immediately removed and placed into ice-cold artificial cerebral spinal fluid (aCSF). The aCSF solution contains the following concentrations: 2.5 mM KCl, 126 mM NaCl, 1.2 mM NaH_2PO_4, 25 mM $NaHCO_3$, 2.4 mM $CaCl_2$, 1.2 mM $MgCl_2$, 20 mM HEPES, 11 mM D-glucose. The pH was adjusted to the physiological pH 7.4. To ensure the tissue received ample oxygen, the aCSF was continuously bubbled with 95% O_2/5% CO_2 throughout the experiment. After chilling for one minute the cerebellum was removed and the brain was bisected using a sterile razor blade. One hemisphere of the brain was then glued to a plate against a cube of agar for support. 300 µm coronal brain slices were then obtained using a vibratome (Leica, Wetzlar, Germany). After obtaining a brain slice containing striatal tissue, it was transferred to a perfusion chamber where oxygenated aCSF was perfused over the slice and was heated to 34 ºC. The slice was equilibrated for one hour before taking any measurements

2.2.18 Optrode fabrication

Optrodes were fabricated by cutting a silica capillary (40 µm ID TSP 040105 polymicro) and a 60 µm fiber optic to a length of 3 cm. The outer coating was removed from the capillary using a flame and the capillary and fiber optic were aligned. A 7µm carbon-fiber purchased from Goodfellow Cambridge Ltd. (Huntingdon, England) was aligned with the silica capillary and the fiber optic so that the carbon fiber extended ~ 3 mm beyond the fiber optic silica capillary unit. This was loaded into a second silica capillary (200 µm TSP 2503506 polymicro) and the unit was aligned with the opening of the second capillary so only the carbon fiber extended beyond the opening using a micromanipulator. This was then sealed by using capillary effects to get a well-mixed epoxy mixture of 0.24g EPI-CURE 3234 Curing Agent (lot FCXC4114/0886GG) and 2.00g EPON Resin 815C (lot HADN0003/1307GG), which had been allowed to pre cure for an hour, into the second capillary until it was completely filled. The epoxy was allowed to cure for 12 hours. The unit was threaded into a glass capillary tubes (1.2 mm D.D and 0.68 mm I.D, 4 in long; A-M System Inc, Carlsborg, WA, USA) and baked for another hour at 100 ºC then the carbon fiber was cut to ~ 30 µm.

2.3 Results and Discussion

2.3.1 Protection and deprotection of phenols

We decided to synthesize a very simple model complex in order to determine if it was possible to cleanly uncage a pHP-phenol bond. Para-cyanophenol was selected for these initial studies because the electron withdrawing nature of the para cyano group causes the phenolic hydrogen to be more acidic when compared to the unmodified phenol. This more acidic phenol

should mean that para-cyanophenol is an ideal leaving group partner for the pHP photochemistry. Compound 1 was synthesized as shown in Scheme 2.

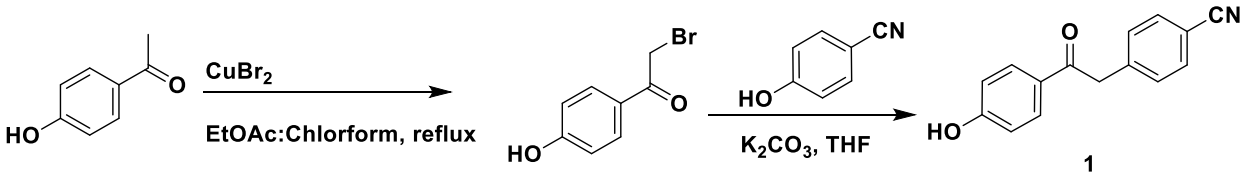

Scheme 2: Synthesis of, 4-(2-(4-hydroxyphenyl)-2-oxoethoxy)benzonitrile (Compound 1)

The photochemical reactivity of Compound 1 was initially studied using UV-vis by irradiating the compound with 300 nm light and taking aliquots of the reaction mixture every six minutes for measurements. As can be seen in Figure 3, as Compound 1 was exposed to 300 nm light, the absorbance peak at 275 nm, characteristic of Compound 1, decreased in intensity. This shows that a photochemically induced reaction is taking place which is consuming the starting material. While this is promising because it shows that the starting material is being consumed after exposure to light, the UV-vis data can only give us insight into what is happening with the protected phenol, it cannot show was what products are being produced. In order to elucidate theses products H^1 NMR was used.

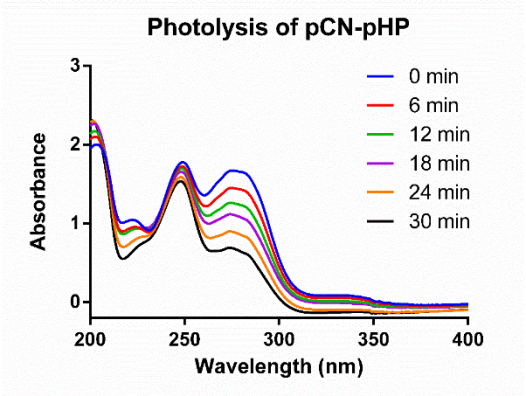

Figure 3: UV-vis study of Compound 1. There is an observed decrease in the absorbance at 275 nm, the peak which is indicative of the phenol on the pHP protecting group, over time implying that Compound 1 is being consumed in the reaction.

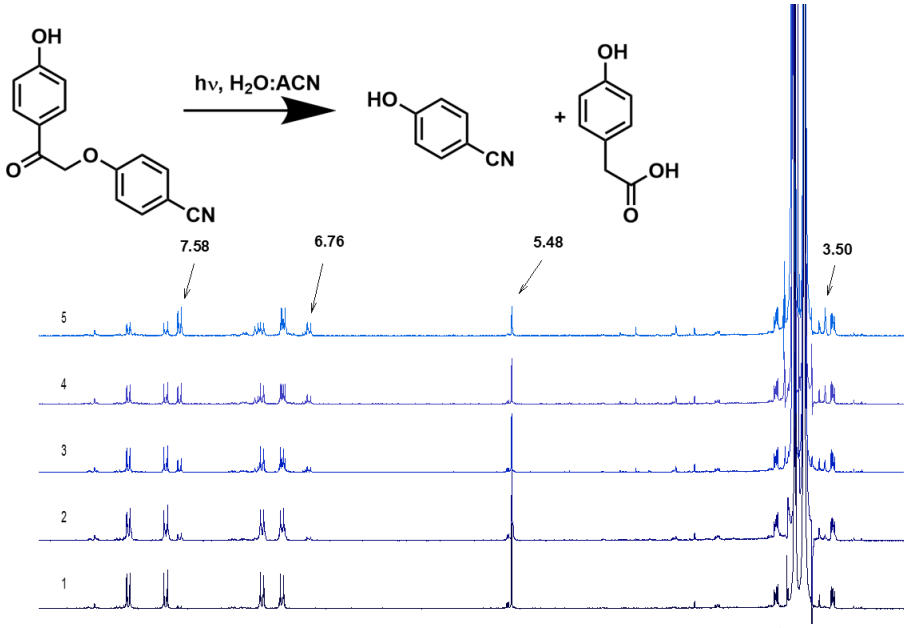

Figure 4: The photochemical uncaging of 1 as tracked by H^1 NMR. The singlet at 5.48, indicative of the caged starting material, is disappearing as the reaction proceeds indicating the starting material is being consume. The peaks at 6.76 and 7.58, representing 4-hpaa and 4-cyanophenol are growing in indicating that these are the two major products.

In order to ascertain the identity of the products the photochemical reaction of compound 1 was tracked via ^{1}H-NMR. In a clean uncaging reaction taking place via the photo-favorskii rearrangement it would be expected that the characteristic peaks of the caged starting material, δ 5.48, would disappear. The peaks indicative of the two main predicted products, 4-HPAA δ 6.76 and 4-cyanophenol δ 7.68, should also appear as the reaction progressed. The H^1 NMR data presented in Figure 4 follows these predications very well. The caged starting material disappeared while the two main product peaks appeared. It is also important to note that from the H^1 NMR it appears that no secondary product peaks are appearing, implying that the reaction is occurring through the photo-favorskii mechanism predominately. Once it was determined that the reaction of Compound 1 underwent a clean photochemical uncaging reaction, the quantum yield of Compound 1 was determined to be 0.33 $\pm$ 0.03. Overall, Compound 1 showed that it is possible to cleanly uncage simple acidic phenols and gave us confidence moving forward that the clean uncaging of our desired targets was possible.

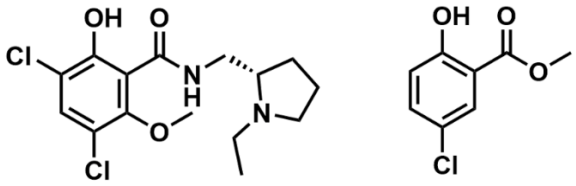

Figure 5: A comparison between the 5-chlorosalciylate and the D2 antagonist raclopride

Our final target, the family of D2 receptor antagonists, including raclopride, are very expensive compounds so we decided to pursue another, more complex, model before committing to the use of our actual targets. The intermediate model chosen was 5-chlorosalciylate because of its similarities to raclopride. As can be seen in Figure 5, 5-chlorosalciylate captures two features we thought would be important to the chemistry of the raclopride target: 1) The two compounds share a chlorine moiety that is para to the phenol group. This chlorine should capture some of the electronic properties of the compound of interest. 2) Both compounds have a carboxy group ortho to the phenol group, with an ester in the case of 5-chlorosalciylate and an amide in the case of raclopride. This carboxy group should help to model the sterics of the target compound.

The synthesis of Compound 2 is shown in Scheme 3. Unlike in the synthesis for Compound 1, a protection step of the pHP groups' phenol moieties was used. This was done because the sterics of 5-chlorosalciylate were predicted to slow down the hetero-coupling. It was thought this would make the homo-coupling more likely than in the case of the para-cyanophenol coupling. A very small amount of Compound 3 was synthesized when the benzyl group was used as the protecting group; however, we were unable to succeed in removing this benzyl protecting group. This protecting group on the phenol of the pHP prevented the photochemistry from proceeding. In order to try to overcome this difficulty in synthesis two other protecting groups were tried, 4-methoxybenzyl and 4-nitrobenzyl. It was found that when these groups were used

the bromination reaction, needed to provide a handle for the coupling chemistry, either went too far causing over bromination or did not proceed.

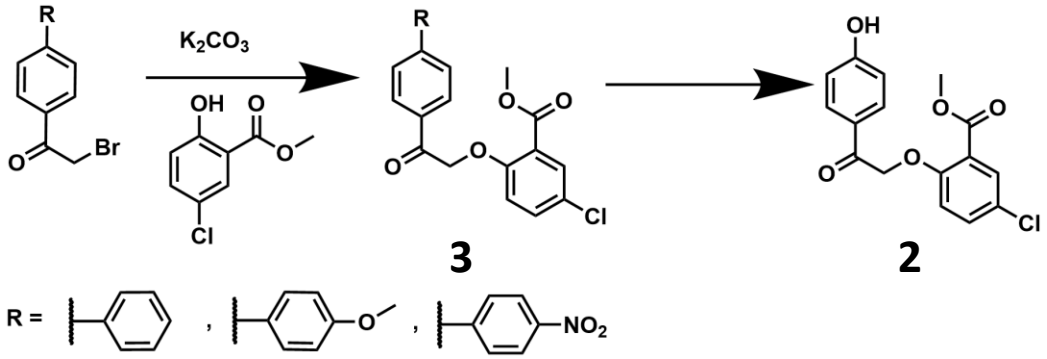

Scheme 3 proposed synthesis of Compound 2

Overall, we were able to show that it is possible to cleanly uncage a simple, acidic phenol in a reaction that follows the photo-favorskii mechanism in reasonable quantum yields. However, we were not able to successfully synthesize a more pertinent model of the target compounds both because of difficulties in synthesizing the protected Compound 2, likely because of steric issues, and difficultly in removal of the benzyl protecting group from Compound 2 to reach Compound 3. When alternative protecting groups were used to make the deprotection chemistry more favorable, it was found that the bromination chemistry was either not occurring at all or was over brominating. Our inability to successful synthesize Compound 2 led us to move on from this line of work to a different, theoretically more favorable moiety.

2.3.2 Protection and deprotection of thiols

This second moiety our group became interested in was thiols. Thiols have two main characteristics that make them a favorable target for this type of chemistry. 1) They are highly nucleophilic moieties meaning that the coupling chemistry should be easier to achieve. 2) Thiols are also a fairly acidic moiety with a pka 8.2-10 [22] which make them good leaving group candidates for the heterolytic uncaging reaction. It has been shown in the past that pHP can be

used as a group to protect thiol containing compounds such as glutathione and cysteine by Specht *et al.*[23] This chemistry was shown to undergo the photo-favorskii rearrangement for the majority of products formed based on ^{1}H-NMR product analysis. [23] We hoped to take this chemistry and apply it to a class of glutathione peroxidase inhibitors that have this thiol moiety.

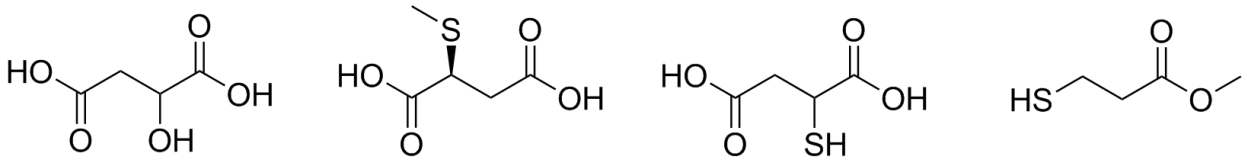

Figure 6 The two compounds to the left did not inhibit glutathione peroxidase because they did not have an unblocked thiol moiety. The two compounds to the right were found to be potent inhibitors of glutathione peroxidase because of their open thiol moieties.

The interest in this thiol moiety biologically arises from the fact that it is the active portion of a class of glutathione peroxidase inhibitors. Examples of these inhibitors are shown in Figure 6. All of these compounds share a common thiol group that has been shown [22] to be the biologically relevant portion of the compound for inhibition to take place. Glutathione peroxidase is a vital enzyme that controls the production of H_2O_2 in mitochondria as shown in Figure 7[24].

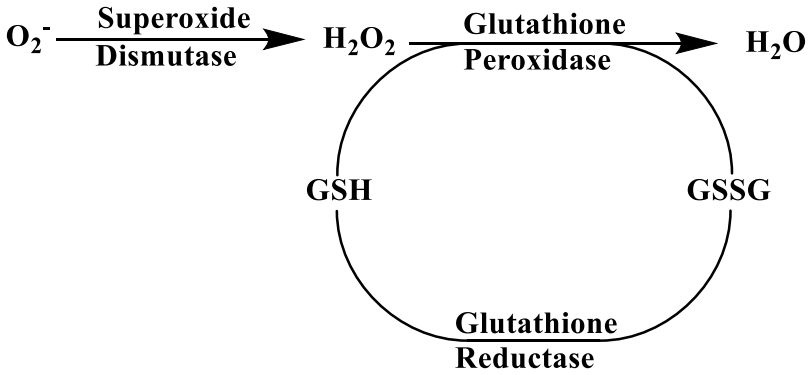

Figure 7: Production of hydrogen peroxide in mitochondria. The thiol based inhibitors increase production by blocking glutathione peroxidase's conversion of hydrogen peroxide to water.(Figure adapted from reference 24)

If glutathione peroxidase is inhibited, the production of hydrogen peroxide, a proposed neuromodulator [25, 26] as well as a ROS [27, 28] , will increase. Since thiols have favorable chemistry for this type of photo caging reactions as outlined above, and the biological activity data [22] points to the thiol being vital for the biochemistry, we hypothesized that caging a glutathione peroxidase inhibitor was an interesting avenue to pursue.

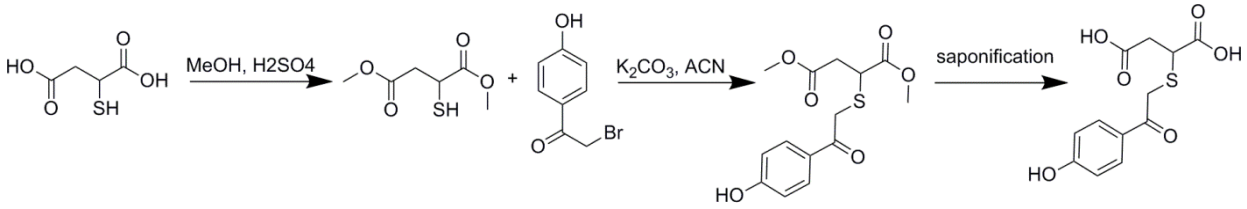

4

Scheme 4: Synthesis of Compound 4.

Mercaptosuccinic acid (MCS) is a potent glutathione peroxidase inhibitor[22] that our lab has used in the past with success. The synthesis for a caged form of mercaptosuccinic acid is shown in Scheme 4. It consisted protecting the carboxylic acid groups on mercaptosuccinic acid by converting them to esters. This was done to prevent the bonding of 3 protecting groups to mercaptosuccinic acid during the coupling reaction. A SN2 coupling was then done to protect the thiol group. Compound 4 was synthesized and photochemical analysis was undertaken.

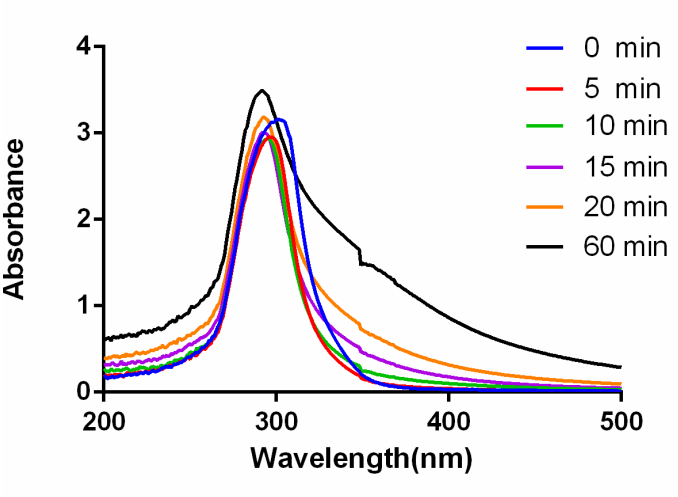

Figure 8: UV-vis taken of Compound 4 at specific time intervals after exposure of the compound to 300 nm light. As the reaction was allowed to continue the absorbance peak observed broadened, which is indicative of a chemical change taking place.

Initially, the compound was exposed to 300 nm light and UV-vis spectra were taken of the reaction at time points 5 minutes apart. These data is shown in Figure 8. These data did not have a clean decrease in a single peak like the data presented above for Compound 1; however, there is a broadening in the absorbance observed at about 295 nm that implies a change is occurring in the starting material. We took this alteration to mean that a reaction was occurring in response to the light exposure; however, it is likely a complex mixture of products.

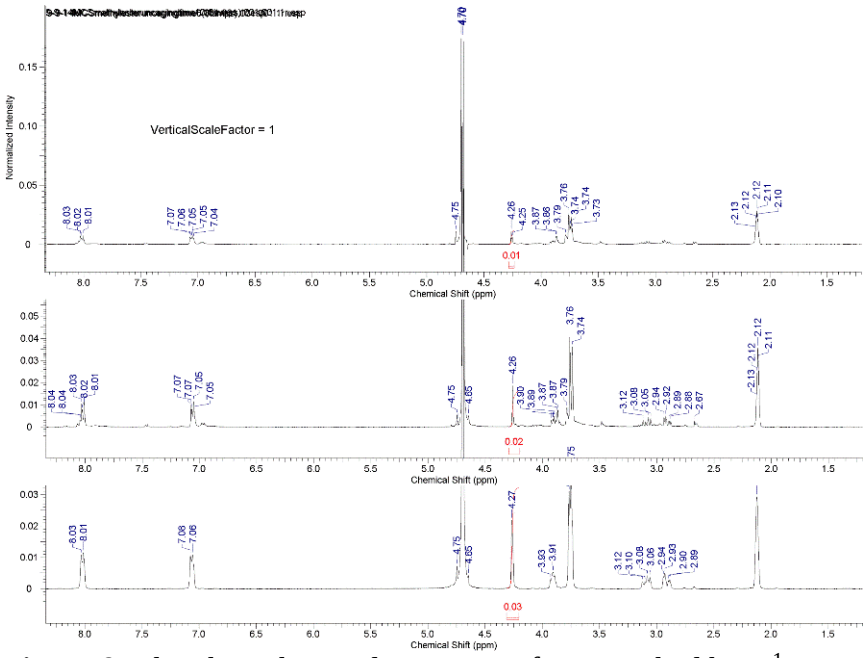

Figure 9: The photochemical uncaging of 4 as tracked by H^1 NMR. The singlet at 4.27, indicative of the caged starting material, is disappearing as the reaction proceeds indicating the starting material is being consume. While this is indicative of product disappearing there seems to be no product peaks appearing during the reaction.

In an attempt to elucidate the identity of these products, the reaction was tracked by H^1-NMR. As seen in Figure 9, as the reaction progresses over time the peak at 4.27, representative of the methylene protons on the carbon bonding the pHP group to the MCS ester is disappearing. This disappearance implies that Compound 4 is being consumed in the reaction. Even though the H^1 NMR shows that the starting material is disappearing no new peaks are appearing from production of products. This result was confusing because it implies that the products being formed in the reaction are either not viewable in our chemical shift range, which is unlikely since they should be similar compounds to the starting material, or that there are many products being formed all below the limits of detection in H^1-NMR.

In order to elucidate what was happening in this presumably complex reaction mixture, it was decided to track the reaction using liquid chromatography mass spectrometry (LC-MS). Compound 4 was exposed to 300 nm light for 10 minutes and then analyzed using a LC

separation coupled to an electrospray ionization source with triple quadrupole detection. When this experiment was done, as seen in Figure 10, a complex mixture of ions was observed. Instead of 3 peaks, one representing starting material, one representing the release of the leaving group, and one representing the expected 4-HPAA byproduct, there was a multitude of peaks present. We were able to identify two of these peaks, one at 16.45 minutes which corresponds to the starting materials mass and one at 8.94 minutes which corresponds to pHP's mass. The fact that a pHP peak was observed after the reaction occurs is telling because it implies that the photo-favorskii mechanism cannot be the only photochemical mechanism occurring. As was outlined above, if the photo-favorskii was the main mechanism of action, 4-HPAA would be expected to be the main byproduct of the uncaging, not a return of the intact pHP cage itself. Since pHP was found to be a major product, as determined by the mass and total ion count, we propose that the reaction proceeded through the mechanism presented in Figure 10b. This mechanism proposes that, instead of a photo-favorskii like mechanism occurring, a homolytic cleavage of the carbon sulfur bond occurs, forming two radicals. The pHP radical could than abstract a hydrogen and form pHP starting material, the peak we see at 8.94 minutes. The sulfur radical could also abstract a hydrogen to form the desired dimethyl-2-mercaptosuccinate product, though this product was not observed in the mass spectrometry data. It is also possible that both radicals are reacting with other species in the reaction mixture. These reactions could lead to the large number of species observed in the mass spectrometry data that were not predicted from our originally hypothesized mechanism. It is clear that a photochemically induced uncaging reaction is occurring; however, because of the hypothesized presence of radicals during the reaction, it is unusable in biological systems.

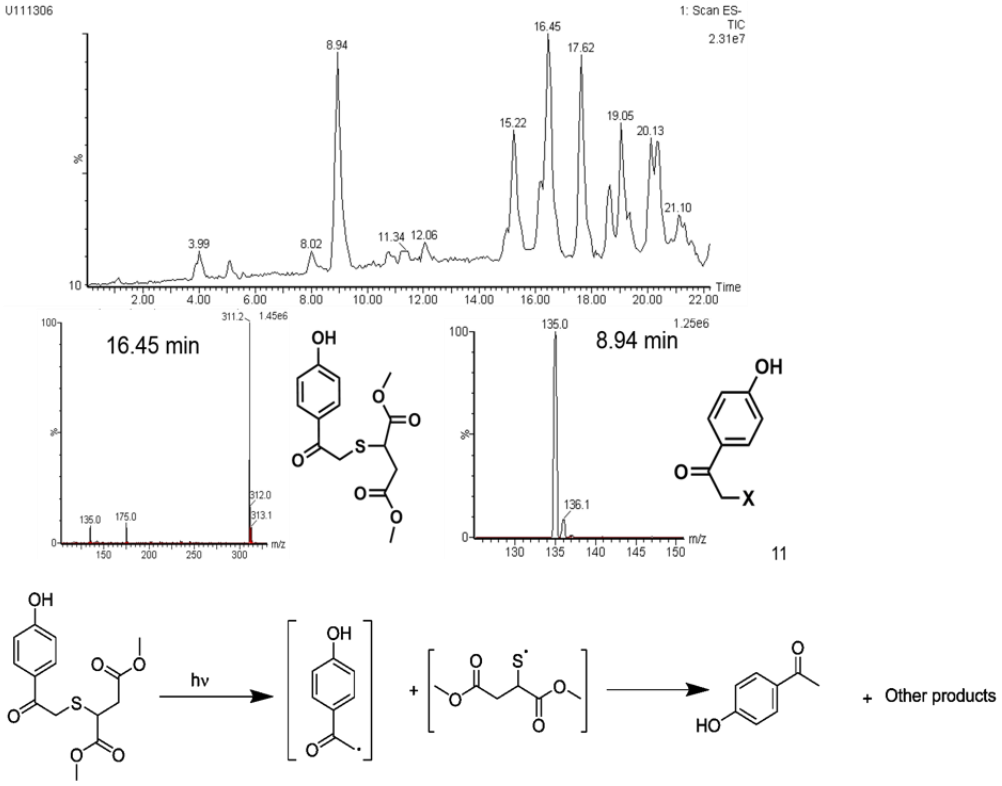

Figure 10: (A) The total ion count chromatogram of the reaction mixture after 10 minutes of exposure to 300 nm light. Instead of the three peaks expected (starting material, 4-HPAA and dimethyl-2-mercaptosuccinate) many peaks were observed. (B) The mass spectra of two of the peaks, one at 8.94 minutes which has been identified as pHP and one at 16.45 minutes which has been identified as starting material. (C) A proposed alternative mechanism for the photochemical uncaging of dimethyl-2-mercaptosuccinate, this mechanism consists of a hemolytic cleavage that is proposed to make two radical intermediates which can then react to make many other products.

2.3.3 An optrode for photochemistry

As briefly discussed above, one of the main reasons that we are interested in the pHP protecting group, beyond the favorable photochemical properties, is the ability to quantify the release of non-electroactive compounds by the measurement of the 4-HPAA byproduct. We have obtained preliminary data showing that it is possible to make these measurements of photochemical release in brain tissue; however, we have discovered there are two main difficulties when doing these experiments: 1) It is difficult to align the fiber optic light guide

with the working electrode using micromanipulators alone. 2) These experiments are difficult to do without using large amounts of expensive photo protected compound because of the large volumes and flow rates needed to keep the tissue alive. Therefore, we set out to design a device that can solve these problems by combining a working electrode for the electrochemical measurements, a fiber optic light guide for the directed delivery of light and a silica capillary for the direct delivery of compound.

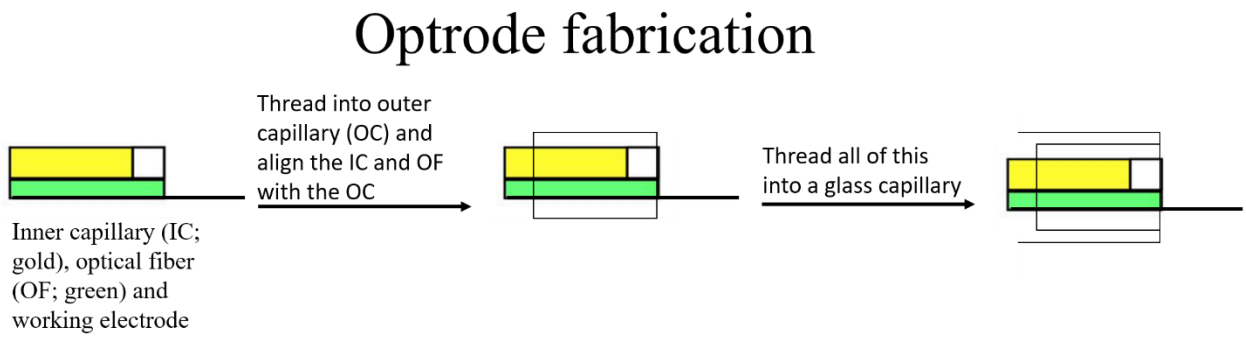

Figure 11: An inner capillary (IC) has its coating burned off and is aligned flush with an optical fiber (OF). Once this alignment is achieved the IC and OF are held in place by wax. A carbon fiber is then attached using static electricity. All of this is threaded into an outer capillary (OC) and the IC and OF are aligned with the end of the OC using micromanipulators. Once everything is aligned the OC is filled with epoxy sealing the IC and OF inside. This is allowed to cure for 12 hours at room temperature. Once the curing process is complete the OC is threaded into a glass capillary and sealed in with epoxy and is then cured for 1 hour at 100 ºC. Once the epoxy has cured the carbon fiber is cut to ~ 50 µm.

The fabrication of our optrode is shown in Figure 11. The optrode consists of a 40 µm inner capillary, a 60 µm optical fiber, and a 7 µm carbon fiber all contained within a 200 µm outer capillary. This unit is then glued and sealed into a glass capillary that is 0.8 mm ID, 1.2 mm OD. Images of the completed optrode are shown in Figure 12. The fiber optic and the inner capillary extend beyond the glass capillary so they can be integrated with light sources and pumps respectively. The inner capillary and optical fiber are located within the outer capillary in order to make sure the injection system and optical fiber are protected from fouling by the tissue.

Finally, the carbon fiber is extended beyond the outer capillary so it can be inserted into the tissue to make measurements.

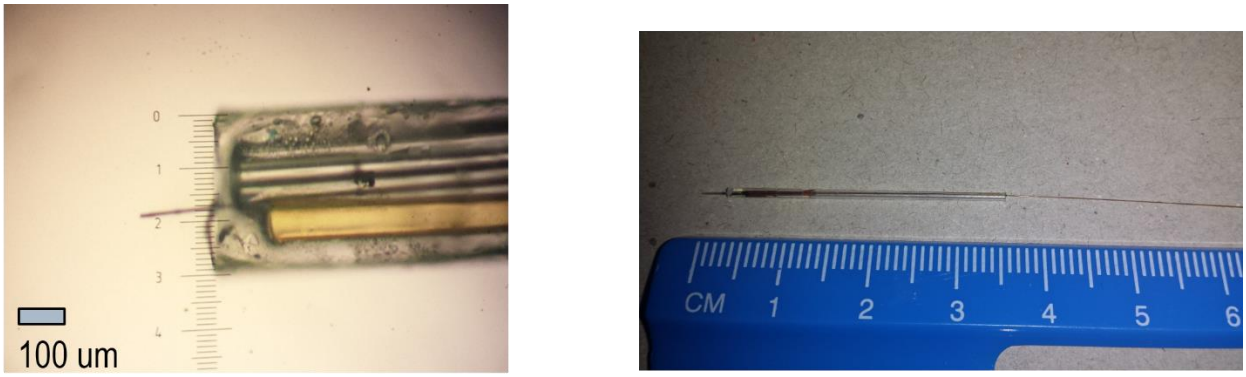

Figure 12. Images of an optrode under the microscope showing how the inner capillary and fiberoptic are contained within the outer capillary while the carbon fiber extends beyond the outer capillary. The second image shows the optrode not under the microscope showing that the outer capillary extends beyond the glass capillary and the inner capillary and fiber-optic extends beyond the glass capillary so they are accessible to be hooked up to apparatus.

To examine the practicability of the electrode, flow cell experiments were conducted to show that the optrode could detect dopamine. Tests were also done to ascertain if fiber optic was able to deliver light to the electrode surface. As can be seen in Figure 13A, the optrode can detect 3 μm dopamine in a flow cell with a CV that is indicative of dopamine. The shape of the current vs time plot is very similar to what is seen in a normal electrode used in our lab. This implies that the optrodes have the same ability to measure dopamine as standard electrodes. The second experiment done to characterize the electrode was a light coupling test. The fiber optic cable was coupled into a mercury light source that was modulated with a shutter. An experiment was done where the shutter was opened, coupling light into the fiber optic, which was able to guide the light to the electrode surface. This light caused a light artifact to appear in the current vs time and color plot as shown in Figure 12B. This strong one point signal is indicative of the light interacting with the electrode surface and producing a current due to the photoelectron effect.

This is indicative of the light guiding fiber optic guiding the light onto the surface of the electrode.

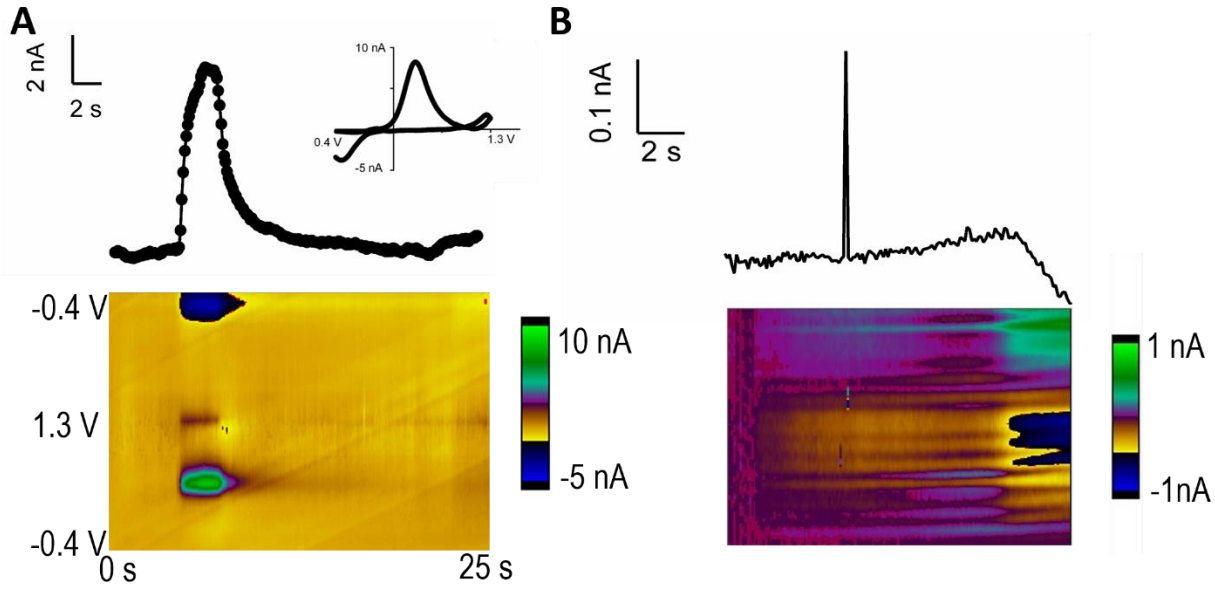

Figure13. (A) Detection of 3 µM dopamine in a flow cell. The CV and current trace shape are consistent with what would be expected in an experiment using a normal electrode used in our lab. (B) A light artifact, the high current signal point peak in the current plot was observed after light was introduced to the fiberoptic in the optrode. This indicates that the optrode is delivering light to the electrode surface.

Overall, the design showed promise in that light hit around the region of the electrode and we were able to detect dopamine in a flow cell. However, the optrodes themselves had two design flaws found during this initial testing: 1) The working electrode portion was very brittle, this made it difficult to cut and use without breaking the electrode.2) The outer capillary was very large leading to tissue damage when the optrode was tested in brain slices.

2.4 Conclusions

This work showed that it was possible to cleanly uncage an acidic phenol, *para*-cyanophenol through a heterolytic cleavage that followed the photo-favorskii rearrangement. Unfortunately, we could not successfully synthesize a more pertinent model compound for our

targeted compounds (D2 receptors antagonist). We were successfully able to synthesize a caged thiol; however, we discovered that the photochemistry likely undergoes a homolytic mechanism involving radical formation. Since this photochemistry produced a multitude of undesired products, it is not a good candidate for biologically relevant experiments.

We were also able to successfully fabricate a combined electrode optical fiber system for the delivery and release of caged compounds on tissue. This served as a good proof of concept as this optrode was shown to be able to detect dopamine in a flow cell. It was also demonstrated that this design could deliver light to the surface of the electrode via the presence of a light artifact.

2.5 References

[1] Yousef, A. L., Lee, J.-I., Conrad, P. G., and Givens, R. S. (2003) Photoremovable Protecting Groups, In *CRC Handbookof Organic Photochemistry and Photobiology, Volumes 1 & 2, Second Edition*, CRC Press.

[2] Ellis-Davies, G. C. (2007) Caged compounds: photorelease technology for control of cellular chemistry and physiology, *Nature methods 4*, 619-628.

[3] Klán, P., Šolomek, T. s., Bochet, C. G., Blanc, A. l., Givens, R., Rubina, M., Popik, V., Kostikov, A., and Wirz, J. (2012) Photoremovable protecting groups in chemistry and biology: reaction mechanisms and efficacy, *Chemical reviews 113*, 119-191.

[4] Kandler, K., Katz, L. C., and Kauer, J. A. (1998) Focal photolysis of caged glutamate produces long-term depression of hippocampal glutamate receptors, *Nature neuroscience 1*, 119-123.

[5] Dong, J., Zeng, Y., Xun, Z., Han, Y., Chen, J., Li, Y.-Y., and Li, Y. (2012) Stabilized Vesicles Consisting of Small Amphiphiles for Stepwise Photorelease via UV Light, *Langmuir 28*, 1733-1737.

[6] Chalmers, S., Caldwell, S. T., Quin, C., Prime, T. A., James, A. M., Cairns, A. G., Murphy, M. P., McCarron, J. G., and Hartley, R. C. (2012) Selective Uncoupling of Individual Mitochondria within a Cell Using a Mitochondria-Targeted Photoactivated Protonophore, *Journal of the American Chemical Society 134*, 758-761.

[7] McCoy, C. P., Rooney, C., Edwards, C. R., Jones, D. S., and Gorman, S. P. (2007) Light-triggered molecule-scale drug dosing devices, *Journal of the American Chemical Society 129*, 9572-9573.

[8] Rock, R. S., and Chan, S. I. (1996) Synthesis and photolysis properties of a photolabile linker based on 3 ‘-methoxybenzoin, *The Journal of Organic Chemistry 61*, 1526-1529.

[9] Wylie, R. G., and Shoichet, M. S. (2008) Two-photon micropatterning of amines within an agarose hydrogel, *Journal of Materials Chemistry 18*, 2716-2721.

[10] Pelliccioli, A. P., and Wirz, J. (2002) Photoremovable protecting groups: reaction mechanisms and applications, *Photochemical & photobiological sciences 1*, 441-458.

[11] Givens, R. S., Jung, A., Park, C.-H., Weber, J., and Bartlett, W. (1997) New Photoactivated Protecting Groups. 7. p-Hydroxyphenacyl: A Phototrigger for Excitatory Amino Acids and Peptides1, *Journal of the American Chemical Society 119*, 8369-8370.

[12] Givens, R. S., and Park, C.-H. (1996) p-Hydroxyphenacyl ATP 1: A new phototrigger, *Tetrahedron letters 37*, 6259-6262.

[13] Ngoy, B. P., Šebej, P., Šolomek, T., Lim, B. H., Pastierik, T., Park, B. S., Givens, R. S., Heger, D., and Klán, P. (2012) 2-Hydroxyphenacyl ester: a new photoremovable protecting group, *Photochemical & Photobiological Sciences 11*, 1465-1475.

[14] Sebej, P., Lim, B. H., Park, B. S., Givens, R. S., and Klán, P. (2011) The power of solvent in altering the course of photorearrangements, *Organic letters 13*, 644-647.

[15] Givens, R. S., Heger, D., Hellrung, B., Kamdzhilov, Y., Mac, M., Conrad, P. G., Cope, E., Lee, J. I., Mata-Segreda, J. F., and Schowen, R. L. (2008) The photo-Favorskii reaction of p-hydroxyphenacyl compounds is initiated by water-assisted, adiabatic extrusion of a triplet biradical, *Journal of the American Chemical Society 130*, 3307-3309.

[16] Park, C.-H., and Givens, R. S. (1997) New Photoactivated Protecting Groups. 6. p-Hydroxyphenacyl: A Phototrigger for Chemical and Biochemical Probes1,2, *Journal of the American Chemical Society 119*, 2453-2463.

[17] Givens, R. S., Weber, J. F. W., Conrad, P. G., Orosz, G., Donahue, S. L., and Thayer, S. A. (2000) New Phototriggers 9: p-Hydroxyphenacyl as a C-Terminal Photoremovable Protecting Group for Oligopeptides, *Journal of the American Chemical Society 122*, 2687-2697.

[18] Givens, R. S., Rubina, M., and Wirz, J. (2012) Applications of p-hydroxyphenacyl (p HP) and coumarin-4-ylmethyl photoremovable protecting groups, *Photochemical & Photobiological Sciences 11*, 472-488.

[19] Shin, M., Kaplan, S. V., Raider, K. D., and Johnson, M. A. (2015) Simultaneous measurement and quantitation of 4-hydroxyphenylacetic acid and dopamine with fast-scan cyclic voltammetry, *Analyst 140*, 3039-3047.

[20] Hatchard, C., and Parker, C. A. (1956) A new sensitive chemical actinometer. II. Potassium ferrioxalate as a standard chemical actinometer, In *Proceedings of the Royal Society of London A: Mathematical, Physical and Engineering Sciences*, pp 518-536, The Royal Society.

[21] Johnson, M. A., Rajan, V., Miller, C. E., and Wightman, R. M. (2006) Dopamine release is severely compromised in the R6/2 mouse model of Huntington's disease, *Journal of neurochemistry 97*, 737-746.

[22] Chaudiere, J., Wilhelmsen, E., and Tappel, A. (1984) Mechanism of selenium-glutathione peroxidase and its inhibition by mercaptocarboxylic acids and other mercaptans, *The Journal of biological chemistry 259*, 1043-1050.

[23] Specht, A., Loudwig, S., Peng, L., and Goeldner, M. (2002) p-Hydroxyphenacyl bromide as photoremoveable thiol label: a potential phototrigger for thiol-containing biomolecules, *Tetrahedron letters 43*, 8947-8950.

[24] Pinto, M., Neves, J., Palha, M., and Bicho, M. (2002) Oxidative stress in Portuguese children with Down syndrome, *Down Syndrome Research and Practice 8*, 79-82.

[25] Avshalumov, M. V., Chen, B. T., Marshall, S. P., Peña, D. M., and Rice, M. E. (2003) Glutamate-dependent inhibition of dopamine release in striatum is mediated by a new diffusible messenger, H2O2, *Journal of Neuroscience 23*, 2744-2750.

[26] Chen, B. T., Avshalumov, M. V., and Rice, M. E. (2001) H2O2 is a novel, endogenous modulator of synaptic dopamine release, *Journal of Neurophysiology 85*, 2468-2476.

[27] Zorov, D. B., Juhaszova, M., and Sollott, S. J. (2014) Mitochondrial reactive oxygen species (ROS) and ROS-induced ROS release, *Physiological reviews 94*, 909-950.

[28] Lushchak, V. I. (2014) Free radicals, reactive oxygen species, oxidative stress and its classification, *Chemico-Biological Interactions 224*, 164-175.

Chapter 3 *Ex vivo* measurement of electrically evoked dopamine release in zebrafish whole brain

Portions of this chapter are reprinted with permission from Shin, M., Field, T. M., Stucky, C. S., Furgurson, M. N., & Johnson, M. A. (2017). Ex vivo measurement of electrically evoked dopamine release in zebrafish whole brain. *ACS Chemical Neuroscience*.Copyright 2017 American Chemical Society." I collected a portion of the release and pharmacology data and I collected all of the modelling and uptake data in this chapter.

Abstract

Zebrafish (*Danio rerio*) have recently emerged as useful model organism for the study of neuronal function. Here, fast-scan cyclic voltammetry at carbon-fiber microelectrodes (FSCV) was used to measure locally-evoked dopamine release and uptake in zebrafish whole brain preparations and results were compared with those obtained from brain slices. Evoked dopamine release ($[DA]_{max}$) was similar in both whole brain and sagittal brain slice preparations (0.49 ± 0.13 µM in whole brain and 0.59 ± 0.28 µM in brain slices). Treatment with α-methyl-p-tyrosine methyl ester (αMPT), an inhibitor of tyrosine hydroxylase, diminished release and the electrochemical signal reappeared after subsequent washout. Although no observed change in stimulated release current occurred after treatment with desipramine and fluoxetine in the whole brain, treatment with desipramine resulted in a modest decrease in uptake, suggesting that norepinephrine may also contribute to the signal. Uptake was inhibited more strongly following treatment with nomifensine compared to GBR 12909, while treatment with sulpiride, a D2 dopamine autoreceptor antagonist, resulted in increased stimulated dopamine release in whole brain, but had no effect on release in slices. Interestingly, dopamine release in whole brains increased progressively up to an electrical stimulation frequency of 25 Hz while release in slices increased up to a frequency of only 10 Hz and then flattened out, highlighting another key difference between these preparations. We also observed a lag in peak dopamine release

following stimulation as well as a secondary current that prevented return to baseline, which we address using diffusion models and pharmacological treatments. Collectively, these results demonstrate, for the first time, the electrochemical measurement of dopamine release in the whole, intact brain of a vertebrate *ex vivo* and are an important step for carrying out more complex experiments.

3.1 Introduction

Zebrafish (*Danio rerio*) are teleosts that were initially established as a model organism in the 1970s by George Streisinger for the study of development [1] Recently, zebrafish have emerged as a desirable model for the study of neuronal function [2] in part because they approximate the human central nervous system more accurately than invertebrates and are easier to genetically manipulate than rodents [3]. Moreover, the optical transparency of zebrafish larvae make this organism well-suited for *in vivo* studies in which intracellular calcium changes [4] and action potentials [5] can be imaged real-time. Also, the zebrafish central nervous system, when studied using cultured cells [6], brain slices [7], and intact brain [8], has proven amenable to electrophysiological measurements of neuronal firing.

In addition to these methods, the use of electrochemistry to measure the release and uptake of neurotransmitters in zebrafish is just now being realized. Fast-scan cyclic voltammetry at carbon-fiber electrodes (FSCV) is an electrochemical technique that provides good chemical selectivity and sub-second temporal resolution, allowing the measurement of the release and uptake of electroactive neurotransmitters[9]. FSCV has been used extensively in rodents to measure the release and uptake dynamics of dopamine, an abundant catecholamine neurotransmitter that plays a role in many aspect of neurological function, including the control of intentional movement [10], cognition [11], and reward [12].

Recently, the release of dopamine and other neurotransmitters was measured in sagittal brain slices acutely harvested from zebrafish, providing important proof of concept[13]. However, it is important to note that, although analysis of slices from various neuronal systems, especially rodents, have yielded much information regarding the study disease state mechanisms [14] as well as fundamental neurotransmitter release properties [15], brain slice preparations in general have several drawbacks, such as cellular damage induced at the surface of the slice [16] and difficulty in capturing entire neuronal pathways [17]. The use of intact brains could mitigate these problems by decreasing the amount of tissue damage and leaving the neuronal pathways intact, thereby allowing remote stimulation of the pathway and eliminating the release of interfering neurotransmitters and neuromodulators that would be present upon local stimulation. Additionally, constant potential amperometry has recently been used to measure stimulus evoked dopamine release in zebrafish larvae[18]. However, to our knowledge, FSCV measurements of neurotransmitter release within the intact brains of adult zebrafish have not yet been reported in the literature; thus, the measurement of locally-stimulated dopamine release from acutely harvested, intact zebrafish brains, and comparison of these measurements with those from brain slices, represents a critical first step.

Here, we describe measurements of dopamine release and uptake in whole, intact zebrafish brains with FSCV. Furthermore, we compare these measurements to those obtained in sagittal and coronal brain slices. We found that, when the working electrode is properly placed by reference to the external features of the removed brain, electrically evoked dopamine release and uptake is easily measured in zebrafish whole brain *ex vivo*. The cyclic voltammograms (CV) obtained suggest that the primary neurotransmitter measured is dopamine, and that norepinephrine may also be released. Moreover, we confirmed the presence of dopamine with

pharmacological agents that alter dopamine release and uptake. Some of the unique characteristics of release and uptake curves are also discussed. These results support the use of FSCV in *ex vivo* whole brain preparations as a useful analytical tool for measuring neurotransmitter release and uptake in zebrafish.

3.2 Methods

3.2.1 Chemicals.

Dopamine, α-methyl-p-tyrosine methyl ester (αMPT), nomifensine, and (±) sulpride, were purchased from Sigma-Aldrich (St. Louis, MO). All aqueous solutions were made with purified (18.2 MΩ) water. A modified artificial cerebrospinal fluid (aCSF) for zebrafish consisted of 131 mM NaCl, 2mM KCl, 1.25 mM KH_2PO_4, 20 mM $NaHCO_3$, 2mM $MgSO_4$, 10 mM glucose, 2.5 mM $CaCl_2 \cdot H_2O$, and 10mM HEPES, and the pH was adjusted to 7.4. Dopamine stock solutions were prepared in 0.2 M perchloric acid and were diluted with aCSF without glucose to 1 µM for calibrations. Solutions of 50 µM aMPT, 10 µM nomifensine, and 10 µM sulpride, were prepared the day of each experiment.

3.2.2 Electrochemical Measurements.

Cylindrical carbon-fiber microelectrodes were fabricated as previously described. Briefly, 7 µm diameter carbon fibers (Goodfellow Cambridge LTD, Huntingdon, UK) were aspirated into a glass capillary tubes (1.2 mm D.D and 0.68 mm I.D, 4 in long; A-M Systems, Inc, Carlsborg, WA, USA). Loaded capillaries were then pulled using a PE-22 heated coil puller (Narishige Int. USA, East Meadow, NY) and carbon fibers were trimmed to a length of 30 µm from the pulled glass tip. To seal the carbon fibers, electrodes were dipped into epoxy resin (EPON resin 815C and EPIKURE 3234 curing agent, Miller-Stephenson, Danbury, CT, USA) and cured at 100℃ for 1 hour. The electrodes were soaked in isopropanol for 10 minutes, and the

electrode surface was electrochemically pretreated by scanning with the waveform –0.4 V to +1.3 V back to –0.4 V at a frequency of 60 Hz for 15 min followed by 10 Hz for 10 min. Electrodes were then backfilled with 0.5 M potassium acetate for electrical connection. A chlorided Ag wire was used as the Ag/AgCl reference electrode. Data were collected and analyzed using an electrochemical workstation consisting of a Dagan Chem-Clamp potentiostat (Dagan, Minneapolis, MN, USA), modified to allow decreased gain settings, a personal computer with TarHeel CV software (provided by R.M. Wightman, University of North Carolina, Chapel Hill, NC, USA.), a UEI breakout box (UNC chemistry department electronics design facility, Chapel Hills, NC), and two National Instruments computer interface cards (PCI 6052 and PCI 6711, National Instruments, Austin, TX). The waveform was applied every 100 ms to the electrode at a scan rate of 400 V/s. Electrodes were calibrated with a 1 µM dopamine solution . To evoke dopamine release both in whole brain and brain slices, multiple stimulus pulses (25 pulses, 2 ms, 350 µA) was applied for 0.5 s at 5 s unless mentioned otherwise. This stimulation was applied by two tungsten electrodes 200 µm apart. A recovery time of 10 min between stimulations was used for both whole brain and brain slices experiments. All statistical analysis was done using GraphPad Prism 6 (GraphPad Software, Inc , La Jolla, CA, USA). All data are reported as a mean plus or minus the standard error of the mean.

3.2.3 Zebrafish**.**

All animal procedures were approved by the University of Kansas Institutional Animal Care and Use Committee. Zebrafish were housed in the Molecular Probes Core of the Center for Molecular Analysis of Disease Pathways at the University of Kansas. Zebrafish were euthanized by rapid chilling, and then decapitated. Brains were harvested under a dissection stereoscope (Leica Microsystem, Bannockburn, IL, USA) and transferred to a superfusion chamber in which

they were kept viable by continuous flow of oxygenated (95% O_2 and 5% CO_2) aCSF maintained at a temperature of 28ºC. The brain was immobilized by placement of a nylon mesh harp on top. Brains were allowed to equilibrate in the chamber for 1 hour prior to collecting measurements. For brain slice preparation, harvested brains were suspended in 2% low gelling point agarose (agarose type VII-A, Sigma-Aldrich, St Louis, MO, USA) prepared in 50% distilled water and 50% aCSF. After hardening, a block of agarose containing the brain was cut off and glued onto a specimen disk and fastened in the buffer tray of a vibratome (Leica Microsystem, Bannockburn, IL, USA). The tray was filled with ice cold oxygenated aCSF and kept at 2-4°C during slicing. Sagittal and coronal slices, 350 µm thick, were transferred to the perfusion chamber and were allowed to equilibrate for 1 hour prior to collecting measurements.

3.2.4 Statistical Analysis**.**

Error bars represent mean ± SEM. Graphpad Prism version 4.03 was used to carry out statistical analyses.

3.3 Results and Discussion

3.3.1 Evoked dopamine release in zebrafish.

A photograph of a viable whole brain acutely harvested from an adult zebrafish is shown in Fig. 2A. The brain is situated ventral side face up to provide easier access to the subpallium in the telencephalon, a region of the brain that contains dopaminergic innervation [19]. The carbon-fiber microelectrode and the stimulation electrodes were micro-manipulated into place by referencing the external features of the ventral side of the brain. The carbon-fiber microelectrode was positioned 100 µm laterally from the medial olfactory tract (MOT) and inserted 280–300 µm

deep. The region was stimulated locally with a biphasic stimulus pulse regimen in which 25 pulses, 2 ms duration and 350 µA current, was applied. Application of this regimen resulted in the release of dopamine detected by FSCV at the carbon-fiber microelectrode (Fig. 2C). A stimulated release plot (concentration versus time profile), sampled from the color plot at the horizontal dotted line, is located above the color plot. A cyclic voltammogram (CV), sampled at the vertical dashed line of the color plot, serves as electrochemical evidence that the neurotransmitter released is dopamine.

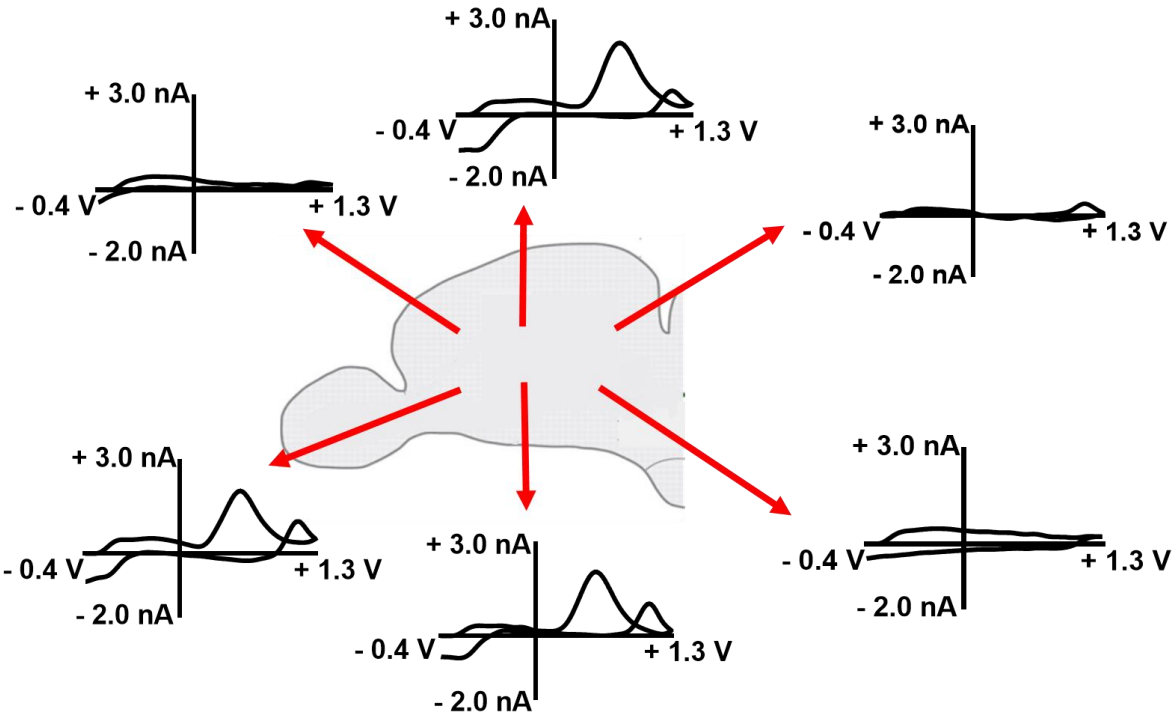

Figure 1 Dopamine release as a function of working electrode placement. The working electrode was moved superior and inferior from the ventral telecephelon. Dopamine release disappeared in both directions, as indicated by the disappearance of the indicative CV.

In order to determine how spatially resolved our method is we kept the stimulation electrode stationary and moved the working electrode inferior and superior from the MOT as well as dorsally. We found that as the electrode was moved away from the MOT both superior

and inferior the release event was no longer observed. We also moved the working electrode up and down 30 µm increments and discovered that the dopamine was found consistently in a 60 µm region (data not show). These results suggest that the region that is dopamine rich is specific (Fig 1).

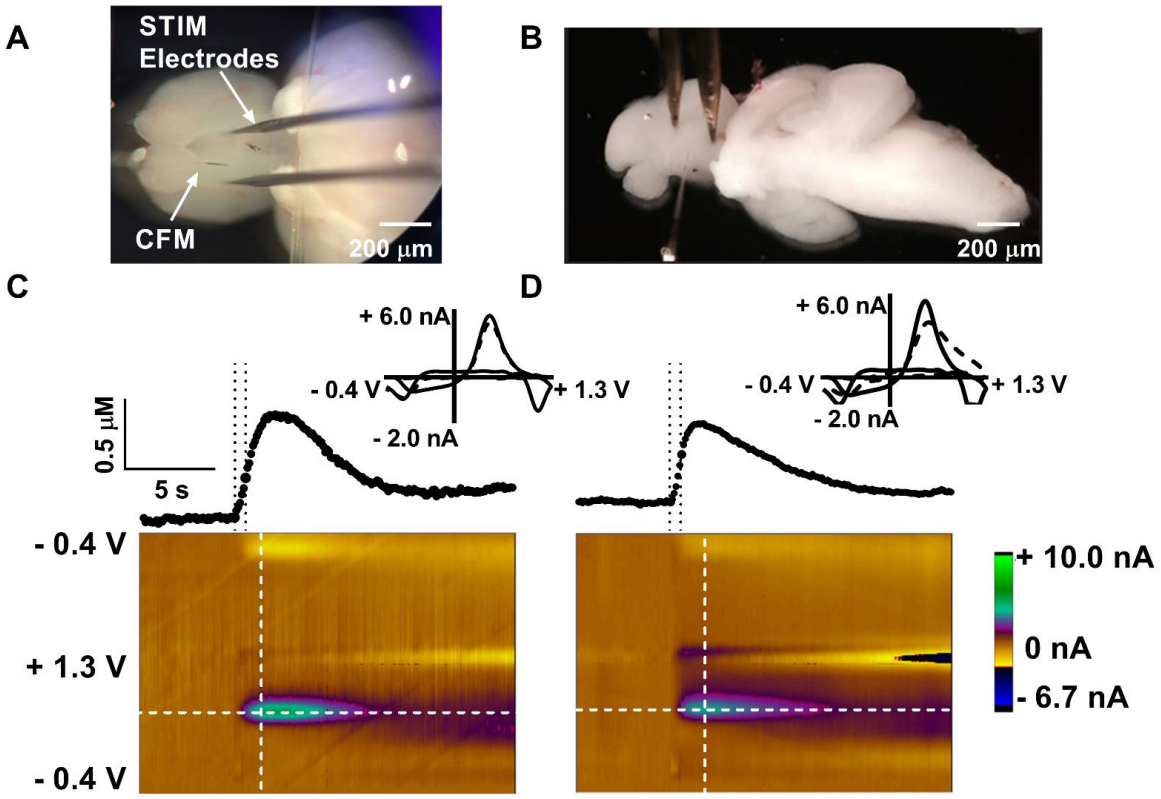

Figure 2. Electrically-evoked dopamine release in zebrafish whole brain and sagittal brain slices. Images of a whole brain (A) and a sagittal slice (B) indicate the placement of carbon-fiber and stimulus electrodes in the ventral telencephalon. Representative data of evoked dopamine release in a whole brain (C) and a sagittal brain slice (D) are shown. For C and D, the stimulated release plots (top) were sampled at the horizontal white dashed lines and the cyclic voltammograms (insets) were sampled at the vertical white dashed lines of the color plots. The stimulation times are indicated on the release plots by the time between the dashed lines. The CVs (dotted lines) are overlaid with sample voltammograms from the flow cell represented by the solid line.

For comparison, dopamine release was also measured in acutely harvested sagittal brain slices (Figs. 2B and C). The stimulation and working electrodes were micro-manipulated into position at the ventral telencephalon. Dopamine release was evoked locally using the same

stimulation parameters used in the whole brain. Both CV and current versus time plots are similar to those obtained in the whole brain preparation. In the representative raw data, $[DA]_{max}$ increased until a peak concentration of about 0.5 µM was measured ~2 s after stimulus application. Current then decreased as uptake occurred. Observation of the color plots suggest that other electroactive species were not released in substantial quantities. Also, electrically evoked $[DA]_{max}$ was consistent throughout each recording session. Dopamine release measurements in both preparations were collected for one hour and compared.

Data pooled from multiple whole brains and brain slices reveal that, under equivalent stimulation conditions, average $[DA]_{max}$ was not significantly different in whole brain and slices: 0.41 ± 0.07 µM in whole brains and 0.54 ± 0.13 µM in slices ($p = 0.40$, n=9 slices and 9 brains, t-test). The concentration of dopamine release evoked by either single or multiple stimulus pulses, both *in vivo* and *ex vivo*, has been reported extensively in the literature. For example, application of single pulses in mouse brain slices resulted in 1.43 ± 0.11 µM (striatum) [20], 1.42 ± 0.14 µM (nucleus accumbens core), and 1.40 ± 0.19 µM (caudate putamen) [21]. Multiple stimulation pulses were applied *in vivo* to evoke dopamine release in the rat striatum at a reported peak concentration of 1.04 ± 0.14 µM[22]. Recently, Jones et al.*(23)* found dopamine to be released in zebrafish sagittal slices at a peak concentration of about 100 nM following stimulation with 20, 4-ms duration pulses applied at a current of 500 µA and an application frequency of 60 Hz. In any case, it appears from our results that less dopamine is released in zebrafish whole brain and slices compared to that of rodents.

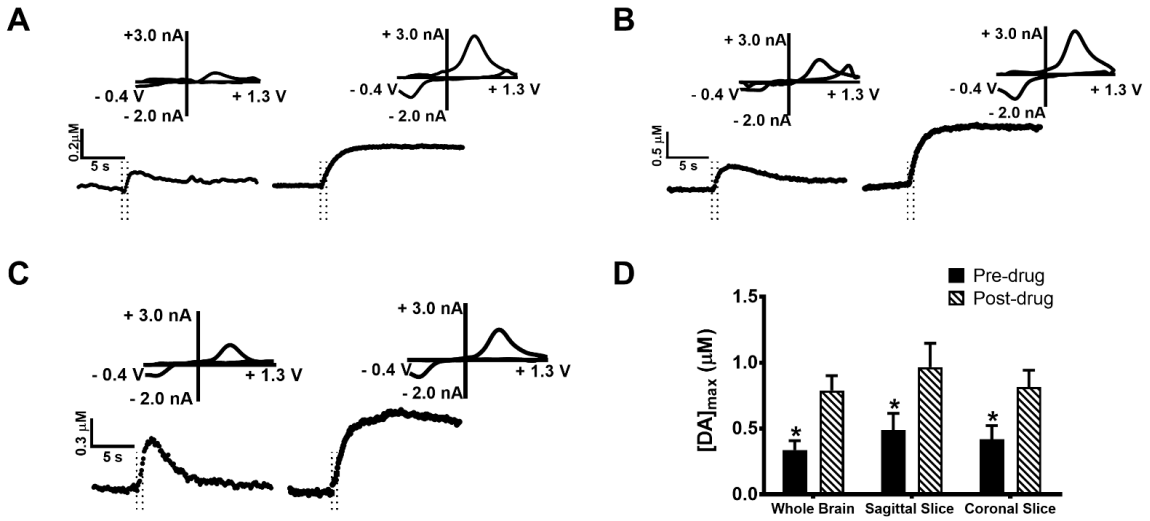

Figure 3. The effect of DAT inhibition on dopamine overflow in whole brain (A) sagittal (B) and coronal (C) brain slices. Dopamine release was measured before and after 10 μM nomifensine was administered to each preparation. The current versus time profiles show that dopamine uptake was diminished. Dopamine overflow after nomifensine was added was significantly increased in whole brain ($p < 0.05$, n = 4 brains, t-test), sagittal slices ($p < 0.05$, n = 5 slices, t-test) and coronal slices ($p<0.05$, n = 4, t-test) (D). Stimulation time is indicated on the release plots by the time between the dashed lines.

3.3.2 Effect of pharmacological agents on evoked dopamine release**.**

Extracellular dopamine levels are tightly regulated by the dopamine transporter (DAT), a membrane-bound protein that transfers dopamine molecules from the extracellular space to the intracellular space within neurons [23]. The stimulated release plot reveals that, similar to the mammalian brain, dopamine is immediately taken up after release. Based on previous measurements in brain slices from mice that lack the DAT [24], it is likely that dopamine is actively taken up and that the decrease in current is not the result of diffusion away from the electrode.

Additional pharmacological studies were conducted in which whole brain preparations, along with sagittal and coronal slices, were treated with 10 μM nomifensine (Fig. 3), a well-established dopamine uptake inhibitor[23]. As a result, the rate of dopamine uptake was sharply

diminished, indicated by the decreased slope of the stimulated release curves after peak dopamine release. This treatment resulted in a ~130% increase in $[DA]_{max}$ in the whole brain preparation (Fig. 2A: pre-drug, 0.34 ± 0.14 µM; post-drug, 0.79 ± 0.22 µM, $p < 0.05$, n = 4 brains, t-test). A similar effect was observed in sagittal slices, with $[DA]_{max}$ increasing ~100% (Fig. 2B: pre-drug, 0.49 ± 0.13 µM; post-drug, 0.97 ± 0.18 µM, $p < 0.05$, n = 5 slices , t-test) and in coronal slices, increasing ~100 % (Fig 2C: pre-drug 0.42 ± 0.11 µM ; post-drug, 0.82 ± 0.13 µM, $p < 0.05$, n = 4 slices, t-test). Our measurements also revealed a nearly complete attenuation of uptake in all three preparations treated with nomifensine (Fig 3A, B, and C).

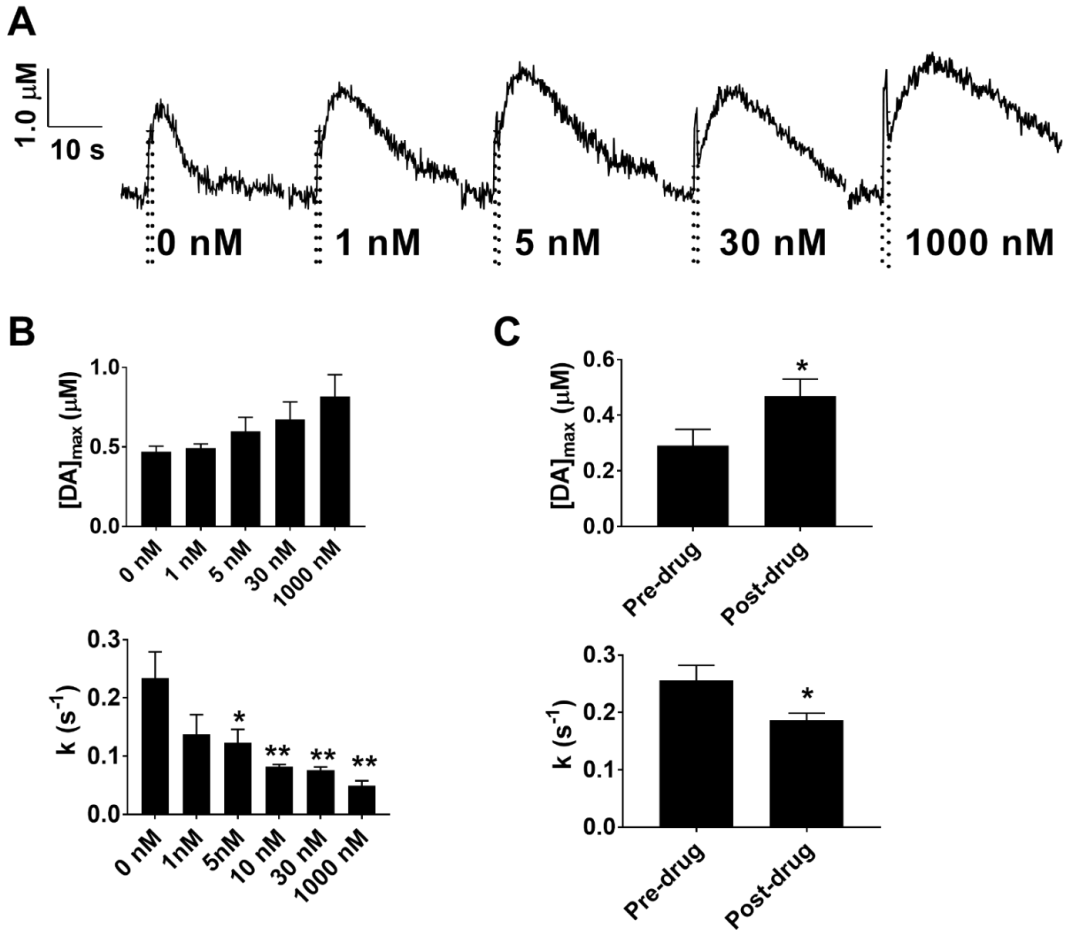

Figure 4. The effect of DAT inhibitors nomifensine and GBR 12909 on dopamine release in the whole brain. (A) Representative stimulated release plots are shown for different concentrations (0, 1, 5, 30, 1000 nM) of nomifensine perfused over whole brain preparations. Stimulation time is indicated on the release plots by the time between the dashed lines. (B) Effect of nomifensine on dopamine release/uptake in whole brain. No effect on $[DA]_{max}$ was observed ($p=0.38$, one-way ANOVA, n=3 brains); however, a significant overall effect on the 1st order rate constant (k) was found ($p < 0.005$, One-way ANOVA, n=3 brains, 5, 10, 30 and 1000 nM, tukey post hoc, * $p<0.05$, ** $p<0.005$ when compared to 0 nM). (C) Treatment with 10 μM GBR-12909 resulted in a significant increase in $[DA]_{max}$ (* $p < 0.05$, t-test, n=5) and a significant decrease in the 1st order rate constant for uptake (* $p < 0.05$, t-test, n = 5).

To investigate its effects in more detail, whole brain preparations were treated with increasing concentrations of nomifensine (1, 5, 30, and 1000 nM). The data were analyzed for changes in concentration as well as uptake. For each plot, the uptake curve was fit to the first order exponential decay equation, $[DA] = [DA]_{max}e^{-kt}$, where [DA] is the concentration of

dopamine at any given time, $[DA]_{max}$ is the experimentally determined maximum dopamine concentration, k is the first order rate constant for decay, and t is time [25]. In order to fit the data, $[DA]_{max}$ was held at the experimentally determined value and k was allowed to float. The data were fit up to the 80% signal decay point and fit was determined to be good if $R^2 > 0.90$. The baseline was corrected using differential subtraction in order to remove the secondary signals observed after the main release event.

A dose dependent increase in the attenuation of the reuptake was observed after the application of nomifensine (Fig. 3B, $p < 0.005$, one-way ANOVA, n = 3 brains)(Fig. 4B). Moreover, $[DA]_{max}$ appeared to increase, although this trend was not quite statistically significant (one-way ANOVA, $p = 0.11$). We also treated whole brain preparations with 10 µM GBR 12909, a selective dopamine uptake inhibitor, and found a significant increase in dopamine release, coupled to a significant decrease in the rate constant for uptake, similar to the findings of Jones *et al*. (Fig 3C; $p< 0.05$, t-test, n = 5). Both nomifensine and GBR 12909 are both effective in zebrafish, but DAT in zebrafish may be more sensitive to nomifensine than GBR 12909.

In order to identify signal contributions from norepinephrine or serotonin, two other common biogenic amine neurotransmitters, 10 µM desipramine [26]**,** a selective norepinephrine uptake inhibitor, and 10 µM fluoxetine [27], a selective serotonin uptake inhibitor, were perfused over *ex vivo* whole brain preparations (Fig 5A and B). These treatments resulted in no statistically significant change in $[DA]_{max}$ (Fig 5C: desipramine pre-drug 0.43 $\pm$ 0.08 µM; post-drug 0.50 ± 0.09 µM; $p = 0.60$, n= 5 brains, t-test and fluoxetine pre-drug 0.27 $\pm$ 0.05 µM, post-drug 0.33 ± 0·04 µM $p = 0.35$, n= 5 brains, t-test). The rate of uptake for both drugs was also compared using the first order rate constant for the decay of the dopamine signal as outlined above. Fluoxetine had no significant effect on the reuptake (Fig 5C: pre-drug 0.24 ± 0.02 s^{-1},

post-drug 0.20 ± 0.01 s^{-1} p = 0.14, n = 5 brains). Desipramine, on the other hand, had a significant effect on uptake (Fig 5C: pre-drug 0.22 ± 0.04 s^{-1}, post-drug 0.13 ± 0.01, $p < 0.05$, t-test, n = 5 brains).

The effect of desipramine on signal decay suggests that norepinephrine also makes up a component of the signal. Although the quantitative determination of the relative contributions of dopamine and norepinephrine is beyond the scope of this particular work, we speculate that dopamine is present in greater amount based on the following observations. First, the peak current observed following stimulation is unaffected by treatment with 10 μM desipramine (Fig. 4) yet is increased by the same concentration of nomifensine (Fig. 3). Given that the inhibition constants (K_i) are in the low nM range for nomifensine at the dopamine and norepinephrine transporters[28] and also for desipramine at the norepinephrine transporter[29], dopamine and norepinephrine uptake should be almost completely inhibited. Thus, differences in measured peak current between these two drug treatments would reflect differences in release between dopamine and norepinephrine since diffusion alone is insufficient to substantially decrease measured extracellular levels on the timescale of our measurements (20 s)[30]. The fact that the high concentration of desipramine used resulted in a relative modest inhibition of uptake (decrease of ~40%) while the same concentration of nomifensine completely abolished uptake further supports this concept. Second, anatomical data obtained from morpholino knockdown experiments in zebrafish larvae suggest that tyrosine hydroxylase-expressing neurons projecting into the forebrain are mostly dopaminergic[31] Finally, work by Shang et al.[32] and Jones et al.[33] suggest that dopamine is the primary catecholamine released in this brain region. Clearly, more work needs to be done to quantify the relative amounts of dopamine, norepinephrine, and other neurotransmitters released in the telencephalon and other brain regions. However, we can

conclude from this work that extracellular dopamine levels are tightly regulated by DAT in the telencephalon immediately after release and that *ex vivo* whole brain preparations can be used to measure locally-stimulated dopamine release.

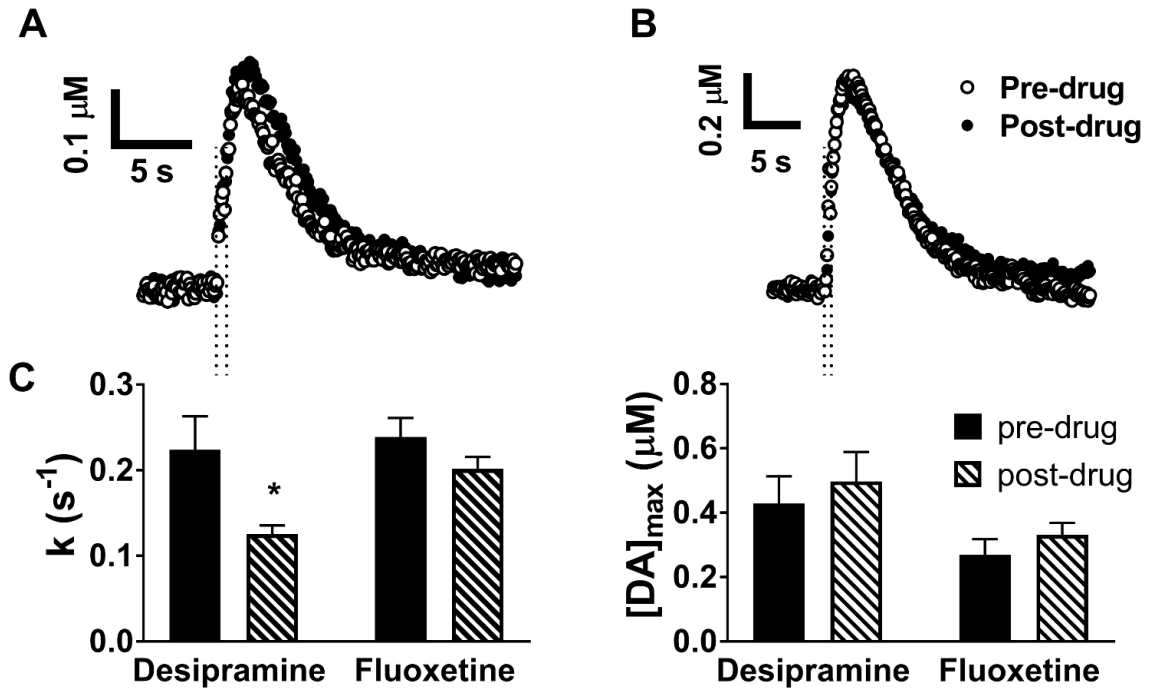

Figure 5. The effects of serotonin transporter (SERT) and norepinephrine transporter (NET) inhibition on dopamine release in whole brains. (A) Stimulated release plots before and after perfusion with 10 µM desipramine. (B) Stimulated release plots before and after perfusion with 10 µM fluoxetine. (C) Comparison of $[DA]_{max}$ and uptake rate constant (k) before and after perfusion with desipramine and fluoxetine. No significant changes in release were noted ($p= 0.595$ and 0.347 for desipramine and fluoxetine, respectively, t-test, n=5). A significant difference in uptake was observed for desipramine (* $p<0.05$, t-test, n=5) while no significant change was noted for fluoxetine ($p= 0.14$, t-test, n =5). Stimulation time is indicated on the release plots by the time between the dashed lines.

To obtain further confirmation of neurotransmitter identity, we examined the effect of α-methyl-p-tyrosine methyl ester (αMPT), which inhibits tyrosine hydroxylase and blocks monoamine neurotransmitter synthesis, (Fig. 6A). Release was electrically-evoked and measured every 10 minutes. Upon stabilization of the dopamine signal, brains were perfused with 50 µM αMPT and, approximately 2 hours later, the observed signal was greatly diminished (pre-drug,

0.56 ± 0.08 µM; post-drug, 0.14 ± 0.07 µM, $p < 0.005$, one-way ANOVA). To ensure that this disappearance of release was not due simply to loss of neuronal viability, the drug was washed out, and release re-appeared approximately 1 hour later (washout, 0.51 ± 0.10 µM, $p = 0.40$, one-way ANOVA), indicating that neurotransmitter release was not significantly different than before the drug was added (Fig. 6B). These measurements, taken in conjunction with the uptake inhibition experiments, further indicate that the neurotransmitters detected are catecholamines, and suggest that other classes of electroactive neurotransmitters, such as serotonin and histamine, are not released.

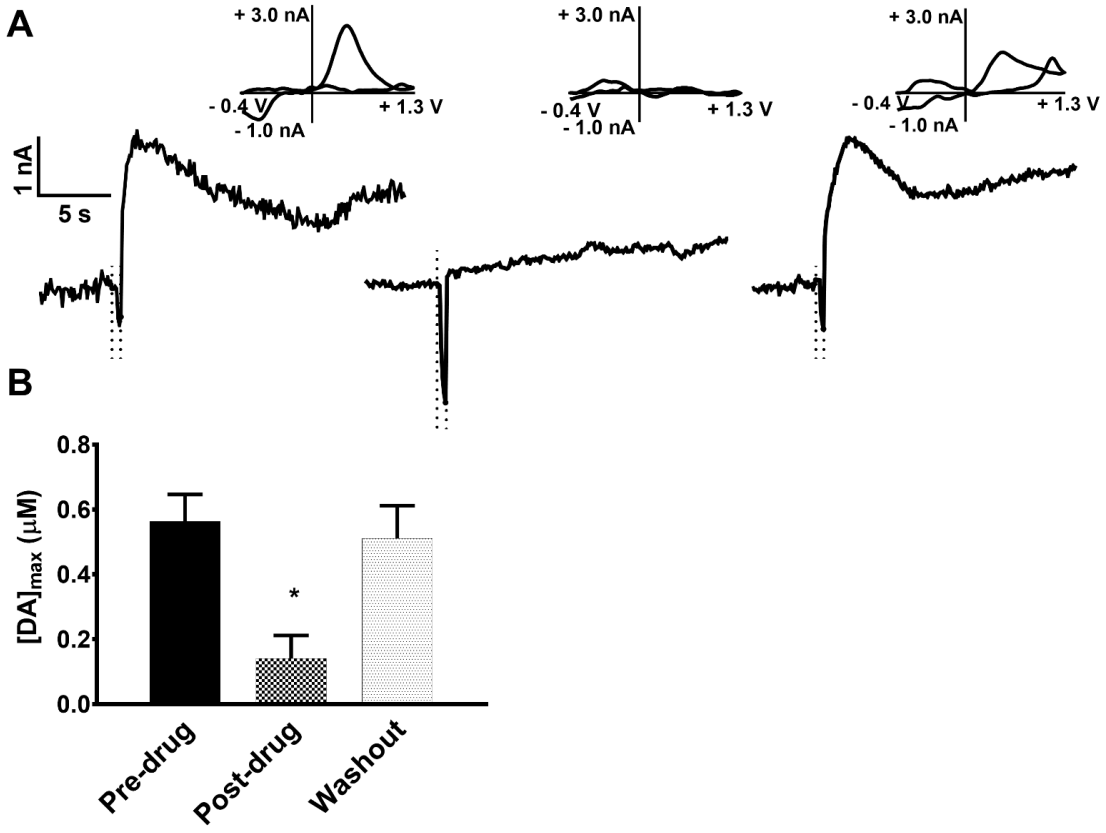

Figure 6. The effect of dopamine synthesis inhibition on stimulated release. (A) Representative data of stimulated dopamine release before (left) and after (center) administration of 50 μM αMPT. Dopamine release reappeared after a 1-hour washout with drug-free buffer solution in the same recording session (right). Cyclic voltammograms for each step (inserts) confirm the release of dopamine. The sharp dip in current prior to the faradaic peak is an artifact occurring due to stimulation. (B) Evoked dopamine release, measured after 2 hours of treatment with αMPT was significantly decreased (n=5, $p < 0.01$, one way ANOVA, tukey post hoc test *$p < 0.05$). Dopamine release after washout was not significantly different from the pre-drug measurement ($p = 0.40$, one way ANOVA, n=5). Stimulation time is indicated by the dotted lines.

Dopaminergic terminals in the mammalian striatum possess D2-family dopamine autoreceptors that serve as a regulatory feedback mechanism for dopamine release[23]. To determine if a similar self-regulatory mechanism is present in dopaminergic terminals of the subpallium, we perfused whole brain *ex vivo* preparations with 10 μM sulpiride, a D2-family dopamine receptor inhibitor (Fig. 7A). Approximately 1 hour after addition of drug, dopamine release increased by about 80% (pre-drug, 0.41 ± 0.12 μM; post-drug, 0.74 ± 0.13 μM, $p < 0.05$,

t-test). Thus, D2 receptors are also present in the zebrafish brain and appear to serve a similar regulatory function. However, given that the circuitry is still intact in the whole brain preparation, it is also possible that sulpiride may enhance the release of dopamine by antagonism of dopamine receptors located not only presynaptically, but also at other locations within the brain [34].

To determine if autoregulation by D2 receptors occurs specifically at terminals, electrically-evoked dopamine release was measured in the subpallium of sagittal and coronal brain slices before and after sulpiride treatment (Fig. 7B). The slicing process could at least partially disrupt the ascending dopaminergic pathway from the diencephalon to the subpallium, leaving only presynaptic terminals without dopaminergic soma [19a, 19b]. In sagittal slices, $[DA]_{max}$ appeared to increase upon drug treatment, but this increase was not statistically significant (pre-drug, 0.33 ± 0.12 µM; post-drug, 0.68 ± 0.29 µM, p = 0.13, n = 5 slices, t-test). Additionally, $[DA]_{max}$ also did not increase in coronal slice preparations (pre-drug, 0.35 ± 0.12 µM; post-drug, 0.38 ± 0.10 µM , p = 0.47, n = 5 slices, t-test). Our results suggests that, while there is an effect on D2 receptors in whole brains, this effect is disrupted in slice preparations. The reason for this lack of effect in fish is not well-understood; however, it is possible that the D2 receptors are not located presynaptically, but rather on the soma [34]. Given that D2 receptors are also found on the cell bodies and axon in rodents, this arrangement would not be unprecedented in zebrafish.[35] Another possibility is that the slicing process induces damage to the terminals. Additional studies will be required to identify the underlying mechanisms of this phenomenon.

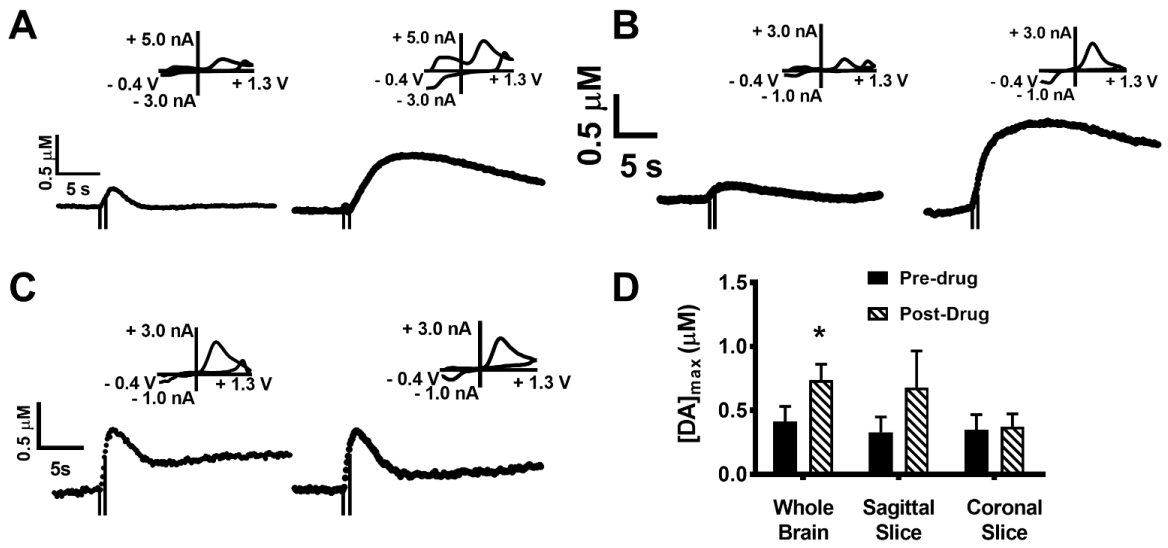

Figure 7. Effect of sulpiride treatment on dopamine release. Evoked dopamine release measured in (A) whole brain, (B) sagittal slice, and (C) coronal slice before and after treatment with 10 µM sulpiride. (D) Dopamine release significantly increased in whole brains (n=5, $p < 0.05$, t-test), but did not significantly increase in sagittal and coronal slices after drug treatment ($p = 0.13$ and $p = 0.47$, respectively, t-test, n= 5). Stimulation times are indicated by vertical lines on release plots.

3.3.4 Kinetics of neurotransmitter release and uptake.

The dopamine release curves in zebrafish whole brain preparations have several interesting characteristics: (1) the curves have a tendency to not return to baseline levels after the release event, (2) $[DA]_{max}$ is observed to occur a certain amount of time after the end of the electrical stimulation, a phenomenon known as overshoot (Δt_O), and (3) dopamine release sometimes appears to occur a very short time after electrical stimulation is initiated, a phenomenon known as lag (Δt_L). Figure 8A illustrates the concepts of overshoot and lag.

In addressing the first point, it was observed from the αMPT measurements that, after application of the inhibitor, the signal observed after the release event was greatly diminished (Fig 4). This phenomenon points to the non-return to baseline being related to the dopamine

initially released and not some secondary release events. From inspection of the CVs, it appears unlikely that the compound being detected is dopamine A chemical species we had considered was 3,4-dihydroxyphenylacetic acid (DOPAC). We had initially hoped to differentiate and identify this component using principal component analysis (PCA)[36]; however, PCA was unreliable in distinguishing between ascorbate, DOPAC, and dopamine in the zebrafish whole brain. This unreliability is probably due to the similarity of the compounds in the training set coupled with the complexity of the matrix. Further experiments will be required to completely resolve this issue.

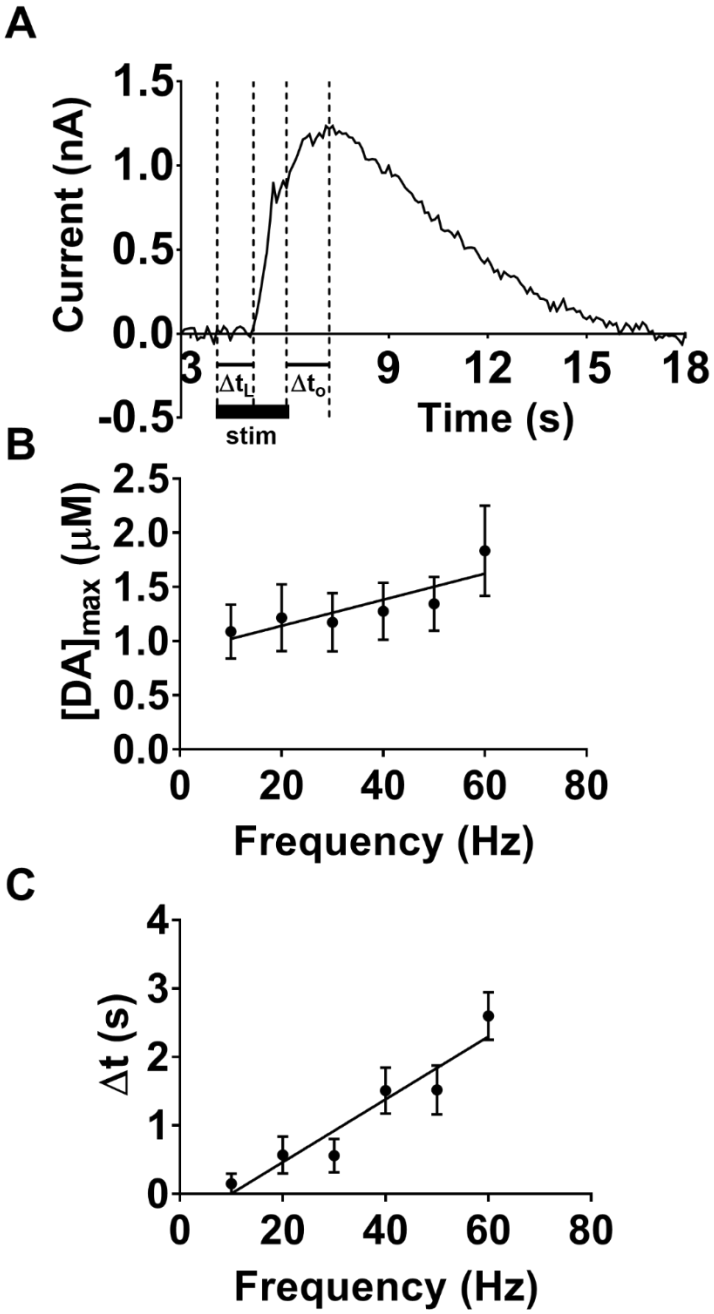

Figure 8 $[DA]_{max}$, lag time (Δt_L), and overshoot time (Δt_O). The concept of lag and overshoot is illustrated in (A). Lag (Δt_L) is the time after the stimulation begins until dopamine release is observed. Overshoot (Δt_O) is the time after the stimulation ends until $[DA]_{max}$ is reached. The duration of stimulation is indicated by the dark line below the release plot. The effect of increasing stimulation frequency on $[DA]_{max}$ (B) and Δt_O (C) is shown. Linear regression analysis showed that both parameters increased with respect to frequency with non-zero slopes (B, slope $\neq 0$ $p < 0.05$, $R^2 = 0.725$; C, slope $\neq 0$ $p < 0.005$, $R^2 = 0.908$ respectively).

In addressing points (2) and (3), it is important to note that overshoot and lag are phenomena also observed in rodents both *in vivo* and *ex vivo* [37]. The concepts of overshoot and lag are explained by the tendency for released dopamine to diffuse from synapse to the electrode; thus, we hypothesize that the time needed for this diffusion leads to Δt_O and Δt_L (Fig 8A) [38]. In order to examine the possible relationship between diffusion and Δt_O and Δt_L in zebrafish whole brain, the stimulation frequency was varied from 10 to 60 Hz while other stimulation parameters were held constant (120 pulses, 350 μA, 4 ms). If simple diffusion is all that is involved, it would be expected that Δt_O and Δt_L would be similar in magnitude and would remain constant while stimulation parameters change. [38a, 39] This is because in the so called diffusion gap model (Equation 1), diffusion is assumed to be independent of any variable except the distance between the electrode (represented by x) and site of release.

$$\frac{d[DA]}{dt} = D\,\frac{\partial^2[DA]}{\partial x^2} + [DA]_p f - \frac{V_{max}[DA]}{[DA] + K_M} \quad (Equation\ 1)$$

In this equation, V_{max} and K_M are the Michaelis–Menten parameters, *f* is stimulation frequency, [DA] is the concentration of dopamine at any given point in time, $[DA]_p$ is the amount of dopamine release per electrical stimulus pulse, a parameter that is corrected for uptake and electrode performance [40], and D is the diffusion coefficient of dopamine. The first term on the right side is from Fick's Second Law[41] and accounts for diffusion of dopamine to the electrode, the second term accounts for the total amount of dopamine released, and the third term accounts for dopamine uptake[40]

When the model is applied, a gap width is used that represents the distance between the electrode and the point of release[38a]. As this gap increases, the lag and overshoot should increase

by approximately equal amounts. On the other hand, if the gap remains the same the lag and overshoot should be approximately constant. We observed that, as the stimulation frequency was increased and the electrode was held in place, both concentration and Δt_O increased in a linear fashion (slope $\neq 0$, $p < 0.05$, $R^2 = 0.73$; slope $\neq 0$ $p < 0.005$, $R^2 = 0.908$ respectively, Figs. 8B and C). As $[DA]_{max}$ is increasing, Δt_O is also increasing. This result directly contradicts the prediction of the diffusion gap model that Δt_O should remain constant[38a]. It is also important to note that, in the vast majority of traces, we did not observe a Δt_L greater than the 100 ms temporal resolution of our method (data not shown), which also points to the diffusion gap model as not holding; therefore, another model must be considered.

This phenomenon of Δt_O being present and independent of Δt_L, and sensitive to the change in stimulation parameters, has been observed by Taylor *et al.* [42] in rats treated with nomifensine. In particular, as dopamine concentration increased due to inhibition of DAT, Δt_O also increased while Δt_L was nonexistent. They explained this phenomenon through a restricted diffusion model[38a]. Briefly, this model assumes that dopamine needs to diffuse to the electrode through tissue, so that that diffusion will not be unhindered, but rather will be interfered with by various characteristics of the tissue such as tortuosity[43] or absorption to specific sites in the tissue[44]. During a release event in the absence of drug, reuptake is much faster than the restricted diffusion so the dopamine that is restricted gets uptaken before it has a chance to move to the electrode, resulting in a small or nonexistent Δt_O. However, after nomifensine treatment, since uptake is significantly slowed, the restricted dopamine molecules are able to diffuse to the electrode for a relatively long time and Δt_O becomes large.

In zebrafish, it is unclear what the amplitude of a naturally occurring transient is; however, we propose that, in the case of stimulated release, the amount of dopamine released is

so great that DAT becomes saturated. This saturation causes dopamine to remain in the tissue for a long period of time. During this time, it can diffuse, resulting in the large Δt_O we observe. More experiments are needed to verify this hypothesis; however, our data clearly show that, in zebrafish, the issue of diffusion and its role in regulation of dopamine concentration is complex.

3.3.5 Effect of stimulation frequency on evoked dopamine release.

The degree of dopamine release is determined, in part, by the number of stimulus pulses and the frequency (number of biphasic pulses applied per second) [45]. Initially, to determine if alteration of stimulation frequency impacts dopamine release similarly in zebrafish, evoked dopamine both in whole brain and sagittal slices was measured and compared at frequencies ranging from 5 Hz to 25 Hz while other stimulus parameters were held constant (120 pulses, 4 ms, and 350 µA; Fig. 8).

We found a trend of increasing dopamine release up to a frequency of 25 Hz in whole brain. Although there appears to be a slight curvature, linear regression analysis revealed a strong correlation coefficient of linearity (R^2=0.96) and also a significantly non-zero slope ($p = 0.003$). In slices, dopamine release increased at 10 Hz; however, beyond 10 Hz, the curve flattened out (R^2=0.17). The overall slope of this curve did not significantly deviate from zero ($p = 0.49$). The difference in curves may suggest that the preparation impacts the availability of vesicles for release. Indeed, progressively diminishing increases of dopamine release [14e] were observed in rodent brain slices and linear increases were observed *in vivo* [46] when stimulation frequency was increased. While the causes underlying these differences are not known, it is possible that higher stimulation frequencies result in mobilization of reserve pool vesicles, as our previous results in striatal mouse brain slices have suggested [14e]. In fact, this decrease in release at higher frequencies was exaggerated in transgenic R6/2 mice, which are commonly used to model

Huntington's disease (HD). Our previous results have suggested that this decrease is likely due to a diminished reserve pool in R6/2 mice. In the future, it will be interesting to determine if these differences between slices and whole brain arise from a diminished reserve pool or have some other cause.

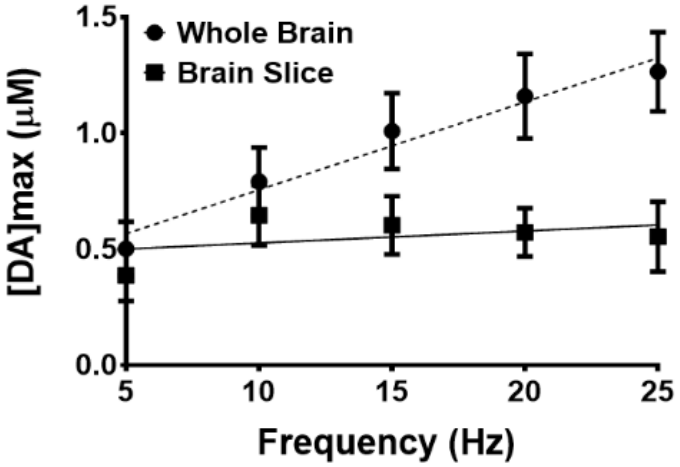

Figure 9. Effect of stimulation frequency on dopamine release. The stimulation frequency was increased while stimulation pulses and width were kept constant (120 pulses, 4 ms pulse duration). Evoked dopamine release was measured both in whole brain and sagittal slices. A linear regression was done for both preparations. The whole brain data had a significant non zero slope ($R^2 = 0.96$, $p = 0.003$) while the slice preparation was found to have no significant slope ($R^2 = 0.17$, $p = 0.49$).

3.4 Conclusion

We have shown that dopamine release can be easily measured with FSCV in the subpallium of zebrafish whole brain. This preparation offers the advantage of keeping the whole brain intact, thereby preserving the three-dimensional neuronal circuitry and offering the future possibility of measuring release evoked by stimulation of pathways. Similar to slices, extracellular dopamine levels are tightly regulated by uptake through the DAT. Our results also

demonstrate that uptake is inhibited by nomifensine in both brain slice and whole brain preparations.

Importantly, in their recent paper, Jones *et al.* showed that evoked neurotransmitter release could be easily measured in slices[13]. Our work has not only built upon these findings, but it has also revealed other release characteristics that are apparently not found in zebrafish sagittal slice preparations. We have identified important differences between slices (sagittal and coronal) and whole brain. For example, even though D2 autoreceptors regulate dopamine release in whole brain and sagittal slice preparations, similar to that observed in rodents, D2 antagonism has no effect in slices. Moreover, stimulated release in sagittal slices responded differently to increasing stimulation frequency compared to release in whole brain. Finally, stimulated release plots in the whole brain preparation had interesting features, including a tendency to not return to baseline following the stimulated release of dopamine and a propensity for dopamine release to continue even after the end of the electrical stimulus. It is apparent that these processes reflect complexities in zebrafish neuronal function that must be sorted out with additional studies. Moreover, our studies reveal not only that release measurements in whole brain is a viable option that may be of particular use in studying circuit function, but also that there are differences between whole brain, coronal slices, and sagittal slices that should be addressed before moving forward.

In summary, these results represent an important step toward more complex studies, such as FSCV experiments that make use of remote stimulation in zebrafish whole brain and measurements of dopamine release *in vivo*. Furthermore, the expanded use of this model organism will allow researchers to exploit the genetic advantages of zebrafish in the analysis of neurotransmitter release properties.

3.5 References

1. (a) Grunwald, D. J.; Eisen, J. S., Headwaters of the zebrafish -- emergence of a new model vertebrate. *Nat Rev Genet* **2002,** *3* (9), 717-24; (b) Williams, R., Thanks be to zebrafish. *Circ Res* **2010,** *107* (5), 570-2; (c) Li, H.-h.; Huang, P.; Dong, W.; Zhu, Z.-y.; Liu, D., A brief history of zebrafish research-toward biomedicine. *Yichuan* **2013,** *35* (4), 410-420.

2. (a) Friedrich, R. W.; Jacobson, G. A.; Zhu, P., Circuit Neuroscience in Zebrafish. *Curr. Biol.* **2010,** *20* (8), R371-R381; (b) Fetcho, J. R.; Liu, K. S., Zebrafish as a Model System for Studying Neuronal Circuits and Behaviora. *Annals of the New York Academy of Sciences* **1998,** *860* (1), 333-345.

3. Kimmel, C. B.; Ballard, W. W.; Kimmel, S. R.; Ullmann, B.; Schilling, T. F., Stages of embryonic development of the zebrafish. *Developmental dynamics : an official publication of the American Association of Anatomists* **1995,** *203* (3), 253-310.

4. (a) Ahrens, M. B.; Li, J. M.; Orger, M. B.; Robson, D. N.; Schier, A. F.; Engert, F.; Portugues, R., Brain-wide neuronal dynamics during motor adaptation in zebrafish. *Nature* **2012,** *485* (7399), 471-477; (b) Higashijima, S.-i.; Masino, M. A.; Mandel, G.; Fetcho, J. R., Imaging neuronal activity during zebrafish behavior with a genetically encoded calcium indicator. *J Neurophysiol* **2003,** *90* (6), 3986-97.

5. Randlett, O.; Wee, C. L.; Naumann, E. A.; Nnaemeka, O.; Schoppik, D.; Fitzgerald, J. E.; Portugues, R.; Lacoste, A. M.; Riegler, C.; Engert, F., Whole-brain activity mapping onto a zebrafish brain atlas. *Nature Methods* **2015,** *12* (11), 1039-1046.

6. Qin, Z.; Lewis, J.; Perry, S., Zebrafish (Danio rerio) gill neuroepithelial cells are sensitive chemoreceptors for environmental CO2. *The Journal of physiology* **2010,** *588* (5), 861-872.

7. Rothenaigner, I.; Krecsmarik, M.; Hayes, J. A.; Bahn, B.; Lepier, A.; Fortin, G.; Götz, M.; Jagasia, R.; Bally-Cuif, L., Clonal analysis by distinct viral vectors identifies bona fide neural stem cells in the adult zebrafish telencephalon and characterizes their division properties and fate. *Development* **2011,** *138* (8), 1459-1469.

8. (a) Baraban, S.; Taylor, M.; Castro, P.; Baier, H., Pentylenetetrazole induced changes in zebrafish behavior, neural activity and c-fos expression. *Neuroscience* **2005,** *131* (3), 759-768; (b) Baraban, S. C., Forebrain electrophysiological recording in larval zebrafish. *Journal of visualized experiments : JoVE* **2013,** (71).

9. (a) Venton, B. J.; Wightman, R. M., Psychoanalytical electrochemistry: dopamine and behavior. *Analytical Chemistry* **2003,** *75* (19), 414 A-421 A; (b) Hermans, A.; Keithley, R. B.; Kita, J. M.; Sombers, L. A.; Wightman, R. M., Dopamine detection with fast-scan cyclic voltammetry used with analog background subtraction. *Analytical chemistry* **2008,** *80* (11), 4040-4048; (c) Wightman, R. M., Probing cellular chemistry in biological systems with microelectrodes. *Science* **2006,** *311* (5767), 1570-1574; (d) Robinson, D. L.; Hermans, A.; Seipel, A. T.; Wightman, R. M., Monitoring rapid chemical communication in the brain. *Chemical reviews* **2008,** *108* (7), 2554-2584.

10. (a) Barnéoud, P.; Descombris, E.; Aubin, N.; Abrous, D. N., Evaluation of simple and complex sensorimotor behaviours in rats with a partial lesion of the dopaminergic nigrostriatal system. *European Journal of Neuroscience* **2000,** *12* (1), 322-336; (b) Cousins, M.; Salamone, J., Involvement of ventrolateral striatal dopamine in movement initiation and execution: a microdialysis and behavioral investigation. *Neuroscience* **1996,** *70* (4), 849-859.

11. Aarts, E.; van Holstein, M.; Cools, R., Striatal dopamine and the interface between motivation and cognition. *Frontiers in psychology* **2011,** *2*.

12. (a) Kelley, A. E.; Berridge, K. C., The neuroscience of natural rewards: relevance to addictive drugs. *The Journal of neuroscience* **2002,** *22* (9), 3306-3311; (b) Oei, N. Y.; Rombouts, S. A.; Soeter, R. P.; van Gerven, J. M.; Both, S., Dopamine modulates reward system activity during subconscious processing of sexual stimuli. *Neuropsychopharmacology* **2012,** *37* (7), 1729-1737.

13. Jones, L. J.; McCutcheon, J. E.; Young, A. M.; Norton, W. H., Neurochemical measurements in the zebrafish brain. *Frontiers in behavioral neuroscience* **2015,** *9*.

14. (a) Good, C. H.; Hoffman, A. F.; Hoffer, B. J.; Chefer, V. I.; Shippenberg, T. S.; Bäckman, C. M.; Larsson, N.-G.; Olson, L.; Gellhaar, S.; Galter, D., Impaired nigrostriatal function precedes behavioral deficits in a genetic mitochondrial model of Parkinson's disease. *The Faseb Journal* **2011,** *25* (4), 1333-1344; (b) Zhang, L.; Le, W.; Xie, W.; Dani, J. A., Age-related changes in dopamine signaling in Nurr1 deficient mice as a model of Parkinson's disease. *Neurobiol. Aging* **2012,** *33* (5), 1001.e7-1001.e16; (c) Robertson, G. S.; Robertson, H. A., Evidence that L-dopa-induced rotational behavior is dependent on both striatal and nigral mechanisms. *J. Neurosci.* **1989,** *9* (9), 3326-31; (d) Covey, D. P.; Garris, P. A., Using fast-scan cyclic voltammetry to evaluate striatal dopamine release elicited by subthalamic nucleus stimulation. *Conf Proc IEEE Eng Med Biol Soc* **2009,** *2009*, 3306-9; (e) Ortiz, A. N.; Kurth, B. J.; Osterhaus, G. L.; Johnson, M. A., Dysregulation of intracellular dopamine stores revealed in the R6/2 mouse striatum. *J. Neurochem.* **2010,** *112* (3), 755-761.

15. Yorgason, J. T.; España, R. A.; Jones, S. R., Demon voltammetry and analysis software: analysis of cocaine-induced alterations in dopamine signaling using multiple kinetic measures. *Journal of neuroscience methods* **2011,** *202* (2), 158-164.

16. (a) Fukuda, A.; Czurko, A.; Hida, H.; Muramatsu, K.; Lenard, L.; Nishino, H., Appearance of deteriorated neurons on regionally different time tables in rat brain thin slices maintained in physiological condition. *Neurosci. Lett.* **1995,** *184* (1), 13-16; (b) Buskila, Y.; Breen, P. P.; Tapson, J.; van Schaik, A.; Barton, M.; Morley, J. W., Extending the viability of acute brain slices. *Sci. Rep.* **2014,** *4*, 5309; (c) Richerson, G. B.; Messer, C., Effect of composition of experimental solutions on neuronal survival during rat brain slicing. *Exp. Neurol.* **1995,** *131* (1), 133-43.

17. (a) Ullrich, C.; Daschil, N.; Humpel, C., Organotypic vibrosections: novel whole sagittal brain cultures. *J Neurosci Methods* **2011,** *201* (1), 131-41; (b) Ferris, M. J.; Calipari, E. S.; Yorgason, J. T.; Jones, S. R., Examining the complex regulation and drug-induced plasticity of dopamine release and uptake using voltammetry in brain slices. *ACS chemical neuroscience* **2013,** *4* (5), 693-703 %@ 1948-7193.

18. Shang, C.-f.; Li, X.-q.; Yin, C.; Liu, B.; Wang, Y.-f.; Zhou, Z.; Du, J.-l., Amperometric Monitoring of Sensory-Evoked Dopamine Release in Awake Larval Zebrafish. *The Journal of Neuroscience* **2015,** *35* (46), 15291-15294.

19. (a) Rink, E.; Wullimann, M. F., The teleostean (zebrafish) dopaminergic system ascending to the subpallium (striatum) is located in the basal diencephalon (posterior tuberculum). *Brain Res.* **2001,** *889* (1,2), 316-330; (b) Rink, E.; Wullimann, M. F., Connections of the ventral telencephalon (subpallium) in the zebrafish (Danio rerio). *Brain Res* **2004,** *1011* (2), 206-20; (c) Tay, T. L.; Ronneberger, O.; Ryu, S.; Nitschke, R.; Driever, W., Comprehensive catecholaminergic projectome analysis reveals single-neuron integration of zebrafish ascending and descending dopaminergic systems. *Nat. Commun.* **2011,** *2* (Jan.), 1-12, 12 pp.

20. Kile, B. M.; Walsh, P. L.; McElligott, Z. A.; Bucher, E. S.; Guillot, T. S.; Salahpour, A.; Caron, M. G.; Wightman, R. M., Optimizing the Temporal Resolution of Fast-Scan Cyclic Voltammetry. *ACS Chem. Neurosci.* **2012,** *3* (4), 285-292.

21. Cragg, S. J.; Greenfield, S. A., Differential autoreceptor control of somatodendritic and axon terminal dopamine release in substantia nigra, ventral tegmental area, and striatum. *J. Neurosci.* **1997,** *17* (15), 5738-5746.

22. Garris, P. A.; Christensen, J. R. C.; Rebec, G. V.; Wightman, R. M., Real-time measurement of electrically evoked extracellular dopamine in the striatum of freely moving rats. *J. Neurochem.* **1997,** *68* (1), 152-161.

23. Cooper, J. R.; Bloom, F. E.; Roth, R. H., *The biochemical basis of neuropharmacology*. Oxford University Press: 2003.

24. (a) Jones, S. R.; Gainetdinov, R. R.; Jaber, M.; Giros, B.; Wightman, R. M.; Caron, M. G., Profound neuronal plasticity in response to inactivation of the dopamine transporter. *Proceedings of the National Academy of Sciences* **1998,** *95* (7), 4029-4034; (b) Jones, S. R.; Joseph, J. D.; Barak, L. S.; Caron, M. G.; Wightman, R. M., Dopamine neuronal transport kinetics and effects of amphetamine. *Journal of neurochemistry* **1999,** *73* (6), 2406-2414.

25. (a) Vickrey, T. L.; Xiao, N.; Venton, B. J., Kinetics of the Dopamine Transporter in Drosophila Larva. *ACS chemical neuroscience* **2013,** *4* (5), 832-837; (b) Sabeti, J.; Adams, C. E.; Burmeister, J.; Gerhardt, G. A.; Zahniser, N. R., Kinetic analysis of striatal clearance of exogenous dopamine recorded by chronoamperometry in freely-moving rats. *Journal of neuroscience methods* **2002,** *121* (1), 41-52.

26. Richelson, E., Antidepressants: pharmacology and clinical use. *Treatments of psychiatric disorders* **1989,** *3*, 1773-1786.

27. Fuller, R. W.; Wong, D. T.; Robertson, D. W., Fluoxetine, a selective inhibitor of serotonin uptake. *Medicinal research reviews* **1991,** *11* (1), 17-34.

28. Lengyel, K.; Pieschl, R.; Strong, T.; Molski, T.; Mattson, G.; Lodge, N. J.; Li, Y.-W., Ex vivo assessment of binding site occupancy of monoamine reuptake inhibitors: methodology and biological significance. *Neuropharmacology* **2008,** *55* (1), 63-70.

29. Roubert, C.; Sagné, C.; Kapsimali, M.; Vernier, P.; Bourrat, F.; Giros, B., A Na+/Cl−-dependent transporter for catecholamines, identified as a norepinephrine transporter, is expressed in the brain of the teleost fish medaka (Oryzias latipes). *Molecular pharmacology* **2001,** *60* (3), 462-473.

30. Jones, S. R.; Gainetdinov, R. R.; Wightman, R. M.; Caron, M. G., Mechanisms of amphetamine action revealed in mice lacking the dopamine transporter. *Journal of Neuroscience* **1998,** *18* (6), 1979-1986.

31. Kastenhuber, E.; Kratochwil, C. F.; Ryu, S.; Schweitzer, J.; Driever, W., Genetic dissection of dopaminergic and noradrenergic contributions to catecholaminergic tracts in early larval zebrafish. *Journal of Comparative Neurology* **2010,** *518* (4), 439-458.

32. Shang, C. F.; Li, X. Q.; Yin, C.; Liu, B.; Wang, Y. F.; Zhou, Z.; Du, J. L., Amperometric Monitoring of Sensory-Evoked Dopamine Release in Awake Larval Zebrafish. *The Journal of neuroscience : the official journal of the Society for Neuroscience* **2015,** *35* (46), 15291-4.

33. Jones, L. J.; McCutcheon, J. E.; Young, A. M.; Norton, W. H., Neurochemical measurements in the zebrafish brain. *Front Behav Neurosci* **2015,** *9*, 246.

34. Boehmler, W.; Obrecht-Pflumio, S.; Canfield, V.; Thisse, C.; Thisse, B.; Levenson, R., Evolution and expression of D2 and D3 dopamine receptor genes in zebrafish. *Developmental dynamics* **2004,** *230* (3), 481-493.

35. Ford, C. P., The role of D2-autoreceptors in regulating dopamine neuron activity and transmission. *Neuroscience* **2014,** *282*, 13-22.

36. (a) Heien, M. L.; Johnson, M. A.; Wightman, R. M., Resolving neurotransmitters detected by fast-scan cyclic voltammetry. *Analytical chemistry* **2004,** *76* (19), 5697-5704; (b) Robinson, D. L.; Wightman, R. M., Rapid dopamine release in freely moving rats. **2007**.

37. Taylor, I. M.; Ilitchev, A. I.; Michael, A. C., Restricted diffusion of dopamine in the rat dorsal striatum. *ACS chemical neuroscience* **2013,** *4* (5), 870-878.

38. (a) Walters, S. H.; Taylor, I. M.; Shu, Z.; Michael, A. C., A novel restricted diffusion model of evoked dopamine. *ACS chemical neuroscience* **2014,** *5* (9), 776-783; (b) Hoffman, A. F.; Spivak, C. E.; Lupica, C. R., Enhanced Dopamine Release by Dopamine Transport Inhibitors Described by a Restricted Diffusion Model and Fast-Scan Cyclic Voltammetry. *ACS chemical neuroscience* **2016**.

39. Wightman, R.; Amatorh, C.; Engstrom, R.; Hale, P.; Kristensen, E.; Kuhr, W.; May, L., Real-time characterization of dopamine overflow and uptake in the rat striatum. *Neuroscience* **1988,** *25* (2), 513-523.

40. Johnson, M. A.; Rajan, V.; Miller, C. E.; Wightman, R. M., Dopamine release is severely compromised in the R6/2 mouse model of Huntington's disease. *Journal of neurochemistry* **2006,** *97* (3), 737-746.

41. (a) Peters, J. L.; Michael, A. C., Modeling voltammetry and microdialysis of striatal extracellular dopamine: the impact of dopamine uptake on extraction and recovery ratios. *Journal of neurochemistry* **1998,** *70* (2), 594-603; (b) Peters, J. L.; Michael, A. C., Changes in the kinetics of dopamine release and uptake have differential effects on the spatial distribution of

extracellular dopamine concentration in rat striatum. *Journal of neurochemistry* **2000,** *74* (4), 1563-1573.

42. Mitch Taylor, I.; Jaquins-Gerstl, A.; Sesack, S. R.; Michael, A. C., Domain-dependent effects of DAT inhibition in the rat dorsal striatum. *Journal of neurochemistry* **2012,** *122* (2), 283-294.

43. Hrabětová, S.; Nicholson, C., Contribution of dead-space microdomains to tortuosity of brain extracellular space. *Neurochemistry international* **2004,** *45* (4), 467-477.

44. Hrabětová, S.; Masri, D.; Tao, L.; Xiao, F.; Nicholson, C., Calcium diffusion enhanced after cleavage of negatively charged components of brain extracellular matrix by chondroitinase ABC. *The Journal of physiology* **2009,** *587* (16), 4029-4049.

45. Wu, Q.; Reith, M. E. A.; Wightman, R. M.; Kawagoe, K. T.; Garris, P. A., Determination of release and uptake parameters from electrically evoked dopamine dynamics measured by real-time voltammetry. *J. Neurosci. Methods* **2001,** *112* (2), 119-133.

46. Kraft, J.; Osterhaus, G.; Ortiz, A.; Garris, P.; Johnson, M., In vivo dopamine release and uptake impairments in rats treated with 3-nitropropionic acid. *Neuroscience* **2009,** *161* (3), 940-949.

Chapter 4 Chemotherapy Treatment in Zebrafish

I collected a portion of the release data and I independently collected the Atomic absorption and modelling data

Abstract

In this chapter, we present work on the effects of chemotherapy treatment on zebrafish dopamine neurotransmission. We treated zebrafish with 5-fluorouracil and carboplatin either through their food or their habitat water. It was found that both drugs had an effect on the release in zebrafish whole brains *ex vivo.* A difference between treatment pathways was also discovered. We showed that platinum did not accumulate in the brain after carboplatin treatment. Finally, we showed that there was no significant difference in uptake between control and treated zebrafish.

4.1 Introduction

Post chemotherapy cognitive impairment, also known as 'chemobrain,' is a neurological condition characterized by a decrease in higher level cognitive and executive function well after the conclusion of the treatment regime[1]. Although the underlying causes of chemobrain are not well understood, mechanisms that have been proposed include chemotherapy-induced DNA damage, disruption of vascular blood flow in the brain[2], inflammatory responses to reactive oxygen species[3, 4] , brain protein modification[5, 6] and impairment of neurotransmitter signals[7, 8].

Recent *in vivo* studies of chemobrain have primarily made use of rats and mice[9]. For example, in our own work, we used fast-scan cyclic voltammetry at carbon-fiber microelectrodes (FSCV) to show that dopamine and serotonin release and cognitive performance were impaired in rats treated with carboplatin[8], a chemotherapeutic agent commonly used in the treatment of cancers of the head, neck, breast, and lung[10, 11]. Although rodents have shown tremendous utility in understanding the cellular processes that underlie chemobrain, their use has drawbacks, including chemotherapy regimen treatment times typically on the order of weeks, the

requirement of i.v. injection of many chemotherapeutic agents, and the need for larger quantities of study compounds to be evaluated as potential therapies. These disadvantages make the evaluation of chemotherapeutic agents on neuronal function, as well as the testing of potential therapies, more difficult by decreasing throughput and increasing costs.

The zebrafish (*Danio rerio*), a teleost originally used to study development, has recently emerged as a useful model of neurochemical signaling[12, 13] and toxicology[14, 15]. As a model of neuronal function, zebrafish represent an ideal compromise between brain complexity, with about ~10 million cells[16], and small size, which allows *ex vivo* studies of whole brain in a perfusion chamber [17]. Zebrafish are useful for toxicological evaluation studies because dosing often requires only adding agents to the water or food, and behavioral and neurochemical analyses can be carried out with greater throughput[18, 19] .

Recently, our group demonstrated the feasibility of using zebrafish whole brain as a preparation for measuring dopamine release and uptake with FSCV [17]. In this work, we extend the application of this preparation toward the evaluation of carboplatin on dopamine release and uptake properties. Zebrafish were administered chemotherapeutic either by addition to their habitat water or their food and then dopamine release and uptake was quantified in whole brain. This study revealed a strong influence of dosing regimen and exposure time on dopamine release. This work suggests that, similar to rats, zebrafish might be an effective model of neurotransmitter release impairment in chemobrain.

4.2 Methods

4.2.1 Drugs

Pharmaceutical grade carboplatin, 10 mg/mL (CD11650AA, Hospira, Lake Forest, IL, USA) and 0.9 % sterile saline (Nova-Tech Inc, Grand Island, NE, USA) solutions were used.

Dopamine was purchased from Sigma-Aldrich (St. Louis, MO, USA). Aqueous solutions were prepared with purified (18.2 MΩ) water. A modified artificial cerebrospinal fluid (aCSF) for zebrafish whole brain preparations consisted of 131 mM NaCl, 2mM KCl, 1.25 mM KH_2PO_4, 20 mM $NaHCO_3$, 2mM $MgSO_4$, 10 mM glucose, 2.5 mM $CaCl_2 \cdot H_2O$, and 10mM HEPES, and the pH was adjusted to 7.4.

4.2.2 Brain preparation

All animal procedures were approved by the University of Kansas Institutional Animal Care and Use Committee. Wild-type adult zebrafish, originally purchased from AquariumFish.net, were housed 20 fish per 2L tank in the University of Kansas Molecular Probes Core (KU-MPC). Zebrafish were maintained on a light dark cycle with a 16 hour light phase and 8 hour dark phase. The temperature of the recirculating water system was maintained at 26℃.

Wholes brains were harvested as previously described[17]. Briefly, for a given experiment, a zebrafish was euthanized by hypothermic shock and decapitated using a 0.009" single edge razor blade (VWR Corporates, Radnor, PA, USA). The head was transferred to a prepared dissection pad made of 2% agarose (BioReagent graded agarose, Sigma-Aldrich, St. Louis, MO, USA) in a 100mm x 15mm petri dish (ThermoFisher Scientific, Waltham, MA, USA). The petri dish was filled with oxygenated (95% O2/5% CO2) ice-cold modified artificial cerebral spinal fluid. The head was then immobilized by pinning it to the agar with a syringe needle. The skull of the zebrafish was carefully removed using forceps, and the brain was removed with a pulled capillary and transferred to the recording chamber, which was perfused with oxygenated-modified aCSF kept at a physiological temperature of 28℃.

4.2.3 Chemotherapy treatment

For chemotherapy exposure through the water environment, fish were housed in 1 L of water to which pharmaceutical grade carboplatin in 0.9% saline (10 mg/mL) was added so that the final concentration of carboplatin was 100 µM. Control fish were housed in 1 L of water treated with an equal volume of 0.9% sterile biological saline. The fish were exposed continuously for 1, 4 or 7 days. Fresh solutions were made every 48 hours.

The oral treatment procedure consisted of soaking 1 g of thawed, strained brine shrimp (San Francisco Bay Brand INC, Newark, CA, USA) for 30 minutes in carboplatin or saline to give the food a drug concentration of 20 mg drug/g of shrimp. A total weight 0.25 g of this shrimp was then added to the habitat water for a 3-minute period, allowing the fish to feed prior to being removed to clean habitat water. This treatment was carried out for 1, 4 or 7 days, after which the fish were sacrificed and analyzed.

4.2.4 Electrochemistry

Cylindrical carbon fiber microelectrodes were fabricated as previously described[20]. Briefly, a 7 µm diameter carbon fiber (Goodfellow Cambridge LTD, Huntingdon, UK) was aspirated into glass capillary tubes (1.2 mm D.D and 0.68 mm I.D, 4 in long; A-M System Inc, Carlsborg, WA, USA). Loaded capillaries were then pulled using a PE-22 heated coil puller (Narishige Int. USA, East Meadow, NY, USA). Pulled carbon fibers were trimmed to a length of 50 to 70 µm from the pulled glass tip. To seal the carbon fiber, electrodes were dipped into epoxy resin (EPON resin 815C and EPIKURE 3234 curing agent, miller-Stephenson, Danbury, CT, USA) and cured at 100℃ for 1 hour.

Electrochemical measurements were collected and analyzed using an electrochemical workstation consisting of a Dagan Chem-Clamp potentiostat (Dagan, Minneapolis, MN, USA),

modified to allow gain settings down to 200 nA/V, a personal computer with TarHeel CV software (provided by R.M. Wightman, University of North Carolina, Chapel Hill, NC, USA), a breakout box, and two National Instruments computer interface cards, PCI 6052 and PCI 6711 (National Instruments, Austin, TX, USA).

During a typical recording session, the brain was allowed to equilibrate in the perfusion chamber for a period of one hour. A carbon-fiber microelectrode and two stimulating electrodes (A-M System Inc, Carlsberg, WA, USA) were micromanipulated into a whole zebrafish brain as previously discussed[17]. The carbon-fiber microelectrode was positioned 50 – 100 µm laterally from the medial olfactory tract (MOT) and inserted about 280 – 300 µm deep. The stimulating electrodes were placed at the center of ventral telencephalon and inserted about 100 µm into the brain so that the carbon-fiber microelectrode was positioned between stimulating electrodes.

To evoke dopamine release, a stimulation train of 35 electrical pulses (350 µA stimulating current, 4 ms of total duration, frequency of 60 Hz) was applied. Evoked dopamine release was measured using a triangular waveform of – 0.4 V to + 1.3 V to – 0.4 V at a scan rate of 400 V/s applied at a 10 Hz frequency. After stimulation and dopamine detection, the brain was allowed a 10 minute resting period before the next stimulation event was applied. Evoked dopamine released was measured from either treated fish brain or control fish brain for 1 hour. Electrodes were pre-calibrated and post-calibrated against standard dopamine solutions. The average of the pre- and post-calibration was used to convert measured current in the brain to dopamine concentration.

4.2.5 Atomic Absorption Spectroscopy

Procedures based on those previously described were used.[21] Briefly, a calibration curve was prepared by making solutions of carboplatin in water. The samples were analyzed using a

flameless method. A 10 µL sample was injected into a graphite furnace (Analytical West, Corona Ca, USA) and a heating regime of a 30 s at 125 ºC, a 20 s ramp to 1500 ºC, 30 s held at 1500 ºC followed by 8 s at 2700 ºC was run. Data was collected using a hollow cathode lamp specific for Pt (Phrotron LTD, Victoria, Australia) measuring at 265.95 nm.

4.2.6 Preparation of brain homogenates

Brains were collected after treatment with carboplatin (whole brains for the zebrafish and hemispheres for the rat brains) and frozen on dry ice. The brains were then stored at -80 ºC until they were analyzed. Homogenates were prepared by mixing the brain tissue with water at a ratio of 1 gram of wet tissue weight with 1 mL of water. This mixture was homogenized using a dounce homogenizer. The homogenized mixture was then centrifuged for 15 minutes and the supernatants were used for analysis.

4.2.7 Data analysis and statistics

All numerical values were represented as mean ± standard error of the mean (SEM). For all analyses, n is equal to the number of zebrafish brains used unless otherwise noted. GraphPad Prism 6 (GraphPad Software Inc, La Jolla, CA, USA) was used to conduct statistical calculations and to present data. The modelling was achieved by analyzing the raw data to determine the point of maximum dopamine signal after stim and the point where that signal has decayed by 80%. This decay curve is then fit with the 1st order exponential decay equation $A_t = A_{max}\, e^{-kt}$. A_{max} is held constant at the experimentally determined value and k, the 1st order rate constant, is allowed to float. The accuracy of the fit is determined by using a Pearson coefficient with a cut off of $R \geq 0.8$ being used. Once this k is determined the half-life of the decay is then calculated using the equation $t_{1/2} = 0.6932/k$. All data analysis and curve fitting was done using GraphPad Prism 6 (GraphPad Software Inc, La Jolla, CA, USA)

4.3 Results and Discussion

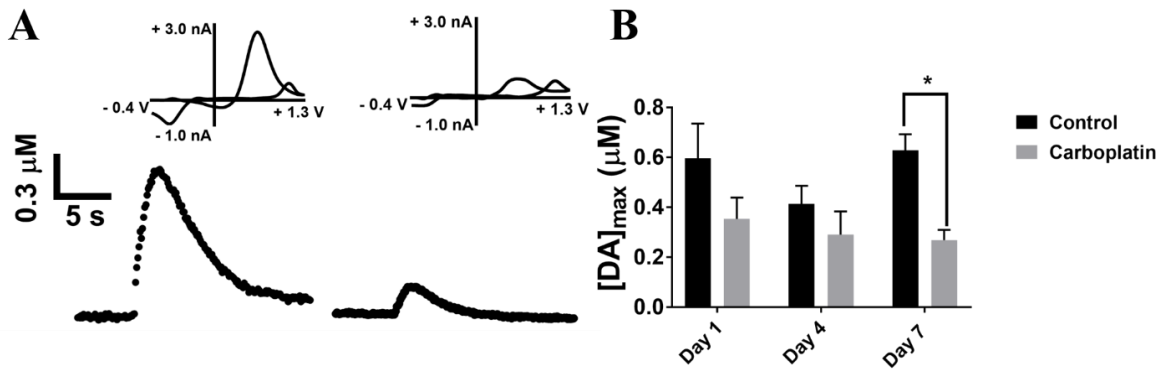

Fig. 1 (A) Shows representative data for the control group and 7 days after 100 µM carboplatin treatment. The cyclic voltammagrams in both cases indicate that the neurotransmitter measured is dopamine. (B) Pooled dopamine concentration data for water treatment with 100 µM, there is a significant drug effect observed ($p < 0.05$ two-way ANOVA n = 5 brains) there is also a significant difference in release observed between the control and 7 day treatment groups (Sidak's test * p, 0.05 n = 5 brains).

4.3.1 Carboplatin water treatment**.**

Recently, our group showed that, in rats, the chemotherapeutic agent carboplatin caused a marked attenuation of dopamine release coupled with behavioral changes related to cognitive decline[8]. With these results in mind, we repeated the drug treatment and neurochemical measurements in zebrafish. In the initial experiments, zebrafish were treated through direct addition of either 100 µM carboplatin or an equal volume of biological saline into their habitat water and neurochemical measurements were taken from *ex vivo* whole brain preparations either 1, 4 , or 7 days after continuous treatment. As shown in Figures 1A and B, release changed significantly until after 7 days of continuous treatment.

Data from multiple fish were analyzed and a significant decrease in dopamine release was found after 7 days of treatment (two-way ANOVA, overall drug effect, $p < 0.05$; Sidak's multiple comparison test: 1-day 0.60 ± 0.14 µM control, 0.35 ± 0.09 µM treated, $p = 0.017$; 4-day 0.41 ± 0.07 µM control, 0.29 ± 0.09 µM treated, $p = 0.70$; 7-day 0.63 ± 0.06 µM control,

0.27 ± 0.04 µM treated, $p < 0.05$, n = 5 brains). This decrease is consistent with previously published results in which rats were treated with carboplatin over the course of four weeks and dopamine release was measured in brain slices[8].

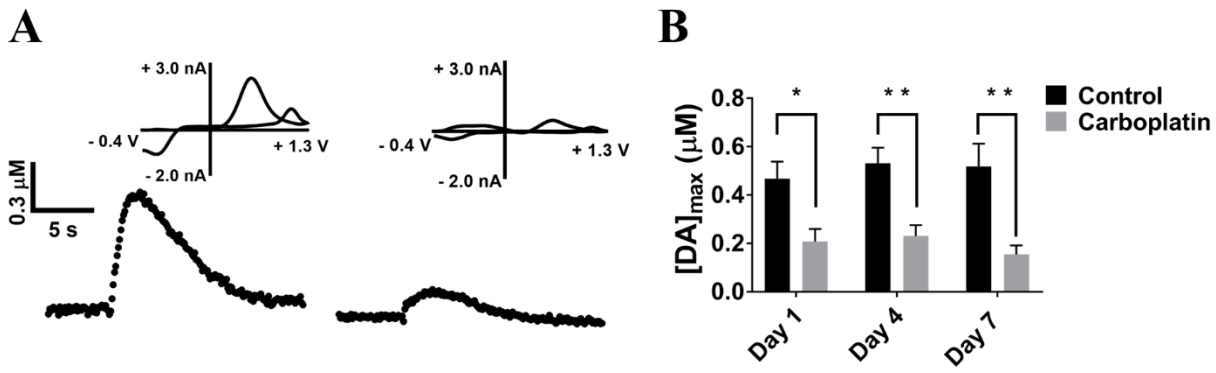

Fig. 2. (A) Representative data showing that there seems to be an attenuation in dopamine release after 7 days off food treatment. The cyclic voltammogram of the compound measured provides evidence that it is dopamine. (B) The pooled data shows a significant drug effect over the 7 days (two-way ANOVA $p < 0.0001$) as well as a significant decrease in the dopamine release after only 1 day that continues to be present at 4 and 7 days as well. (Sidak's test * $p < 0.05$, ** $P < 0.01$)

4.3.2 Carboplatin food treatment.

Although treatment through the water habitat resulted in an overall drug effect and a measurable decrease in dopamine release by day 7, we sought to determine a treatment method that would yield more robust results. While it has been shown that fish gills can accumulate unwanted metals in contaminated water, food contamination has been found in laboratory experiments to be the more important pathway for the delivery of molecules[22,23]; therefore, we administered the drug through their food. This was done for two reasons: 1) treatment through food is convenient and 2) carboplatin is known to cross the intestines in rodent models[24]. During this treatment, fish were fed brine shrimp with a concentration of 20 mg carboplatin/gram of drug once per day for 1, 4, or 7 days after which dopamine measurements were made from whole

zebrafish brain *ex vivo*. As shown in Figure 2 the representative data reveal a significant attenuation in the dopamine release after just one day of food treatment. This attenuation appears to remain constant even after further treatments. Analysis of multiple fish show a dose dependent change in dopamine release (Two-way ANOVA, overall drug effect, $p < 0.0001$; Sidak's multiple comparison test: 1-day 0.47 ± 0.07 µM control, 0.21 ± 0.05 µM, treated $p < 0.05$; 4-day 0.53 ± 0.065 µM control, 0.23 ± 0.045 µM treated, $p < 0.01$; 7-day 0.52 ± 0.094 µM control, 0.15 ± 0.037 µM treated, $p < 0.01$) that was significant compared to the control.

These phenomena suggests that the effect of carboplatin on dopamine release in zebrafish is similar to that of results in rodent animal models. However, when the chemotherapy drug was delivered orally, chemotherapy treatment was more efficient than when the drug was delivered by treating habitat water. This observed difference in release may be related to the amount of intact drug that reaches the animal. It is not clear how much carboplatin can cross the skin and enter the blood stream. As such, it is likely that the water-treated fish are receiving less than a 100 µM dose. During food treatment, since the fish are ingesting the drug instead of absorbing it through the skin, and it is known that carboplatin can cross the small intestine of rats[24], they are more likely to receive the entire intended dose leading to the observed increase in attenuation. This theory is supported by the fact that in the water-treated fish the significant changes were not observed until after day 7, whereas, in the shrimp-treated fish the effect was immediate (Figures 1 and 2).

4.3.3 Atomic absorption spectroscopy

Our data have clearly shown that there is a dose- and treatment pathway-dependent attenuation of dopamine release in zebrafish. Our next concern was to determine where the drug was accumulating during treatment. There is a debate in the literature about whether platinum-

based drugs can cross the blood brain barrier effectively without the aid of drugs that disrupt the blood brain barrier[25-27]. Thus, we sought to determine if the drug was crossing the blood brain barrier in zebrafish and, if it could, how much accumulated in the brain. In order to do this, we used flameless atomic absorption spectroscopy to measure the platinum in zebrafish whole brains.

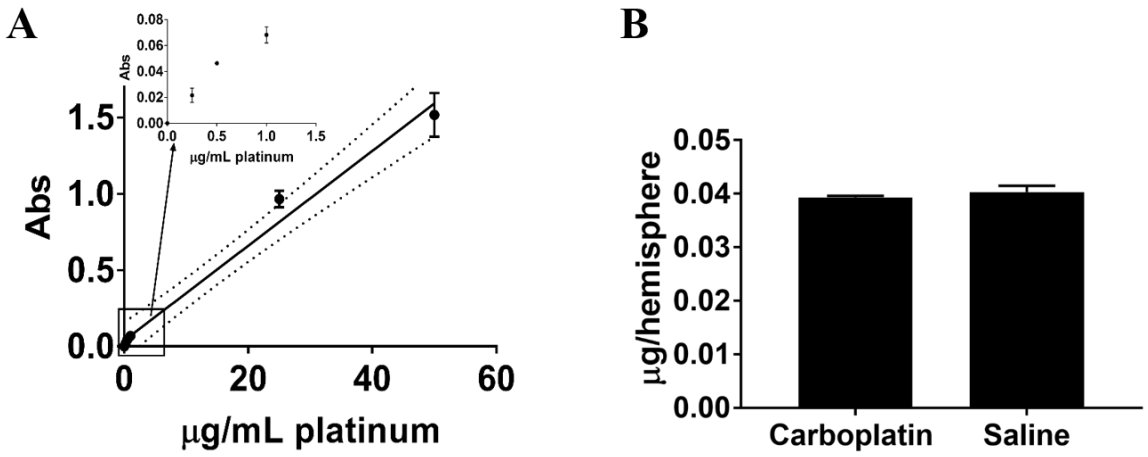

Figure 3: (A) Calibration curve for carboplatin in water measured by flameless atomic absorption spectroscopy. There is a linear relationship between concentration and response with significant positive slope ($p<0.0001$) and good correlation $R^2 = 0.99$. (B) Amount of platinum measured in rate brain hemispheres, there was no significant difference between the amount measured in saline vs carboplatin treated (n = 4 brains).

As shown in Figure 3 platinum was detectable in calibration samples making a curve with good linearity and a limit of detection of 20 ng/mL. When rat brain hemispheres were analyzed we found that, while there were observable peaks, these peaks were found in both the saline and treated samples. This conclusion is based on the finding that when the data are pooled the concentration measured is the same for both treatments groups (saline 0.040 $\pm$ 0.0001 µg/hemisphere; treated 0.039 $\pm$ 0.0003 µg/hemisphere, t-test, $p = 0.44$, n = 4 brains). Thus, the observed peaks likely arise from organic contaminants, suggesting that this method did not detect platinum in the treated rats.

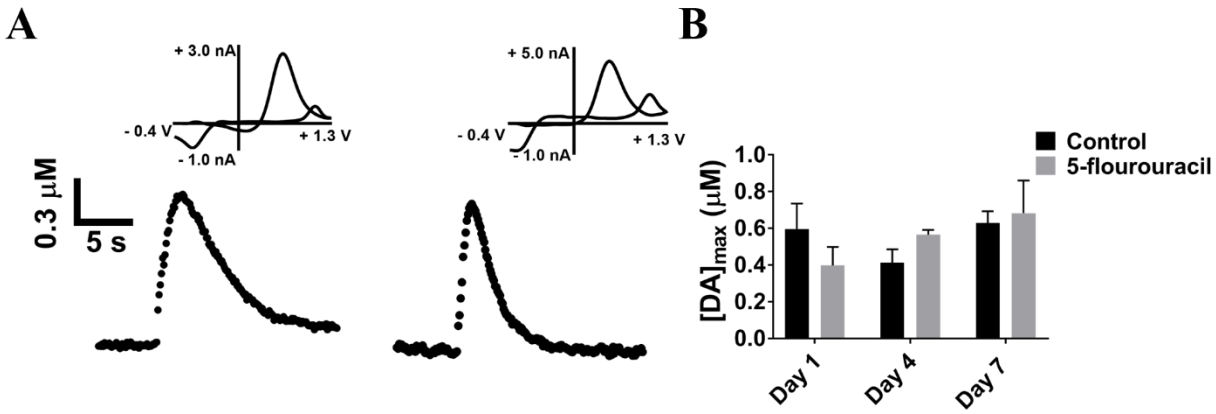

Figure 4 (A). Representative data for 5-FU water treatment after 7 days. The signal has not changed significantly and the CV continues to look like that of dopamine. (B) The pooled data shows no significant drug effect throughout the treatment (two way ANOVA p = 0.98 n= 5 brains)

4.3.4 5-fluorouracil water treatment.

Once we had established that carboplatin seemed to have a similar effect in zebrafish as it did in rats, we sought to extend our study to a second chemotherapeutic agent in order to see if it was a generalized effect, or if it was limited to carboplatin. The drug chosen was the chemotherapeutic agent 5-fluorouracil (5-FU), a derivative of uracil that can disrupt both protein formation as well as the synthesis of thymine.

For the initial water treatment, a regime was followed that matched the one used for carboplatin: 1, 4, or 7 days of constant exposure to 100 µM 5-FU followed by neurochemical measurements from whole brain preparations *ex vivo* using fast scan cyclic voltammetry. As can be seen from the representative data in Figure 4, panel A, dopamine is present; however, there is no significant change in dopamine release after 7 days. This observation is born out when the data is pooled with no observed drug effect (no significant drug effect, two way ANOVA p = 0.98, Sidak's multiple comparison test; 1-day 0.60 $\pm$ 0.14 µM control, 0.40 $\pm$ 0.10 µM treated p = 0.51; 4-day 0.41 $\pm$ 0.072 µM control, 0.565 $\pm$ 0.12 µM treated p = 0.70; 7-day 0.63 $\pm$ 0.064

μM control 0.68 ± 0.18 μM treated p = 0.978 n = 5 brains). Unlike carboplatin treatment, there was no significant effect observed after 7 days of 5-FU treatment. It is possible this lack of effect was because the animal's gills are more effective at filtering 5-FU then carboplatin. In any case based on our data, 5-FU does not cause a significant change in the release of dopamine after water treatment.

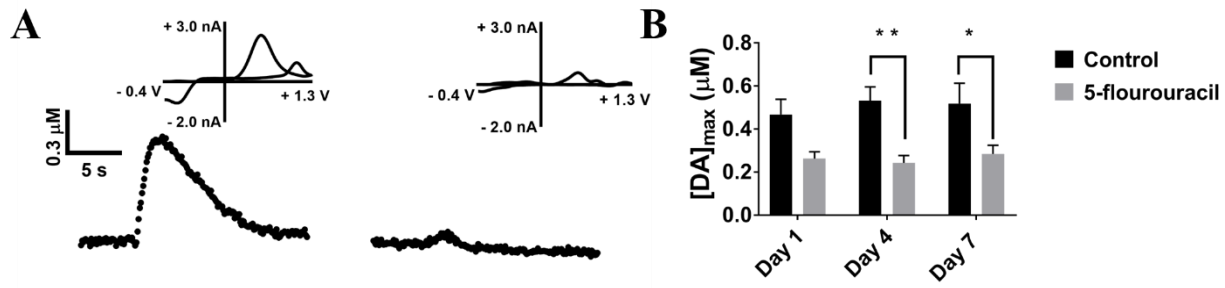

Figure 5 (A). Representative data for 5-FU treatment after 7 days. The signal has clearly been significantly attenuated while the CV continues to look like dopamine's. (B) The pooled data shows a significant drug effect throughout the treatment (two way ANOVA $p < 0.001$ n= 5 brains) while there are significant attenuations in the dopamine release after 4 and 7 days (* $p < 0.05$, ** $p < 0.01$ Sidak's multiple comparisons).

4.3.5 5-fluorouracil food treatment

It was found that water treatment did not cause a significant change in observed release. It is also important to note that, while there is extensive evidence for metal accumulation through and in the gills for organics, it is known that some organics cannot cross the barrier.[23] Also, it was found in LC50 experiments that 5-FU was nontoxic when it was administered through their habitat water[28]. Since more efficient uptake was observed in carboplatin after food treatment we treated the fish with 5-FU through their food.

For these experiments, similar to the carboplatin experiments, brine shrimp with a concentration of 20 mg 5-FU/ g of shrimp were fed to the zebrafish for 3 minutes a day for either 1, 4, or 7 days. The fish were then euthanized and neurochemical measurements were made form the whole brain *ex vivo* using fast scan cyclic voltammetry. As can be seen from the

representative data there appears to be a significant attenuation in release after 7 days (Figure 5 A). Pooled data reveal a significant drug effect observed over the treatment regime, with statistically significant effects observed after 1 day of treatment (significant drug affect two way ANOVA $p<0.001$, Sidak's multiple comparison test; 1-day 0.47 ± 0.071 µM control, 0.263 ± 0.032 µM treated $p = 0.073$; 4-day 0.53 ± 0.065 µM control, 0.243 ± 0.034 µM treated $p< 0.01$; 7-day 0.52 ± 0.094 µM control, 0.29 ± 0.040 µM treated $p <0.05$, $n = 5$ brains). These data agree well with what was observed in carboplatin treatment with both a significant drug effect as well as a significant attenuation after only 1 day.

Our data show that, for both carboplatin and 5-FU, the food treatment method displayed a quicker effect then the water data and in the case of 5-FU the only effect observed. This is an interesting phenomenon that may be occurring for several reasons. It is possible that the gills are able to efficiently filter out unwanted ions and small molecules such as Pt and 5-FU. This filtering could explain the much less pronounced effect for both of the compounds studied when they were delivered through the system water. It is also possible the effective concentration that the fish received from the food treatment was much higher than the concentration they received from the water treatment. It is difficult to estimate how much of the drug actually reached the fish because drug is allowed to diffuse away when the food hits the water. If the drug concentration is relatively higher for the food then the water treatment, it offers a possible explanation for the observed data.

Overall, we can make three conclusions with a high level of confidence from these data: (1) Chemotherapy treatment leads to an attenuation in dopamine release, similar to that observed in rats. (2) When administered through the habitat water, carboplatin has a greater effect on

dopamine release than 5-FU. (3) When administered by addition to food, carboplatin and 5-FU have approximately the same effect on release, decreasing it by ~ 60%.

4.3.6 Kinetics of dopamine release

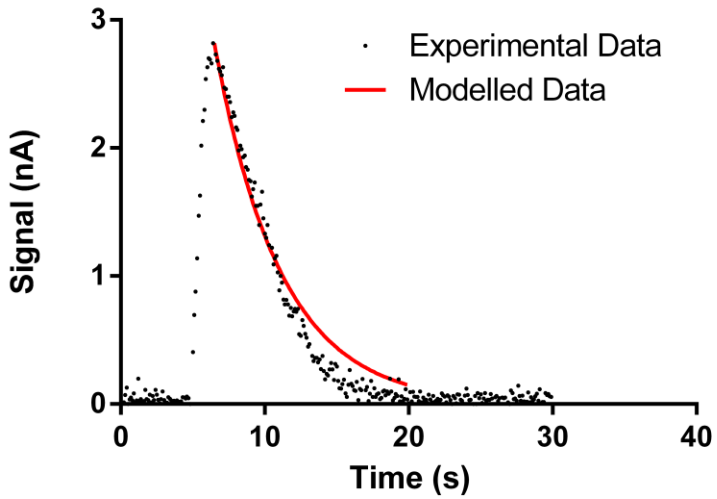

Figure 6: Representative figure showing the raw experimental data with the simulated data from the modeled parameters overlaid.

In the preceding sections it has been shown that chemotherapeutic treatment attenuates dopamine release in zebrafish. With this result in mind we wanted to determine if uptake was also affected by modelling the 1st order rate constant of uptake (k). Understanding uptake is important because of the influence it has on the length of time dopamine is available to activate signaling pathways as well as the peak concentration of extracellular dopamine observed. Both of these phenomena can cause the effects discussed above.

The red line in Figure 6 represents a fit of the release data from the point where maximum signal is observed to the point were 80% of the signal has disappeared. This fit is achieved using Equation 1

$A_t = A_{max}\, e^{-kt}$ **Equation 1**

In Equation 1, A_t is the signal at a given point of time, A_{max} is the maximum single observed, k is the 1st order rate constant for uptake and t is time[29, 30]. During the modelling, A_{max} was held at the experimentally determined value for the file of interest and k was allowed to float. The fit was determined to be valid if the modeled data had a Pearson coefficient greater than 0.8 when it was overlaid with the raw experimental data[29, 30]. The rate constant is a measure of the efficiency of the transporters as they uptake the released dopamine. This rate constant can also be used to calculate $t_{1/2}$ for the uptake of dopamine. The results of the modelling are shown in Figure 7.

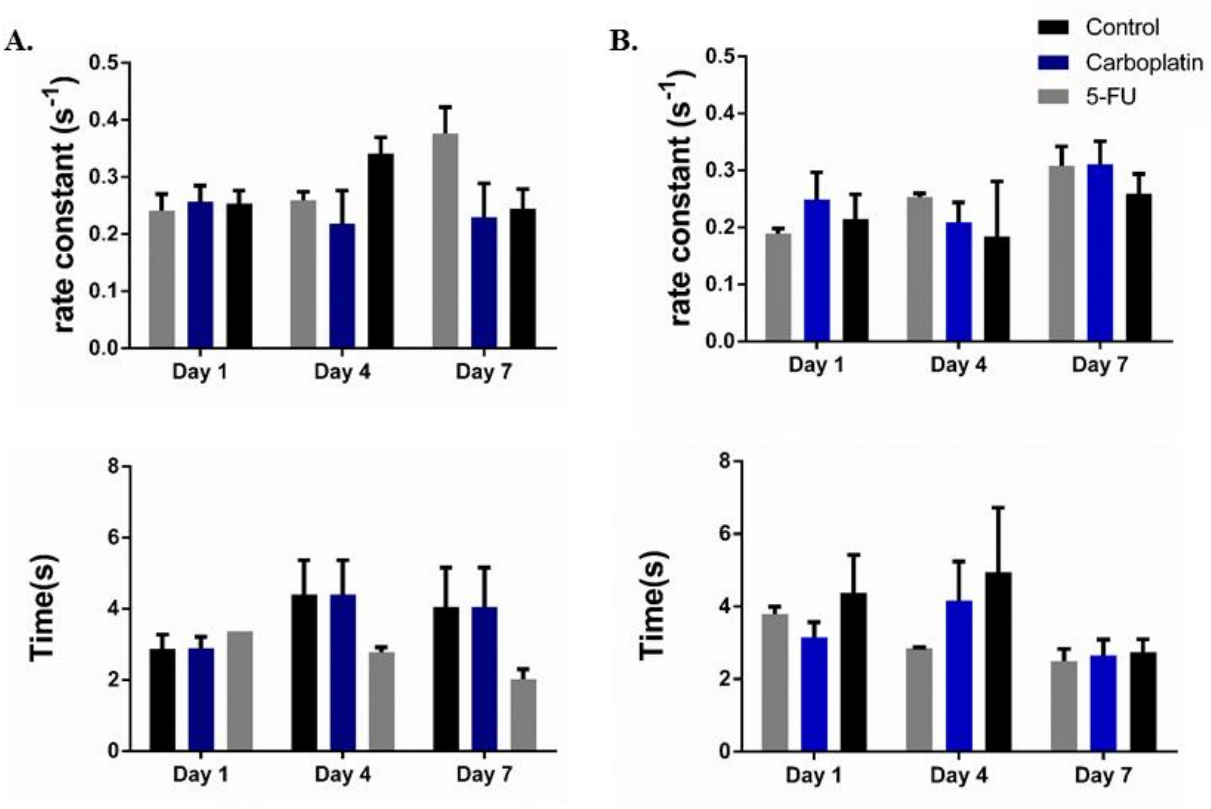

Figure 7. The averages of the 1st order rate constant (A and B top) and $t_{1/2}$ (A and B bottom) in both water (A) and shrimp treated (B) zebrafish over the treatment time. There was no significant difference observed in either treatment pathway or treatment time.

It was determined that there was no significant difference between any of the treatment groups. Since this was the case all the control data was pooled and an average k was determined to be $0.2418 s^{-1} \pm 0.018$ with an n of 25 fish. This value is much larger than the reported numbers for both rats (0.012 to 0.027 s^{-1})[30] and fruit flies (0.062 ± 0.004 s^{-1})[29] and, therefore, indicates a fast reuptake in the zebrafish when compared to these species. We propose that this is because the model used does not account for diffusion as a factor and, as such, is over estimating the rate of uptake. While it is likely that the modelling is over estimating the rate value, it still points to uptake having no contribution to the attenuation in release observed. More work needs to be done to both calculate the Michaelis-Menten kinetic parameters for zebrafish as well as to take into account diffusion, which this current model assumes does not exist, in order to fully support this hypothesis.

4.4 Conclusions

In this work we demonstrated that zebrafish are a candidate to be a model for chemobrain. We found that treatment pathway was significant to the observed attenuation of release. Food treatment was found to have a significant effect on release for both of the drugs studied after 1, 4 and 7 days of treatment. On the other hand, water treatment was only found to be effective when the fish were treated with carboplatin after 7 days. Furthermore, we showed that uptake was unchanged before and after treatment implying that it was not an explanation for the observed attenuation in release. Finally, we demonstrated that Pt was not present in rat brains after treatment, and is unlikely to be present in zebrafish brains after treatment using AA.

4.5 References

[1] Raffa, R. B., Duong, P. V., Finney, J., Garber, D. A., Lam, L. M., Mathew, S. S., Patel, N. N., Plaskett, K. C., Shah, M., and Weng, H. F. J. (2006) Is 'chemo-fog'/'chemo-brain' caused by cancer chemotherapy, *J. Clin. Pharm. Ther. 31*, 129-138.

[2] Nudelman, K. N. H., Wang, Y., McDonald, B. C., Conroy, S. K., Smith, D. J., West, J. D., O'Neill, D. P., Schneider, B. P., and Saykin, A. J. (2014) Altered Cerebral Blood Flow One Month after Systemic Chemotherapy for Breast Cancer: A Prospective Study Using Pulsed Arterial Spin Labeling MRI Perfusion, *PLoS ONE 9*, e96713.

[3] Joshi, G., Aluise, C. D., Cole, M. P., Sultana, R., Vore, M., St Clair, D. K., and Butterfield, D. A. (2010) Alterations in brain antioxidant enzymes and redox proteomic identification of oxidized brain proteins induced by the anti-cancer drug Adriamycin: Implications for oxidative stress-mediated chemobrain, *Neuroscience 166*, 796-807.

[4] Gaman, A. M., Uzoni, A., Popa-Wagner, A., Andrei, A., and Petcu, E.-B. (2016) The Role of Oxidative Stress in Etiopathogenesis of Chemotherapy Induced Cognitive Impairment (CICI)-"Chemobrain", *Aging and Disease 7*, 307-317.

[5] Scheibel, R. S., Valentine, A. D., O'Brien, S., and Meyers, C. A. (2004) Cognitive dysfunction and depression during treatment with interferon-alpha and chemotherapy, *J. Neuropsychiatry Clin. Neurosci. 16*, 185-191.

[6] Meyers, C. A., Albitar, M., and Estey, E. (2005) Cognitive impairment, fatigue, and cytokine levels in patients with acute myelogenous leukemia or myelodysplastic syndrome, *Cancer (Hoboken, NJ, U. S.) 104*, 788-793.

[7] Ahles, T. A., and Saykin, A. J. (2007) Candidate mechanisms for chemotherapy-induced cognitive changes, *Nature Reviews Cancer 7*, 192-201.

[8] Kaplan, S. V., Limbocker, R. A., Gehringer, R. C., Divis, J. L., Osterhaus, G. L., Newby, M. D., Sofis, M. J., Jarmolowicz, D. P., Newman, B. D., and Mathews, T. A. (2016) Impaired Brain Dopamine and Serotonin Release and Uptake in Wistar Rats Following Treatment with Carboplatin, *ACS chemical neuroscience*.

[9] Seigers, R., Schagen, S., Van Tellingen, O., and Dietrich, J. (2013) Chemotherapy-related cognitive dysfunction: current animal studies and future directions, *Brain imaging and behavior 7*, 453.

[10] Boulikas, T., and Vougiouka, M. (2004) Recent clinical trials using cisplatin, carboplatin and their combination chemotherapy drugs, *Oncology reports 11*, 559-595.

[11] Muggia, F. M. (1989) Overview of carboplatin: replacing, complementing, and extending the therapeutic horizons of cisplatin, In *Seminars in oncology*, pp 7-13, Elsevier.

[12] Panula, P., Chen, Y.-C., Priyadarshini, M., Kudo, H., Semenova, S., Sundvik, M., and Sallinen, V. (2010) The comparative neuroanatomy and neurochemistry of zebrafish CNS systems of relevance to human neuropsychiatric diseases, *Neurobiology of disease 40*, 46-57.

[13] Kalueff, A. V., Stewart, A. M., and Gerlai, R. (2014) Zebrafish as an emerging model for studying complex brain disorders, *Trends in pharmacological sciences 35*, 63-75.

[14] Hill, A. J., Teraoka, H., Heideman, W., and Peterson, R. E. (2005) Zebrafish as a model vertebrate for investigating chemical toxicity, *Toxicological sciences 86*, 6-19.

[15] McGrath, P., and Li, C.-Q. (2008) Zebrafish: a predictive model for assessing drug-induced toxicity, *Drug discovery today 13*, 394-401.

[16] Hinsch, K., and Zupanc, G. K. H. (2007) Generation and long-term persistence of new neurons in the adult zebrafish brain: A quantitative analysis, *Neuroscience 146*, 679-696.

[17] Shin, M., Field, T. M., Stucky, C. S., Furgurson, M. N., and Johnson, M. A. (2017) Ex Vivo Measurement of Electrically Evoked Dopamine Release in Zebrafish Whole Brain, *ACS Chemical Neuroscience*.

[18] Richendrfer, H., and Créton, R. (2013) Automated High-throughput Behavioral Analyses in Zebrafish Larvae, *Journal of Visualized Experiments : JoVE*, 50622.

[19] Gerlai, R., Chatterjee, D., Pereira, T., Sawashima, T., and Krishnannair, R. (2009) Acute and chronic alcohol dose: population differences in behavior and neurochemistry of zebrafish, *Genes, Brain and Behavior 8*, 586-599.

[20] Kraft, J., Osterhaus, G., Ortiz, A., Garris, P., and Johnson, M. (2009) In vivo dopamine release and uptake impairments in rats treated with 3-nitropropionic acid, *Neuroscience 161*, 940-949.

[21] Pera, M. F., and Harder, H. C. (1977) Analysis for platinum in biological material by flameless atomic absorption spectrometry, *Clinical Chemistry 23*, 1245-1249.

[22] Dallinger, R., Prosi, F., Segner, H., and Back, H. (1987) Contaminated food and uptake of heavy metals by fish: a review and a proposal for further research, *Oecologia 73*, 91-98.

[23] Heath, A. G. (1995) *Water pollution and fish physiology*, CRC press.

[24] Binks, S. P., and Dobrota, M. (1990) Kinetics and mechanism of uptake of platinum-based pharmaceuticals by the rat small intestine, *Biochemical pharmacology 40*, 1329-1336.

[25] Emerich, D., Snodgrass, P., Dean, R., Agostino, M., Hasler, B., Pink, M., Xiong, H., Kim, B. S., and Bartus, R. (1999) Enhanced delivery of carboplatin into brain tumours with intravenous CereportTM (RMP-7): dramatic differences and insight gained from dosing parameters, *British journal of cancer 80*, 964.

[26] Black, K. L. (1995) Biochemical opening of the blood-brain barrier, *Advanced drug delivery reviews 15*, 37-52.

[27] Ishida, S., Lee, J., Thiele, D. J., and Herskowitz, I. (2002) Uptake of the anticancer drug cisplatin mediated by the copper transporter Ctr1 in yeast and mammals, *Proceedings of the National Academy of Sciences 99*, 14298-14302.

[28] Kovacs, R., Bakos, K., Urbanyi, B., Kovesi, J., Gazsi, G., Csepeli, A., Appl, A. J., Bencsik, D., Csenki, Z., and Horvath, A. (2016) Acute and sub-chronic toxicity of four cytostatic drugs in zebrafish, *Environmental science and pollution research international 23*, 14718-14729.

[29] Vickrey, T. L., Xiao, N., and Venton, B. J. (2013) Kinetics of the Dopamine Transporter in Drosophila Larva, *ACS Chemical Neuroscience 4*, 832-837.

[30] Sabeti, J., Adams, C. E., Burmeister, J., Gerhardt, G. A., and Zahniser, N. R. (2002) Kinetic analysis of striatal clearance of exogenous dopamine recorded by chronoamperometry in freely-moving rats, *Journal of neuroscience methods 121*, 41-52.

Chapter 5 conclusions and future directions

5.1 Conclusions

Our work in zebrafish has developed multiple interesting results. We have shown that it is possible to measure neurotransmitter release from intact whole brain tissue *ex vivo*, the first time that has been demonstrated. We examined the release in zebrafish and were able to compare it to the release in rodents and have shown that, though there were distinct difference between the shapes of the release curve in zebrafish when compared to rodents there were many similarities. Dopamine release is regulated both by uptake at the DAT, as demonstrated by the reuptake inhibitor experiments. The release events are also clearly regulated by D2 autoreceptors, at least in the intact whole brains, as demonstrated by the sulpiride experiments.

We have also been able to show that the zebrafish's neurochemistry seems to react in similar ways to the rodent's neurochemistry upon introduction of chemotherapeutic agents. There is a marked decrease in dopamine release in both model organisms. Overall we feel that we have made a great amount of progress in showing that zebrafish are a valuable and viable model organism for neurochemistry that can complement other current model organisms like rodents and fruit flies.

5.2 Future Directions

These are promising conclusions but there is still a lot of information that needs to be teased out to completely understand what is going on. The first main question that needs to be answered is what the identity of all of the analytes released during an experiment.. In order to try to determine the identity of the released species we tried to use principal component analysis[1, 2]as shown in Figure 1. While we had a limited amount of success with isolating signals by this method it was inconsistent. In the future it is possible that by optimizing the training sets, and

coating the electrodes with polymers such as nafion[3] to limit possible extra signals we will be able to use PCA to successfully isolate signals in zebrafish. This would allow us to replicate what other groups have reported.

Determining how much of the signal comes from norepinephrine quantitatively can't be done by using PCA because of the similarity of the CVs of dopamine and norepinephrine. Another experimental method must be used to deconvulate these signals. It is possible that treatment with a drug that can either selectively stop norepinephrine synthesis or one that can selectively effect norepinephrine or dopamine release would allow us to deconvulate the signals. Stopping norepinephrine synthesis independently of dopamine synthesis is difficult, however, effecting dopamine release selectively using a drug such as quinpirole[4, 5] is much easier.

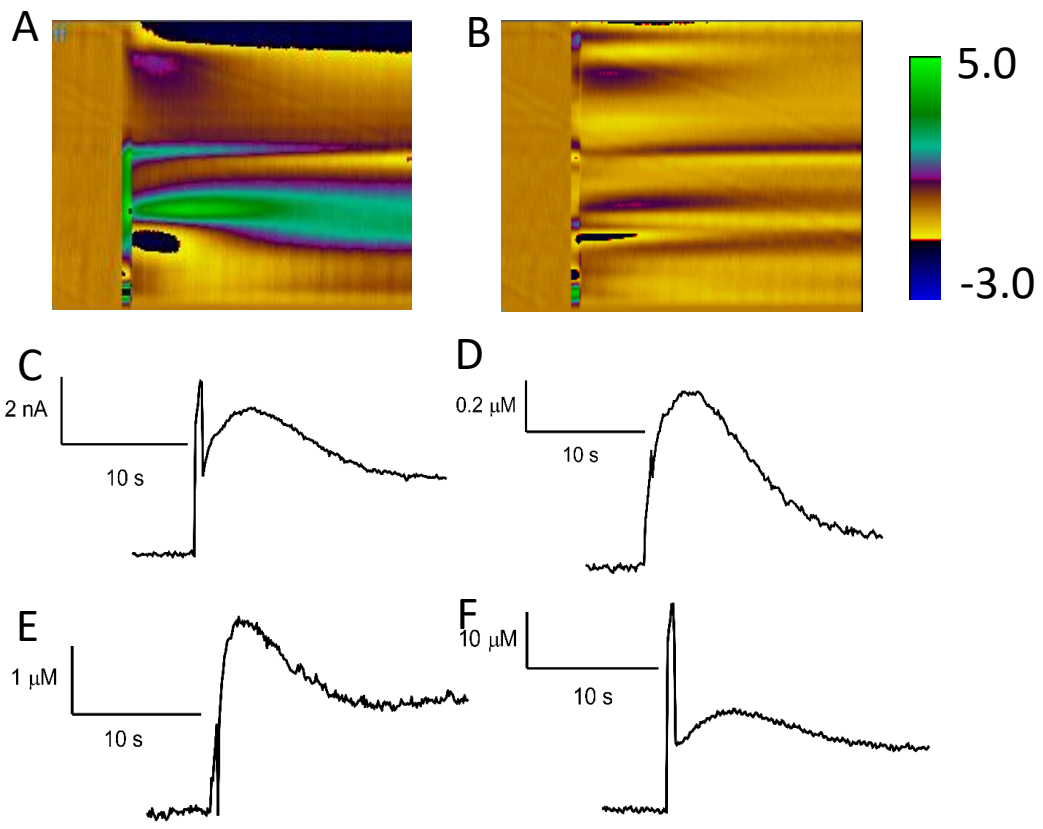

Figure 1: Example of PCA work in a zebrafish whole brain. (A) Shows the orginal color plot before the application of principal component analysis. (B) Shows the color plot after the analysis has been applied, as can be seen most of the signals not found where the stim artifact is have been accounted for. (C) Is the raw current vs time plot before the PCA analysis has been applied. (D) Is the dopamine component of the signal, the concentration of ~ 0.4 um was in good agreement with the average signal we would expect from a whole brain. (E) Is the DOPAC component and (F) is the ascorbate component.

Another important question is how large a natural occurring dopamine release event is. This is important to know because it will give us a gauge of how similar induced release events are to natural occurring events. This information would allow us to probe the hypothesis in chapter 3 that one of the reasons that we see such extreme overshoot in zebrafish is that much more dopamine is being released during an electrical stimulation event then would be observed in a naturally occurring event. We have done the experiment to see naturally occurring events are

observed from an intact brain *ex vivo* and have seen none. We believe that in order to see events some sort of chemical stimulation, such as nicotine[6], is needed. We think chemical stimulation is promising because we have observed unstimulated release events after treatment of the brain with deprenyl, a MAO inhibitor that has been found to be effective in zebrafish[7]. (Figure 3). We do not completely understand the underlying biochemical reasons for these observations at this point, however, we do believe that it is promising.

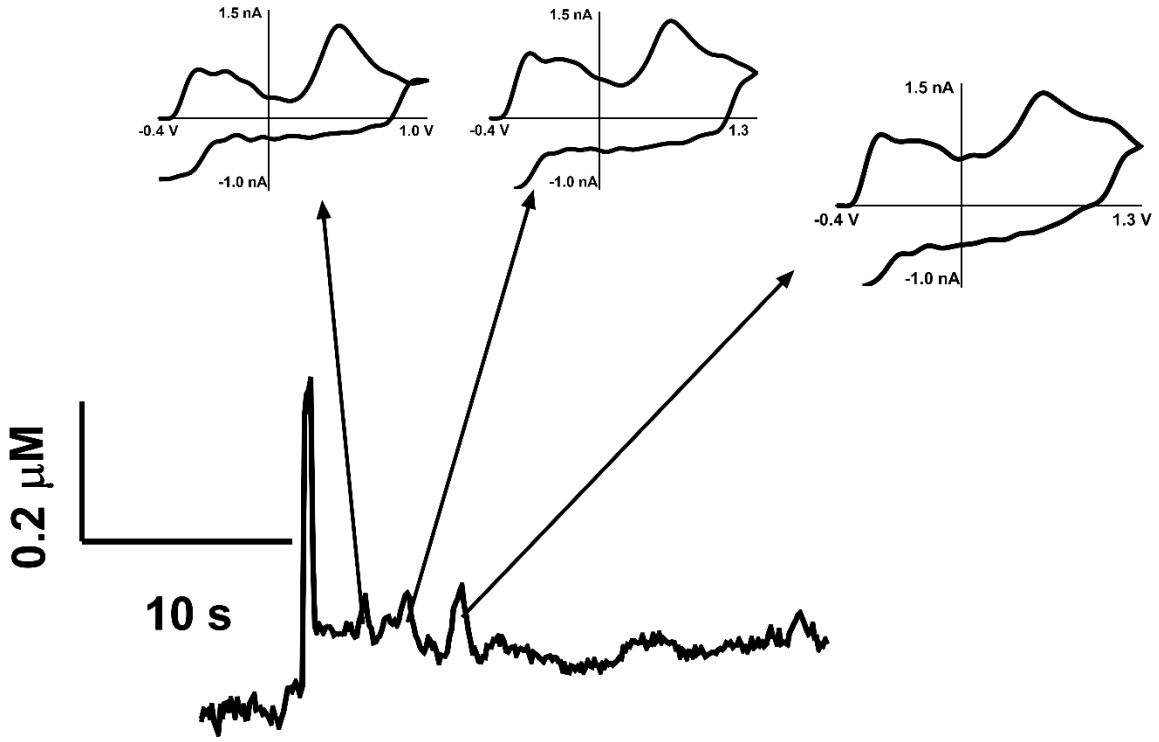

Figure 3: After the initial electrical stimulation 3 transient like events were observed with CV similar to dopamine's when the brain was treated with 10 uM deprenyl.

One of the distinct advantages of using whole brains is the fact that the neuronal circuitry should be intact. In order to take full advantage of this methods need to be developed to allow for remote stimulation of the neurons of interest. As was discussed in chapter 1 one of the main

dopamine systems in zebrafish extends from the diencephalon to the telencephalon. With this in mind we worked to stimulate in the diencephalon and measure the signal in the telencephalon, as seen in Figure 4. We were able to see clean dopamine release when this was done in 2 brains. While these results are promising they are inconsistent, without any disinguising features it is difficult to consistently place the stim electrodes in the diencephalon. We believe moving forward that some form of green fluorescence protein (GFP) labeling of neurons to allow for consistent placement of the electrodes is needed. GFP has been used in the past to study the development of and toxicity towards monoamine neurons[8, 9] In order to use these technologies for our work staining needs to be specific for dopamine and we need to be able to image simultaneously with our electrochemical measurements.

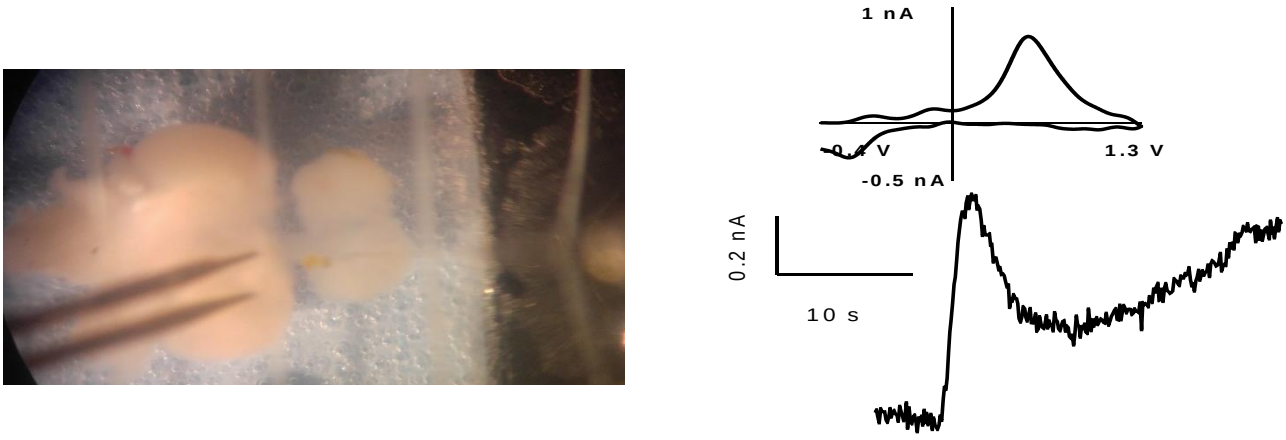

Figure 4 An example of remote stimulation, the stim electrode is placed in the diencephalon and the working electrode in the telencephalon. Clean release is observed with a clean CV.

Another promising avenue of work in the zebrafish is related to the mitigation of the neurochemical effects observed after treatment with the chemotherapeutic agent's carboplatin and 5-FU. In order to examine this we treated the fish with the drug in their water at a concentration of 100 μM for two week then allowed the fish to recover for 2 weeks. The results are shown in Figure 5. After treatment with both drugs there was no recovery back to the release

levels of saline fish (Carboplatin 0.419 ± 0.197 µM n=3 brains, 5-FU 0.485 ± 0.116 µM n=5 brains, and Saline 1.39 ± 0.335 µM n=4 brains). Also interestingly, unlike what was seen in chapter 4 after 1 week of treatment, 2 weeks of water treatment with 5-FU caused release to be significantly released, even with 2 weeks of recovery, ($p<0.05$ 2 tailed t-test).

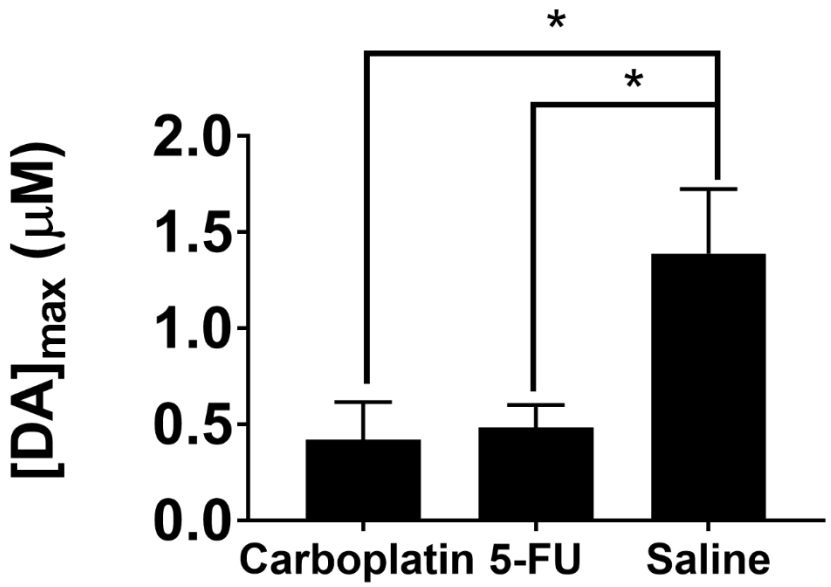

Figure 5 Dopamine release after water treatment with 100 µM carboplatin or 5-FU. Both 5-FU (2-tailed t-test $p<0.05$) and carboplatin treatment (one-tailed t-test $p<0.05$) were significantly decreased when compared to the saline treated fish's release.

5.3 References

[1] Keithley, R. B., Wightman, R. M., and Heien, M. L. (2009) Multivariate concentration determination using principal component regression with residual analysis, *TrAC Trends in Analytical Chemistry 28*, 1127-1136.

[2] Rodeberg, N. T., Johnson, J. A., Cameron, C. M., Saddoris, M. P., Carelli, R. M., and Wightman, R. M. (2015) Construction of training sets for valid calibration of in vivo cyclic voltammetric data by principal component analysis, *Analytical chemistry 87*, 11484-11491.

[3] Zimmerman, J. B., and Wightman, R. M. (1991) Simultaneous electrochemical measurements of oxygen and dopamine in vivo, *Analytical chemistry 63*, 24-28.

[4] Eilam, D., and Szechtman, H. (1989) Biphasic effect of D-2 agonist quinpirole on locomotion and movements, *European journal of pharmacology 161*, 151-157.

[5] Einat, H., and Szechtman, H. (1993) Longlasting consequences of chronic treatment with the dopamine agonist quinpirole for the undrugged behavior of rats, *Behavioural brain research 54*, 35-41.

[6] Eddins, D., Petro, A., Williams, P., Cerutti, D. T., and Levin, E. D. (2009) Nicotine effects on learning in zebrafish: the role of dopaminergic systems, *Psychopharmacology 202*, 103.

[7] Setini, A., Pierucci, F., Senatori, O., and Nicotra, A. (2005) Molecular characterization of monoamine oxidase in zebrafish (Danio rerio), *Comparative Biochemistry and Physiology Part B: Biochemistry and Molecular Biology 140*, 153-161.

[8] Wen, L., Wei, W., Gu, W., Huang, P., Ren, X., Zhang, Z., Zhu, Z., Lin, S., and Zhang, B. (2008) Visualization of monoaminergic neurons and neurotoxicity of MPTP in live transgenic zebrafish, *Developmental biology 314*, 84-92.

[9] Suen, M. F., Chan, W., Hung, K. W., Chen, Y., Mo, Z., and Yung, K. K. (2013) Assessments of the effects of nicotine and ketamine using tyrosine hydroxylase-green fluorescent protein transgenic zebrafish asbiosensors, *Biosensors and Bioelectronics 42*, 177-185.